



Analysis of Mechanisms for Early Waste Package / Drip Shield Failure

**NOTICE OF OPEN CHANGE DOCUMENTS - THIS DOCUMENT IS IMPACTED BY
THE LISTED CHANGE DOCUMENTS AND CANNOT BE USED WITHOUT THEM.**

1) ACN-001, DATED 09/28/2007



Prepared for:
U.S. Department of Energy
Office of Civilian Radioactive Waste Management
Office of Repository Development
1551 Hillshire Drive
Las Vegas, Nevada 89134-6321

Prepared by:
Sandia National Laboratories
OCRWM Lead Laboratory for Repository Systems
1180 Town Center Drive
Las Vegas, Nevada 89144

Under Contract Number
DE-AC04-94AL85000

DISCLAIMER

This report was prepared as an account of work sponsored by an agency of the United States Government. Neither the United States Government nor any agency thereof, nor any of their employees, nor any of their contractors, subcontractors or their employees, makes any warranty, express or implied, or assumes any legal liability or responsibility for the accuracy, completeness, or any third party's use or the results of such use of any information, apparatus, product, or process disclosed, or represents that its use would not infringe privately owned rights. Reference herein to any specific commercial product, process, or service by trade name, trademark, manufacturer, or otherwise, does not necessarily constitute or imply its endorsement, recommendation, or favoring by the United States Government or any agency thereof or its contractors or subcontractors. The views and opinions of authors expressed herein do not necessarily state or reflect those of the United States Government or any agency thereof.

QA: QA

**Analysis of Mechanisms for Early Waste Package / Drip Shield
Failure**

ANL-EBS-MD-000076 REV 00

June 2007



Scientific Analysis/Calculation Signature Page/Change History

Page iii

1. Total Pages: 168

Complete only applicable items.

2. Document Title Analysis of Mechanisms for Early Waste Package / Drip Shield Failure			
3. DI (Including Revision No. and Addendum No.) ANL-EBS-MD-000076 REV 00			
	Printed Name	Signature	Date
4. Originator	John A. McClure	<i>John A. McClure</i>	06/29/2007
5. Checker	James K. Knudsen	<i>James K. Knudsen</i>	6/29/2007
6. QCS/Lead Lab QA Reviewer	Brian T. Mitcheltree	<i>Brian T. Mitcheltree</i>	6/29/2007
7. Responsible Manager/Lead	Clifford L. Howard	<i>Cliff Howard</i>	6-29-07
8. Responsible Manager	M. Kathryn Knowles	<i>M. Kathryn Knowles</i>	6/29/07
9. Remarks Acknowledgements to Chris Kimura for his efforts creating the waste package SAPHIRE model, and to Russell Jarek for revisions to the weld flaw analysis.			
Change History			
10. Revision No. and Addendum No.	11. Description of Change		
00	<p>Initial issue.</p> <p>This analysis report is a complete revision of and supersedes <i>Analysis of Mechanisms for Early Waste Package/Drip Shield Failure</i>, CAL-EBS-MD-000030 REV 00C.</p> <p>Upon completion, this analysis report addresses all actions in Condition Reports CR-9845 and CR-10052 associated with this or prior revisions of <i>Analysis of Mechanisms for Early Waste Package/Drip Shield Failure</i>.</p> <p>CR-9845, Action Number 9845-001 is to remove citations of certain IEDs as Direct Inputs from the document. This action item was addressed in this document by citing only the design information TDIPs as direct design input.</p> <p>CR-10052 noted two errors in the calculation CAL-EBS-MD-000030: Item Error 1 that identified a mathematical error in a minimization method and Item Error 2 that identified an incorrect citation.</p> <p>Item Error 1 was addressed by using a different approach for evaluating Error Factors that does not use the referenced minimization method.</p> <p>Item Error 2 was an incorrect section citation from ANL-EBS-MD-000003 that was resolved as ANL-EBS-MD-000003 is not a reference for this revision.</p>		

INTENTIONALLY LEFT BLANK

CONTENTS

	Page
ACRONYMS.....	xiii
1. PURPOSE	1-1
2. QUALITY ASSURANCE	2-1
3. USE OF SOFTWARE.....	3-1
4. INPUTS.....	4-1
4.1 DIRECT INPUTS	4-1
4.1.1 Estimates of Human Error Probabilities	4-1
4.1.2 Alloy 22 Weld Flaw Characteristics.....	4-2
4.1.3 Miscellaneous Inputs	4-6
4.1.4 Qualification of External Source Data.....	4-7
4.2 YUCCA MOUNTAIN REVIEW PLAN CRITERIA	4-11
4.3 CODES, STANDARDS, AND REGULATIONS.....	4-13
5. ASSUMPTIONS.....	5-1
5.1 CLOSURE WELD-FLAW SCREENING SIZE	5-1
5.2 PROBABILITY DISTRIBUTION FOR IMPROPER MATERIAL SELECTION.....	5-1
5.3 UNCERTAINTY DISTRIBUTIONS FOR PROBABILITY VALUES.....	5-1
5.4 CRITICAL PHASE OF THE WASTE PACKAGE OUTER CORROSION BARRIER HEAT TREATMENT	5-2
5.5 MONITORS FOR WASTE PACKAGE OUTER CORROSION BARRIER FABRICATION PROCESSES	5-2
5.6 QUENCHING OF WASTE PACKAGE OUTER CORROSION BARRIER	5-3
5.7 PROBABILITY FOR MECHANICAL MALFUNCTIONING OF LIFTING AND MOVING EQUIPMENT	5-3
5.8 FLUID MAKEUP SYSTEM FOR THE HEAT-TREATMENT QUENCHING PROCESS	5-4
5.9 INDEPENDENT CHECKS OF MECHANICAL AND OPERATIONAL PROCESSES ASSOCIATED WITH WASTE PACKAGES AND DRIP SHIELDS.....	5-4
5.10 AUTOMATED SYSTEMS USED FOR FABRICATION PROCESSES ASSOCIATED WITH WASTE PACKAGES AND DRIP SHIELDS.....	5-5
6. DISCUSSION OF EARLY FAILURE PROBABILITY CALCULATIONS.....	6-1
6.1 REVIEW OF DEFECT-RELATED FAILURES OF CONTAINERS IN VARIOUS INDUSTRIES	6-1
6.1.1 Boilers and Pressure Vessels	6-1
6.1.2 Nuclear Fuel Rods	6-3
6.1.3 Underground Storage Tanks	6-4
6.1.4 Radioactive Cesium Capsules.....	6-5

CONTENTS (Continued)

	Page
6.1.5 Dry Storage Casks for Spent Nuclear Fuel.....	6-6
6.1.6 Summary	6-8
6.2 FABRICATION AND HANDLING PROCESSES RELEVANT TO EARLY FAILURE OF ENGINEERED BARRIER COMPONENTS.....	6-11
6.2.1 Waste Package Fabrication and Handling Processes.....	6-11
6.2.2 Drip Shield Fabrication and Handling Processes	6-12
6.2.3 Disposition of Possible Engineered Barrier Component Fabrication or Handling Processes That Could Lead to Defects.....	6-14
6.3 WASTE PACKAGE POTENTIAL DEFECTS.....	6-17
6.3.1 Evaluation of Weld Flaws in Waste Package Outer Lid Weld.....	6-18
6.3.2 Improper Base-Metal Selection for Waste Package Outer Corrosion Barrier	6-36
6.3.3 Improper Heat-Treatment Implementation for Waste Package Outer Corrosion Barrier	6-38
6.3.4 Improper Heat-Treatment Implementation for Waste Package Outer Corrosion Barrier Lid.....	6-45
6.3.5 Low-Plasticity Burnishing Treatment Implementation	6-50
6.3.6 Improper Handling of Waste Package.....	6-52
6.3.7 Improper Weld Filler Material Selection for Waste Package.....	6-54
6.4 DRIP SHIELD FABRICATION, HANDLING, AND POTENTIAL DEFECTS	6-55
6.4.1 Drip Shield Base Metal Flaw Implementation	6-56
6.4.2 Drip Shield Improper Heat-Treatment Implementation	6-57
6.4.3 Drip Shield Weld-Filler Defects	6-60
6.4.4 Drip Shield Emplacement Failure.....	6-61
6.5 WASTE PACKAGE AND DRIP SHIELD DEFECT SUMMARY PROBABILITIES AND CONSEQUENCES.....	6-63
6.5.1 Combining Defect Probabilities.....	6-63
6.5.2 Assessing Consequences of Defects	6-70
7. CONCLUSIONS.....	7-1
7.1 WASTE PACKAGE AND DRIP SHIELD EARLY FAILURE IMPLEMENTATION.....	7-1
7.2 TSPA WELD-FLAW IMPLEMENTATION.....	7-3
7.3 EVALUATION OF YUCCA MOUNTAIN REVIEW PLAN CRITERIA	7-3
8. INPUTS AND REFERENCES	8-1
8.1 DOCUMENTS CITED.....	8-1
8.2 CODES, STANDARDS, REGULATIONS, AND PROCEDURES.....	8-5
8.3 SOURCE DATA, LISTED BY DATA TRACKING NUMBER	8-6
8.4 OUTPUT DATA, LISTED BY DATA TRACKING NUMBER	8-6
8.5 SOFTWARE CODES.....	8-6

CONTENTS (Continued)

	Page
APPENDIX A – EVALUATION OF WELD-FLAW TEST DATA.....	A-1
APPENDIX B – EVENT TREES AND FAULT TREES.....	B-1
APPENDIX C – TESTS ON PROTOTYPE WASTE PACKAGE OUTER CORROSION BARRIER	C-1

INTENTIONALLY LEFT BLANK

FIGURES

	Page
4-1. Schematic Representation of the Cross Section of the Alloy 22 Weld	4-4
6-1. Illustration of Closure Welds for the VSC-24 Dry Storage Cask	6-7
6-2. Basic Waste Package Defect Event Tree.....	6-18
6-3. Initial Flaw Size PDF and Its CDF Compared with the Alternate Distribution.....	6-24
6-4. PDF and CDF for Flaw-Density Parameter before Ultrasonic Inspection.....	6-25
6-5. Schematic Representation of Flaw Orientation on Specimen Ring	6-27
6-6. Comparison of Several Ultrasonic PND Curves	6-30
6-7. PDF for Flaw Size before and after Ultrasonic Inspection and Repair in 25-mm- Thick Weld.....	6-33
6-8. CDF of Weld-Flaw Density before and after Ultrasonic Inspection and Repair in 25 mm-Thick Weld	6-34
6-9. Event Tree for Evaluating Improper Base Metal Selection for Waste Package Outer Corrosion Barrier	6-38
6-10. Event Tree for Evaluating Improper Heat Treatment of the Waste Package Outer Corrosion Barrier	6-44
6-12. Event Tree for Evaluating Low-Plasticity Burnishing Treatment of the Waste Package Outer Corrosion Barrier Lid	6-52
6-13. Event Tree for Evaluating Mishandling of the Waste Package Outer Corrosion Barrier	6-54
6-14. Event Tree for Evaluating Weld-Filler Material Defects in the Waste Package Outer Corrosion Barrier	6-55
6-15. Basic Drip Shield Defect Event Tree	6-56
6-16. Event Tree for Evaluating Improper Base-Metal Selection for Drip Shield.....	6-57
6-17. Event Tree for Evaluating Improper Heat-Treatment of the Drip Shield	6-60
6-18. Event Tree for Evaluating Weld-Filler Material Flaws in the Drip Shield	6-61
6-19. Event Tree for Evaluating Improper Emplacement of the Drip Shield.....	6-63
6-20. Cumulative Uncertainty Distribution for Undetected Waste Package Defects (UNC_WP_EF).....	6-67
6-21. Cumulative Uncertainty Distribution for Undetected Drip Shield Defects (UNC_DS_EF).....	6-68
B-1. Basic Waste Package Defect Event Tree.....	B-1
B-2. Event Tree for Evaluating Improper Base-Metal Selection for Waste Package Outer Corrosion Barrier	B-2
B-3. Event Tree for Evaluating Improper Heat-Treatment of the Waste Package Outer Corrosion Barrier	B-3
B-4. Fault Tree for Waste Package Outer Corrosion Barrier Heat-Treatment Move	B-4
B-5. Fault Tree for Waste Package Outer Corrosion Barrier Heat-Treatment Move Check	B-5
B-6. Fault Tree for Waste Package Outer Corrosion Barrier Heat-Treatment Quench	B-6
B-7. Fault Tree for Waste Package Outer Corrosion Barrier Heat-Treatment Quench Check	B-7

FIGURES (Continued)

	Page
B-8. Event Tree for Evaluating Improper Heat Treatment of the Waste Package Outer Corrosion Barrier Lid.....	B-8
B-9. Fault Tree for Waste Package Outer Corrosion Barrier Lid Heat-Treatment Move.....	B-9
B-10. Fault Tree for Waste Package Outer Corrosion Barrier Lid Heat-Treatment Move Check.....	B-10
B-11. Fault Tree for Waste Package Outer Corrosion Barrier Lid Heat-Treatment Quench Check	B-11
B-12. Event Tree for Evaluating Low-Plasticity Burnishing Treatment of the Waste Package Outer Corrosion Barrier Lid.....	B-12
B-13. Fault Tree for Evaluating Low-Plasticity Burnishing Process for the Waste Package Outer Corrosion Barrier Lid.....	B-13
B-14. Event Tree for Evaluating Mishandling of the Waste Package Outer Corrosion Barrier.....	B-14
B-15. Fault Tree for Evaluating Mishandling of the Waste Package Outer Corrosion Barrier.....	B-15
B-16. Event Tree for Evaluating Weld-Filler Material Defects for the Waste Package Outer Corrosion Barrier	B-16
B-17. Basic Drip Shield Defect Event Tree	B-17
B-18. Event Tree for Evaluating Improper Base-Metal Selection for the Drip Shield.....	B-18
B-19. Event Tree for Evaluating Improper Heat Treatment of the Drip Shield.....	B-19
B-20. Fault Tree for Check on Improper Heat Treatment of the Drip Shield.....	B-20
B-21. Event Tree for Evaluating Weld-Filler Material Flaws in the Drip Shield.....	B-21
B-22. Event Tree for Evaluating Improper Emplacement of the Drip Shield.....	B-22
C-1. Prototype Waste Package Outer Corrosion Barrier Entering Quench Tank	C-1
C-2. Postannealed View of the Prototype Waste Package Outer Corrosion Barrier.....	C-2

TABLES

	Page
4-1. Estimates of Human Error Probabilities.....	4-2
4-2. Weld Dimensions	4-3
4-3. Dimensions of the Ultrasonic Indications	4-5
4-4. Weld Flaw Data.....	4-6
4-5. Input to Early Failure Mechanisms for Waste Package Outer Corrosion Barrier and Drip Shield.....	4-6
6-1. Summary of VSC-24 Weld Cracking Events.....	6-6
6-2. Summary of Defect-Related Failures in Various Welded Metallic Containers	6-8
6-3. Expected Distribution of As-Welded Waste Package Weld Flaws (informational only)	6-26
6-4. Parameters Needed for Calculating Weld-Flaw Characteristics	6-35
6-5. Parameter Summary for Evaluating Flaw Characteristics	6-36
6-6. Main Characteristics of Flaws in Welds of Waste Package (informational only)	6-36
6-7. Parameters for End-State Uncertainty Distributions of Undetected Defects	6-64
6-8. Parameters from Scenario End-State Uncertainty Distributions for Undetected Defects	6-65
6-9. Cumulative Uncertainty Distribution for Undetected Waste Package Defects.....	6-66
6-10. Cumulative Uncertainty Distribution for Undetected Drip Shield Defects	6-67
6-11. Joint Probability for Co-Location of Flawed Drip Shield and Waste Package.....	6-69
7-1. TSPA Waste Package and Drip Shield Early Failure Parameter Specification	7-2

INTENTIONALLY LEFT BLANK

ACRONYMS

ASME	American Society of Mechanical Engineers
BWR	boiling water reactor
CDF	cumulative distribution function
DOE	U.S. Department of Energy
HEP	human error probability
NBBPVI	National Board of Boiler and Pressure Vessel Inspectors
NDE	nondestructive examination
NRC	U.S. Nuclear Regulatory Commission
PDF	probability density function
PND	probability of nondetection
PWR	pressurized water reactor
QA	quality assurance
SCC	stress corrosion cracking
TAD	transportation, aging, and disposal (canister)
TSPA	total system performance assessment
TWP	technical work plan
YMP	Yucca Mountain Project
YMRP	<i>Yucca Mountain Review Plan, Final Report</i>

INTENTIONALLY LEFT BLANK

1. PURPOSE

The purpose of this analysis is to evaluate the types of defects or imperfections that could occur in a waste package or a drip shield and potentially lead to its early failure, and to estimate a probability of undetected occurrence for each type. An early failure is defined as the through-wall penetration of a waste package or drip shield due to manufacturing or handling-induced defects, at a time earlier than would be predicted by mechanistic degradation models for a defect-free waste package or drip shield. A single waste package design has been specified with several configurations for the various waste forms as cited in *Total System Performance Assessment Data Input Package for Requirements Analysis for DOE SNF/HLW and Navy SNF Waste Package Overpack Physical Attributes Basis for Performance Assessment* (SNL 2007 [DIRS 179567], Table 4-1, Item 03-02). The waste package consists of a stainless steel inner shell and an outer corrosion barrier. For this analysis, the transportation, aging, and disposal (TAD) canister type waste package is a surrogate for all of the waste package configurations since all the configurations are subject to the same fabrication and handling processes. The scope of this analysis is limited to the manufacturing or handling-induced defects that might lead to the early failure of the waste package outer corrosion barrier and drip shield. The structural (stainless steel) vessel of the waste package was not analyzed.

This document was developed in accordance with the *Technical Work Plan for Postclosure Engineered Barrier Degradation Modeling* (SNL 2007 [DIRS 178849]), except for deviations as noted.

1. All of the acceptance criteria from Section 2.2.1.3.1.3 of *Yucca Mountain Review Plan, Final Report* (YMRP) (NRC 2003 [DIRS 163274]) were designated in the technical work plan (TWP) for consideration in this analysis. However, most of the criteria in Section 2.2.1.3.1.3 relate to degradation of the engineered barriers model abstraction that is beyond the scope of this analysis. The one subsection from Section 2.2.1.3.1.3 of *Yucca Mountain Review Plan, Final Report* (NRC 2003 [DIRS 163274]) applicable to this analysis is Acceptance Criterion 3, subsection 4, addressed in Section 4.2.
2. The TWP cites the procedure IM-PRO-001, *Managing Electronic Mail Records*, as the procedure for handling electronic information. The correct procedure is IM-PRO-002, *Control of the Electronic Management of Information*, as cited in Section 2.

If a waste package is affected by a type of defect that may lead to its early failure, it does not mean that this waste package is due to fail at emplacement in the repository. Failure of the waste package will only occur after degradation processes take place, which may happen hundreds or even thousands of years after emplacement. If a waste package were to fail early because of a defect, its radionuclide inventory would not necessarily be available for transport. This is because most through-wall penetrations, especially cracks from stress corrosion cracking (SCC), are usually tight and of limited length. Likewise, for drip shields, these types of failures do not necessarily lead to a loss of function, as seepage ingress through stress corrosion cracks is expected to be minimal (SNL 2007 [DIRS 177417], Section 6.7).

This analysis receives no direct input from other analyses or model reports. The intended use of this analysis is to provide information and inputs to repository license activities, particularly performance assessment and postclosure criticality analyses. The output will be estimates of drip shield and waste package early failure probabilities. This analysis provides direct inputs to *Total System Performance Assessment Model/Analysis for the License Application* (SNL 2007 [DIRS 178871]) and *Screening Analysis of Criticality Features, Events, and Processes for License Application* (SNL 2007 [DIRS 173869]).

There are no limitations on the use of the data from this analysis, with the exception that results are based, in part, on assumptions (Section 5) about process procedural steps that must be verified when the approved process procedures become available.

2. QUALITY ASSURANCE

This document has been developed under the Yucca Mountain Quality Assurance (QA) Program in accordance with SCI-PRO-005, *Scientific Analyses and Calculations*. This activity is subject to *Quality Assurance Requirements and Description* (DOE 2006 [DIRS 177092]) requirements. All waste package configurations have been determined to be important for waste isolation in accordance with LS-PRO-0203, *Q-List and Classification of Structures, Systems, and Components*.

The inputs to this analysis are documented in accordance with SCI-PRO-004, *Managing Technical Product Inputs*. The methods used to control the electronic management of data, as required by IM-PRO-002, have been accomplished in accordance with the TWP (SNL 2007 [DIRS 178849]).

INTENTIONALLY LEFT BLANK

3. USE OF SOFTWARE

The computer code SAPHIRE (V. 7.26, STN: 10325-7.26-00 [DIRS 177010]) was used to develop and quantify event trees for this analysis. SAPHIRE was selected for use in this analysis since it is an appropriate software product for use with event tree/fault tree analyses and was used only within its range of validation in accordance with IM-PRO-003, *Software Management*. It is a qualified software code that was obtained from Software Configuration Management. There are no limitations on the use of the SAPHIRE software product.

SAPHIRE was installed on a Dell Optiplex GX260 PC running Microsoft Windows 2000 with Service Pack 4, SNL tag number S884983, which is use-restricted for qualified and controlled software. Compressed files from the SAPHIRE computation labeled "SAPHIRE OUTPUT" are included in output DTN: MO0701PASHIELD.000 and DTN: MO0705EARLYEND.000.

Microsoft Excel 2003 SP2, bundled with Microsoft Office 2003, is a commercial off-the-shelf software program used in this report. Microsoft Excel 2003 SP2 was installed on a Dell Celeron PC equipped with the Windows XP Version 2002 operating system and is appropriate for this application as it offers the mathematical and graphical functionality necessary to perform and document the numerical manipulations used in this report. The Excel computations performed in this report use only standard built-in functions and are documented in sufficient detail to allow an independent technical reviewer to reproduce or verify the results by visual inspection or hand calculation without recourse to the originator. The Excel files are included in output DTN: MO0701PASHIELD.000. The analysis results are not dependent upon the use of this particular software; therefore use of this software is not subject to IM-PRO-003.

Mathcad® Version 13 is a commercial off-the-shelf software program used in this report. This program was installed on a Dell Celeron PC equipped with the Windows XP Version 2002 operating system and is appropriate for this application as it offers the mathematical and graphical functionality necessary to perform and document the numerical manipulations used in this report. The Mathcad® computations performed in this report use only standard built-in functions and are documented in sufficient detail in Appendix A to allow an independent technical reviewer to reproduce or verify the results by visual inspection or hand calculation without recourse to the originator. The Mathcad® file is included in output DTN: MO0701PASHIELD.000. The analysis results are not dependent upon the use of this particular software; therefore use of this software is not subject to IM-PRO-003.

The software code CWD (V. 2.0, STN: 10363-2.0-00 [DIRS 162809]) computes the cumulative probability of a manufacturing defect based on the probability for the nondetection of weld flaws in the total system performance assessment (TSPA) model. The code is referenced since inputs for computations with this software are within the parameters in Table 7-1 but the software is not used in this analysis. The details of the CWD calculation are given in Section 2 of the software management report for CWD (DOE 2003 [DIRS 167564]).

INTENTIONALLY LEFT BLANK

4. INPUTS

4.1 DIRECT INPUTS

Direct inputs to this analysis are listed in Table 4-1 through Table 4-5. Supporting information for the direct input data is also provided in this section to aid in transparency and clarity. In particular, Section 4.1.1 includes a description of the human error probability (HEP) distributions equations and Section 4.1.2.2 includes a discussion of the weld-flaw detection techniques.

4.1.1 Estimates of Human Error Probabilities

The specific HEP data used are summarized in Table 4-1. Based on information by Swain and Guttman (1983 [DIRS 139383], pp. 2-17 to 2-19), the estimated HEPs are considered to follow a lognormal distribution. For such distributions, Swain and Guttman (1983 [DIRS 139383], p. 2-19) recommend choosing the 5th and the 95th percentiles (100 quantiles) of a lognormal distribution when evaluating lower and upper bounds for HEP uncertainty. The range for the uncertainty is expressed as an error factor EF , given by Equation 2. The nominal probabilities from Swain and Guttman (1983 [DIRS 139383]) represent the median of the uncertainty distribution with an assigned error factor. The mean value for these error probability distributions, derived from Equation 4, are also shown in Table 4-1 and are used subsequently in the SAPHIRE computations. Values derived from Benhardt et al. (1994 [DIRS 157684]) and shown in Table 4-1 are the distribution means and, thus, the median values are derived from Equation 4.

The distribution median m_{50} and the error factor for lognormal distributions can be obtained from the 5th and the 95th percentiles using the following formulae (Modarres 1993 [DIRS 104667], p. 266):

$$m_{50} = \sqrt{5^{th} \text{ percentile} \times 95^{th} \text{ percentile}} \quad (\text{Eq. 1})$$

$$EF = \sqrt{\frac{95^{th} \text{ percentile}}{5^{th} \text{ percentile}}} \quad (\text{Eq. 2})$$

The distribution mean (m) of a lognormal distribution (k) as a function of its median (m_{50}) and its error factor is given as follows (Modarres 1993 [DIRS 104667], p. 266), where the factor, 1.645, is the standard normal value of the 0.95 quantile of the cumulative distribution function (CDF):

$$\sigma_k = \frac{\ln(EF_k)}{1.645} \quad (\text{Eq. 3})$$

$$m_k = m_{50k} \cdot \exp\left[\frac{1}{2} \cdot (\sigma_k)^2\right] \quad (\text{Eq. 4})$$

Using Equations 1 to 4 yields expected or mean error probability values shown in the “Expected (Mean) Probability” column of Table 4-1 or median values as shown in “Nominal (Median) Probability” column.

Table 4-1. Estimates of Human Error Probabilities

Item #	Description	Nominal (Median) Probability	Error Factor	Expected (Mean) Probability	Source:
1	Failure to use written test or calibration procedure	0.05	5	8.1×10^{-2}	Swain and Guttman 1983 [DIRS 139383], Item 6 of Table 20-6
2	Error of commission in reading and recording quantitative information from unannounced digital readout (less than four digits)	0.001	3	1.25×10^{-3}	Swain and Guttman 1983 [DIRS 139383], Item 2 of Table 20-10
3	Error of commission in check-reading ^a analog meter with difficult-to-see limit marks, such as scribe lines	0.002	3	2.50×10^{-3}	Swain and Guttman 1983 [DIRS 139383], Item 3 of Table 20-11
4	Selection of wrong control on a panel from an array of similar-appearing controls identified by labels only	0.003	3	3.75×10^{-3}	Swain and Guttman 1983 [DIRS 139383], Item 2 of Table 20-12
5	Improperly mate a connector (this includes failures to seat connectors completely and failure to test locking features of connectors for engagement)	0.003	3	3.75×10^{-3}	Swain and Guttman 1983 [DIRS 139383], Item 13 of Table 20-12
6	Checker failure to detect error made by others during routine tasks	0.1	5	1.6×10^{-1}	Swain and Guttman 1983 [DIRS 139383], Item 1 of Table 20-22
7	Failure to complete change of state of a component if a switch must be held down until completion	0.003	3	3.75×10^{-3}	Swain and Guttman 1983 [DIRS 139383], Item 10 of Table 20-12
8	Checking routine tasks with alerting factors	0.05	5	8.1×10^{-2}	Swain and Guttman 1983 [DIRS 139383], Item 3 of Table 20-22
9	Failure of administrative control	1.9×10^{-4}	10	0.0005	Benhardt et al. 1994 [DIRS 157684], Table 4, Item 1 (routine, repetitive circumstances)
10	Failure to respond to a compelling signal	1.1×10^{-3}	10	0.003	Benhardt et al. 1994 [DIRS 157684], Table 4, Item 2 (few competing signals)

^a Check-reading means reference to a display merely to see if the indication is within allowable limits; no quantitative reading is taken.

The fact that the HEP values given in Table 4-1 correspond to nominal probabilities should be emphasized. No performance-shaping factors are used for this evaluation. In general, performance-shaping factors are utilized to alter the nominal HEP in order to account for the effects of factors such as equipment design, operator skills, and psychological and physiological stresses. Because the procedures and equipment that will be put into service to perform the fabrication and handling of the waste package outer corrosion barrier and the drip shield have not yet been precisely identified, use of performance shaping factors is inappropriate.

4.1.2 Alloy 22 Weld Flaw Characteristics

Sixteen weld rings of Alloy 22 (UNS N06022) were fabricated and examined using various nondestructive examination techniques, followed by a metallographic examination as discussed in *Weld Flaw Evaluation and Nondestructive Examination Process Comparison Results for*

High-Level Radioactive Waste Package Manufacturing Program (Smith 2003 [DIRS 163114]). Information gathered from these experiments has been used to develop a flaw density and size distribution applicable to the closure welds of the waste package. The parameters used are summarized in the following subsections.

4.1.2.1 Weld Ring Dimensions

Weld ring dimension inputs are summarized in Table 4-2 with visualization and reference points of the weld given in Figure 4-1. Dimensions are given in the units provided in the corresponding source of information.

Table 4-2. Weld Dimensions

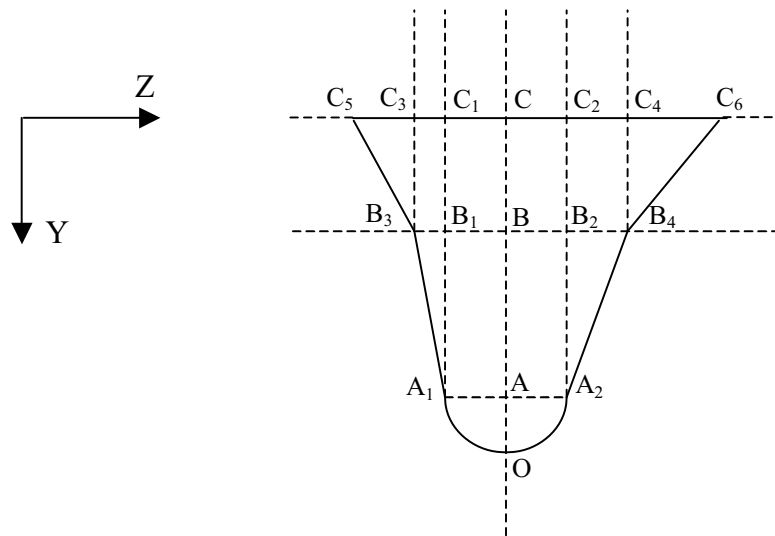
Parameter Description (see Figure 4-1)	Parameter Value ^a
Radius of the half-circle A_1OA_2	0.125 in
Distance OC	0.97 in
Distance BC	0.30 in
Angle $B_3A_1B_1$	3°
Angle $C_5B_3C_3$	25°
Angle $B_2A_2B_4$	6°
Angle $C_4B_4C_6$	29°
Diameter of the ring from centerline of the weld	60.765 in ^b

^a Values derived from dimensions given in Figures 1 and 2 of the drawing cited in the source listed below. Certain values may be derived, such as "OC," which is obtained from the specimen thickness minus remaining thickness from bottom of weld trench: 2.75 in - 1.780 in = 0.97 in.

^b Average value between inner diameter (60.785 in) and outer diameter (60.745 in) dimensions given in Figure 1 of the source given below. Same weld centerline determination as contained in Smith (2003 [DIRS 163114], Section 6.3).

Source: SNL 2007 [DIRS 179394], Section 4.1.2.3.

The parameters given above are appropriate for use in this analysis because the general form and size of the welds in the weld rings are the same as for the current design of the Alloy 22 closure welds of the waste package.



Source: Combination of Figures 1 and 2 from the drawing cited in SNL 2007 [DIRS 179394], Section 4.1.2.3.

Figure 4-1. Schematic Representation of the Cross Section of the Alloy 22 Weld

4.1.2.2 Parameters for Ultrasonic Inspection and Flaw Characteristics

Several nondestructive examination (NDE) techniques were used to detect weld flaws in the specimen rings. Surface examinations included liquid penetrant and eddy current inspections. Volumetric examinations included radiographic and ultrasonic testing. The surface indications, which consisted of nonwelding-related indications such as tooling marks, were irrelevant as discussed in the drawing cited in *Total System Performance Assessment Data Input Package for Requirements Analysis for TAD Canister and Related Waste Package Overpack Physical Attributes Basis for Performance Assessment* (SNL 2007 [DIRS 179394], Section 4.1.2.3) and are eliminated from further consideration in this analysis. For volumetric inspection, the radiographic testing was mainly used for a secondary check of the ultrasonic testing inspections. Therefore, only the volumetric indications of the ultrasonic testing are further considered.

Discussion in the “Study Summary” from the drawing cited in *Total System Performance Assessment Data Input Package for Requirements Analysis for TAD Canister and Related Waste Package Overpack Physical Attributes Basis for Performance Assessment* (SNL 2007 [DIRS 179394], Section 4.1.2.3) indicates that the nondestructive ultrasonic examination employed was comparable to radiographic examination; as the discussion states, both were “capable of detecting volumetric flaws as small as 1 millimeter in size.” This was confirmed by the metallographic inspections performed on the specimen rings: the weld imperfections discovered through this process were the same weld imperfections discovered during the ultrasonic testing and radiographic testing inspections. However, three flaws that were indicated by ultrasonic testing and/or radiographic testing were not located upon metallographic examination, as discussed in “Results of Metallographic Study” from the drawing cited in Section 4.1.2.3 of the abovementioned report.

Based on the information provided in the “Results of Metallographic Study” from the drawing cited in *Total System Performance Assessment Data Input Package for Requirements Analysis for TAD Canister and Related Waste Package Overpack Physical Attributes Basis for Performance Assessment* (SNL 2007 [DIRS 179394], Section 4.1.2.3), ultrasonic testing inspections revealed seven flaws that were confirmed by metallography. Two of the weld flaws listed in Table 1 from the drawing cited in that report as discovered during the ultrasonic testing and radiographic examination could not be verified by metallographic methods (Rings K2 and S1F) and therefore were not included in this evaluation. (A third flaw not confirmed by metallography was discovered in Ring S3F only by radiographic examination.) The weld flaw volumetric dimensions (here called the X, Y, and Z directions) as evaluated by the ultrasonic testing inspections are presented in Table 4-3. Metallographic examinations confirmed the ultrasonic testing dimensions or showed that ultrasonic testing slightly overestimated the actual flaw dimensions as discussed in “Volumetric Flaws” from the drawing cited in the report.

Table 4-3. Dimensions of the Ultrasonic Indications

Ultrasonic Testing Flaw No.	X-Direction, Length (in)	Y-Direction, Thickness (in)	Z-Direction, Width (in)
Ring K3	1/8 (0.125)	1/16 (0.0625)	1/16 (0.0625)
Ring K4	5/8 (0.625)	1/16 (0.0625)	1/16 (0.0625)
Ring R1F	3/4 (0.75)	1/8 (0.125)	1/16 (0.0625)
Ring R3F	1 3/8 (1.375)	1/8 (0.125)	1/16 (0.0625)
Ring R5F	3/8 (0.375)	1/8 (0.125)	1/16 (0.0625)
Ring W1F	1/2 (0.50)	3/16 (0.188)	1/8 (0.125)
Ring X1F	3/8 (0.375)	9/16 (0.563)	0

Source: Values calculated from dimensions given in Table 1 of the drawing cited in SNL 2007 [DIRS 179394], Section 4.1.2.3.

Based on Figure 3 from the drawing cited in *Total System Performance Assessment Data Input Package for Requirements Analysis for TAD Canister and Related Waste Package Overpack Physical Attributes Basis for Performance Assessment* (SNL 2007 [DIRS 179394], Section 4.1.2.3), the X direction gives the azimuthal location of the flaws in the direction of the weld (starting from some fixed point on the ring); the Y direction shows the position of the flaw in the through-wall extent of the weld; and the Z direction shows the radial position of the flaw in the weld. The Y and Z directions are shown in Figure 4-1. The X direction is shown in Figure 6-5, given in Section 6.3.1.5.

The flaws in Ring K are the result of a poor weld preparation, as discussed in “Weld Root Flaws Section” from the drawing cited in *Total System Performance Assessment Data Input Package for Requirements Analysis for TAD Canister and Related Waste Package Overpack Physical Attributes Basis for Performance Assessment* (SNL 2007 [DIRS 179394], Section 4.1.2.3), that was performed under conditions that are not representative of the highly controlled environment in which future manufacturing of the waste packages will take place. Nevertheless, following a conservative approach these flaws have been kept in this analysis. The other flaws reported in Table 4-3 are lack of fusion-type defects, as described in the “Weld Flaw Section” from the drawing cited in the abovementioned report.

Table 4-4 summarizes the direct input data for the weld-flaw analyses provided in Section 6.1.

Table 4-4. Weld Flaw Data

Parameter Description	Parameter Value	Source
Lower limit for ultrasonic testing of probability of nondetection (PND)	5×10^{-3}	Bush 1983 [DIRS 107696], p. 13A.5.7
Geometry of specimen welds examined during testing	Various dimensions	SNL 2007 [DIRS 179394], Figures 1 and 2, Section 4.1.2.3
Number of flaws found and confirmed from ultrasonic testing	7	SNL 2007 [DIRS 179394], Section "Results of Metallographic Study," Section 4.1.2.3
Detection limit for weld flaws	$\geq 1/16$ th of an inch	SNL 2007 [DIRS 179394], Section 4.1.2.3
Volumetric information on ultrasonic testing of flaws	Length, thickness, and width of flaws	SNL 2007 [DIRS 179394], Table 1, Section 4.1.2.3

The parameters given previously are appropriate for use in this analysis because they yield characteristics of flaws of Alloy 22 welds, whose design conforms to that of the closure weld of the waste package.

4.1.3 Miscellaneous Inputs

Table 4-5 summarizes the miscellaneous input data for evaluating the various scenarios leading to defects that have potential for becoming early failure mechanisms for waste packages and drip shields. All of the input data identified in Table 4-5 are from appropriate sources that are qualified for their use in Section 4.1.4.

Table 4-5. Input to Early Failure Mechanisms for Waste Package Outer Corrosion Barrier and Drip Shield

Description	Value	Source
Probability of selecting improper material	65 to 350 lbs of wire out of 1,706,556 lbs	Babcock & Wilcox 1979 [DIRS 108219], pp. 2, I-4, I-6; Part II, Table 1
Probability of inducing defects through handling	4.8×10^{-5} per fuel assembly moved	BSC 2001 [DIRS 157560], Table 5
Drip shield weld filler material	Titanium Grades 7, 28, and 29	SNL 2007 [DIRS 179354], Table 4-2, Item 07-12
Drip shield material	Titanium Grades 7 and 29	SNL 2007 [DIRS 179354], Table 4-2, Items 07-04 and 07-04A
Drip shield heat treatment	No maximum time requirement for stress-relief heat treatment, 1,100°F \pm 50°F for two hours with air cooling	SNL 2007 [DIRS 179354], Table 4-2, Item 07-13
Drip shield emplacement	Requirement for interlock and inspections	SNL 2007 [DIRS 179354], Table 4-2, Items 07-02 and 07-02B
Waste package outer corrosion barrier heat treatment	Requirements for heat treatment process; temperature (2,050°F \pm 50°F), duration (minimum of 20 min), and quenching (>275°F/min)	SNL 2007 [DIRS 179394], Table 4-1, Item 03-20

Table 4-5. Input to Early Failure Mechanisms for Waste Package Outer Corrosion Barrier and Drip Shield (Continued)

Description	Value	Source
Stress relief of closure welds on waste package outer corrosion barrier lid	Requirements for use of low-plasticity burnishing as stress-relief method	SNL 2007 [DIRS 179394], Table 4-1, Item 03-21
Waste package outer corrosion barrier handling and inspections	Requirements for inspections for surface defects during handling and prior to emplacement	SNL 2007 [DIRS 179394], Table 4-1, Items 03-26, 03-27, and 03-28
Alarm failure for duration heat treatment of waste package outer corrosion barrier	3×10^{-5} per hour Error factor of 10	Blanton and Eide 1993 [DIRS 141700], Table 6f
Failure of makeup water system represented by failure of motor-operated valve to open	Failure rate = 3×10^{-3} Error factor of 5	Blanton and Eide 1993 [DIRS 141700], Table 6a
Pressure failure	Mean value = 1×10^{-6} per hour Error factor of 3	Blanton and Eide 1993 [DIRS 141700], Table 6f
Probability distribution for HEPs	Lognormal	Swain and Guttman 1983 [DIRS 139383], pp. 2-18 and 2-19
Upper and lower bounds for probability distributions	5% to 95%	Swain and Guttman 1983 [DIRS 139383], p. 2-19

4.1.4 Qualification of External Source Data

Estimates of HEPs from unqualified external sources were used in this analysis to evaluate operational events. These probability estimates are “data” per SCI-PRO-004. The basis for using this information is that such data are recommended for use by *PRA Procedures Guide, A Guide to the Performance of Probabilistic Risk Assessments for Nuclear Power Plants* (NRC 1983 [DIRS 106591], Sections 4.1 and 4.5.7) and/or are used in evaluations of the probability of occurrence of human errors in the conduct of probabilistic risk assessments for nuclear power plants. This section presents planning and documentation for the data qualification of the unqualified external source data used as direct input only for the intended use in this analysis. Data qualification is performed in accordance with SCI-PRO-005.

4.1.4.1 Data for Qualification

There are five external sources of data used as direct input for this analysis:

1. Data for the probability for humans failing to respond to administrative and engineered controls from Benhardt et al. (1994 [DIRS 157684]) identified in Section 4.1.1 and Table 4-1 of this report
2. Data for the probability for failure of engineered controls from Blanton and Eide (1993 [DIRS 141700]) identified in Section 4.1.3 and Table 4-5 of this report
3. Weld-flaw data revealed through ultrasonic testing from Bush (1983 [DIRS 107696]) identified in Table 4-4 of this report

4. Probability of system failures related to human error, Swain and Guttman (1983 [DIRS 139383]) identified in Table 4-1 and Table 4-5 and discussed in Section 4.1.1 of this report
5. Probability of failures related to selection of improper welding wire from Babcock & Wilcox (1979 [DIRS 108219]) identified in Table 4-5 of this report.

4.1.4.2 Method of Qualification Selected

The method for qualification of all five external sources of data is the “technical assessment method.” The rationale for using this method is that all three of the qualification approaches for technical assessment (SCI-PRO-001, *Qualification of Unqualified Data*, Attachment 3) of external source data are appropriate for consideration. Other qualification methods are not considered because they require information not available through the original source (i.e., scientific journal or publication). Qualification process attributes used in the technical assessment of each external source are selected from the list provided in Attachment 4 of SCI-PRO-001. Attributes used specifically as data qualification attributes in this report are:

1. Qualifications of personnel or organizations generating the data are comparable to qualification requirements of personnel generating similar data under an approved program that supports the Yucca Mountain Project (YMP) license application process or postclosure science
2. The extent to which the data demonstrate the properties of interest (e.g., physical, chemical, geologic, mechanical)
3. Prior uses of the data and associated verification processes
4. Prior peer or other professional reviews of the data and their results
5. Extent and reliability of the documentation associated with the data.

4.1.4.3 Technical Assessment of External Data from Benhardt et al.

The following criteria were used to assess the external data from *Savannah River Site Human Error Data Base Development for Nonreactor Nuclear Facilities (U)* (Benhardt et al. 1994 [DIRS 157684]):

1. Data must be sufficiently extensive to cover the context of this application
2. Data must be demonstrated to be reliable as judged by the experience of the originators and reputation of the originating organization
3. Data must have received an appropriate review.

As the title suggests, this document presents methodologies for safety analyses of nonreactor nuclear facilities. It was developed to meet the needs of risk analysts preparing safety analyses reports and gives probabilities for a variety of human errors associated with nonreactor nuclear facilities, which are applicable to the activities that will be occurring at the YMP during waste

receipt, handling, and emplacement operations. Methods used to generate data were thoroughly described and documented in the report prepared by the Westinghouse Savannah River Company for the Savannah River Site, a U.S. Department of Energy (DOE) defense laboratory and industrial complex. The authors, H. C. Benhardt and S. A. Eide, have published extensively on the topic of human errors and risk analysis in nonreactor environments in publications sponsored by the DOE or the U.S. Nuclear Regulatory Commission (NRC).

As discussed in Section 4 of the report by Benhardt et al. (1994 [DIRS 157684]), the document underwent an external independent technical review and an internal peer review. The independent review focused on reasonableness of the assumptions, consistency of the models, and accuracy of the calculations. The internal review focused on the representativeness of human errors to be quantified, the selection of appropriate search criteria for human error events, and the validity of the model used.

Based on the assessment made above, data from Benhardt et al. (1994 [DIRS 157684]) are qualified for use as direct input for this analysis.

4.1.4.4 Technical Assessment of External Data from Blanton and Eide

The following criteria were used to assess the external data from *Savannah River Site, Generic Data Base Development (U)* (Blanton and Eide 1993 [DIRS 141700]):

1. Qualifications of personnel generating the data must be comparable to the qualification requirements of personnel generating similar data under an approved program that supports YMP postclosure science
2. Data must have been used for other similar investigations requiring verification processes.

This document presents a generic component-failure database for safety analyses of nuclear facilities. It combined data from the Savannah River Site, as well as the *Nuclear Computerized Library for Assessing Reactor Reliability (NUCLARR)* (Gertman et al. 1989 [DIRS 157687]) and failure data from the Idaho Chemical Processing Plant. The document was developed to meet the needs of risk analysts preparing safety analysis reports and provides probability data for a variety of components associated with nuclear and nuclear-related facilities, each requiring a stringent data verification process.

The report was prepared by the Westinghouse Savannah River Company for the Savannah River Site, a DOE defense laboratory and industrial complex. One of the authors, S. A. Eide, has published extensively on the topic of risk analysis related to component failure and human error in nuclear-related environments in publications sponsored by the DOE or the NRC.

Based on the assessment made above, data from Blanton and Eide (1993 [DIRS 141700]) are qualified for use as direct input for this analysis.

4.1.4.5 Technical Assessment of External Data from Bush

The following criterion was used to assess the external data from *Reliability of Nondestructive Examination* (Bush 1983 [DIRS 107696]):

Data must have been used for other investigations requiring verification processes.

This report was developed for the NRC program, “Integration of NDE Reliability and Fracture Mechanics.” The objectives of the NRC program included 1) improving examination procedures for incorporation into the American Society for Mechanical Engineers (ASME), Boiler and Pressure Vessel Codes, Section III, V, XI; and 2) gaining a better insight into the influence of improved reliability of NDE in detecting, locating, and sizing flaws on component failure probabilities (NUREG/CR-3110, Volume 3 (Bush 1983 [DIRS 107696], Abstract)). Because the data were used to support development of ASME procedures for improved NDE methods, they underwent a thorough verification process.

Based on the assessment made above, data from Bush (1983 [DIRS 107696]) are qualified for use as direct input for this analysis.

4.1.4.6 Technical Assessment of External Data from Swain and Guttman

The following criteria were used to assess the external data from *Handbook of Human Reliability Analysis with Emphasis on Nuclear Power Plant Applications Final Report* (Swain and Guttman 1983 [DIRS 139383]):

1. Qualifications of personnel generating the data must be comparable to the qualification requirements of personnel generating similar data under an approved program that supports YMP post closure science
2. Data must appropriately demonstrate properties of interest.

This handbook presents methods, models, and estimated human error probabilities to enable analysts to make quantitative or qualitative assessments of occurrences of human errors that may affect the availability or operational reliability of engineered safety features and components in nuclear power plants as a part of probabilistic risk assessments. It was prepared by Sandia National Laboratories in collaboration with the NRC and is applicable for estimating human errors associated with nuclear facilities and relevant to activities that will occur at the YMP during waste receipt, handling, and emplacement operations.

The authors have published extensively on the topic of risk analysis related to human errors in nuclear-related environments in publications sponsored by the DOE or the NRC.

Based on the assessment made above, data from Swain and Guttman (1983 [DIRS 139383]) are qualified for use as direct input for this analysis.

4.1.4.7 Technical Assessment of External Data from Babcock & Wilcox

The following criteria were used to assess the external data from *Records Investigation Report Related to Off-Chemistry Welds in Material Surveillance Specimens and Response to IE Bulletins 78-12 and 78-12A – Supplement* (Babcock & Wilcox 1979 [DIRS 108219]):

1. Qualifications of personnel generating the data must be comparable to the qualification requirements of personnel generating similar data under an approved program that supports YMP post closure science
2. Data must appropriately demonstrate properties of interest.

This report was made in response to the NRC staff who requested a generic investigation to assess the potential for off-chemistry conditions in a reactor vessel after the discovery of such a condition at the Crystal River 3 nuclear power plant. The investigation sought to quantify the extent of condition for similar occurrences—that is, the wrong weld material being used to weld reactor pressure vessels. The NRC request was issued in *Atypical Weld Material in Reactor Pressure Vessel Welds* (NRC 1978 [DIRS 165403]), dated September 26, 1978. This paper is applicable to the YMP in two ways relating to the fabrication of waste packages and drip shields: (1) it has a direct analog to welding that will occur on waste packages and drip shields and can be used to estimate the probability of using incorrect weld material, and (2) it is analogous to receiving and using an improper material (such as base metal that is either the incorrect alloy or has manufacturing defects) that is not detected through the manufacturing inspection processes.

Babcock & Wilcox is a leading supplier to the nuclear power industry and has provided service and equipment to the energy industry for more than 100 years.

Based on the assessment made above, data from Babcock & Wilcox (1979 [DIRS 108219]) are qualified for use as direct input for this analysis.

4.2 YUCCA MOUNTAIN REVIEW PLAN CRITERIA

Because this report serves, in part, as the basis for the repository license application, the information contained herein must conform to applicable acceptance criteria. The *Yucca Mountain Review Plan, Final Report* (NRC 2003 [DIRS 163274]) contains acceptance criteria intended to establish the basis for the review of the material contained in the license application and, in particular, material applicable to the barrier system. This analysis addresses the degradation of two features of the Engineered Barrier System—the waste package outer corrosion barrier and the drip shield. Thus, based on the processes involved with the degradation of the waste package outer corrosion barrier and drip shield and the potential impact of such degradation, the acceptance criteria that are applicable to this analysis are listed below.

YMRP Section 2.2.1.1—System Description and Demonstration of Multiple Barriers – Subsection 2.2.1.1.3 Acceptance Criteria

Acceptance Criterion 1—Identification of Barriers Is Adequate.

Barriers relied upon to achieve compliance with 10 CFR 63.113(b), as demonstrated in the total system performance assessment, are adequately identified and clearly linked to their capability.

Acceptance Criterion 2—Description of Barrier Capability Is Acceptable.

The capability of the identified barriers to prevent or substantially reduce the movement of water or radionuclides from the Yucca Mountain repository to the accessible environment or prevent the release or substantially reduce the release rate of radionuclides from the waste is adequately identified and described:

(1) The information on the time period over which each barrier performs its intended function, including any changes during the compliance period, is provided;

(2) The uncertainty associated with barrier capabilities is adequately described;

(3) The described capabilities are consistent with the results from the total system performance assessment;

(4) The described capabilities are consistent with the definition of a barrier at 10 CFR 63.2.

Acceptance Criterion 3—Technical Basis for Barrier Capability Is Adequately Presented.

The technical bases are consistent with the technical basis for the performance assessment. The technical basis for assertions of barrier capability is commensurate with the importance of each barrier's capability and the associated uncertainties.

YMRP Section 2.2.1.3.1—Degradation of Engineered Barriers (Model Abstraction) – Subsection 2.2.1.3.1.3 Acceptance Criteria

Acceptance Criterion 3—Data Uncertainty Is Characterized and Propagated Through the Model Abstraction.

(4) The US DOE uses appropriate methods for nondestructive examination of fabricated engineered barriers to assess the type, size, and location of fabrication defects that might lead to premature failure as a result of rapidly initiated engineered barriers degradation. The US DOE specifies and justifies the allowable distribution of fabrication defects in the engineered barriers and assesses the effects that cannot be detected on the performance of the engineered barriers.

4.3 CODES, STANDARDS, AND REGULATIONS

No codes, standards, or regulations were referenced in this analysis.

INTENTIONALLY LEFT BLANK

5. ASSUMPTIONS

5.1 CLOSURE WELD-FLAW SCREENING SIZE

It is assumed that a minimum required size for the detection and screening of closure weld flaws will be 1/16 in (1.5875 mm).

The rationale for selecting 1/16 in as the minimum size for the weld flaw detection and screening limit is that standards for the calibration of ultrasonic testing equipment for detecting a flaw size of 1/16 in are readily available. For example, the calibration block used for the ultrasonic testing examination of the Alloy 22 weld-flaw evaluation contained a reference flaw of 1.0 mm (Smith 2003 [DIRS 163114], Section 3.1). In addition, design requirements specify detection and repair of weld flaws at 1/16th of an inch or greater (SNL 2007 [DIRS 179394], Table 4-1, Item 03-19). Thus, for flaw sizes of 1/16 in and above, the fabrication process equipment is capable of locating closure weld flaws, permitting the operator to either repair the weld section or make a screening determination that it will not adversely affect the postclosure performance of the welded item. The probability of nondetection (PND) of weld flaws (Equation 17) represents that only half of the flaws of this size will actually be detected although actual detection limits are lower, per use of a 1.0-mm reference flaw for tests. Thus, a minimum size of 1/16 in for detection and screening of flaws is conservative since the evaluation of the PND with a parameter of this size overestimates the number of undetected closure weld flaws for postclosure analysis purposes (Section 6.3.1.6).

This assumption, which is used in Sections 6.3.1.6 and 6.3.1.7, is conservative, as stated, and does not require confirmation.

5.2 PROBABILITY DISTRIBUTION FOR IMPROPER MATERIAL SELECTION

It is assumed that the probability distribution for improper selection of fabrication materials can be represented by a lognormal distribution.

The rationale for this assumption is the similarity between the operations of selecting materials for fabrication and the selection of weld filler material. This type of error can be represented by HEPs (Swain and Guttman 1983 [DIRS 139383], p. 2-17), which are represented by lognormal distributions (Swain and Guttman 1983 [DIRS 139383], Section 7). For such distributions, Swain and Guttman (1983 [DIRS 139383], p. 2-19) recommend choosing the 5th and the 95th percentiles of a lognormal distribution when evaluating lower and upper bounds for HEP uncertainty that is characterized as an error factor.

This assumption, which is used in Section 6.3.2, does not require confirmation.

5.3 UNCERTAINTY DISTRIBUTIONS FOR PROBABILITY VALUES

It is assumed that probabilities given as point values represent the mean value of probability distributions and that the uncertainty values for the distributions can be represented by lognormal distributions with a range delimited by an error factor between 3 and 15.

The rationale for this assumption is that there is uncertainty associated with any probability value, whether explicitly specified or not, and the lognormal distribution is one possible representation for distributions that cannot be negative. In addition, assigning a lognormal attribute to nonspecified uncertainty distributions makes them consistent with HEPs, which are represented by lognormal distributions (Swain and Guttman 1983 [DIRS 139383], pp. 2-18 and 2-19).

The specification of an error factor range between 3 and 15 is a reasonable value that is consistent with the range of HEPs. This spread in error factor values allows the uncertainty distribution for the associated probability a range that is on the order of 10 to 100 (Equation 2).

This assumption is used in Sections 5.7, 6.3.3, 6.3.4, 6.3.5, and 6.4.2 and does not require confirmation.

5.4 CRITICAL PHASE OF THE WASTE PACKAGE OUTER CORROSION BARRIER HEAT TREATMENT

It is assumed that the critical portion of the heat treatment process for the waste package outer corrosion barrier is the final phase of the operation that is the time-sensitive solution annealing of the outer corrosion barrier.

The rationale for this assumption is that strict time constraints are imposed on the solution-annealing phase of the waste package outer corrosion barrier heat treatment to prevent the development of undesirable phases in the outer corrosion barrier material during cool-down (SNL 2007 [DIRS 179394], Table 4-1, Item 03-20). The purpose of the heat treatment is to produce a uniform phase in the outer corrosion barrier material and then avoid an undesirable phase transition during cooling (SNL 2007 [DIRS 179394], Section 4.1.2.2). In addition, the heat treatment will be applied to the outer corrosion barrier as a complete unit with the exception of the closure lid. The overall outer corrosion barrier fabrication is to be performed in a controlled manner (SNL 2007 [DIRS 179394], Table 4-1, Item 03-16). Performance constraints on the operation prior to the solution-annealing phase are less stringent than those pertaining to the solution-annealing phase, permitting potential process faults or failures to be more readily identified and corrected, minimizing the likelihood of nondetection of such events.

This assumption is used in Sections 6.3.3 and 6.3.4 and does not require confirmation since additional phases of the operation can be modeled, if identified as important as a mechanism contributing to early failures.

5.5 MONITORS FOR WASTE PACKAGE OUTER CORROSION BARRIER FABRICATION PROCESSES

It is assumed that the fabrication processes for the waste package outer corrosion barrier will be monitored with appropriate systems (e.g., timers, thermocouples) equipped with recording capability and alarms that serve as surrogates for operational monitoring processes.

The rationale for this assumption is that, firstly, recording capability is a normal part of operations performed under quality assurance procedures to provide the necessary documentation records. This capability applies to all fabrication processes. Secondly, in the

event of process malfunctions or failures, it is anticipated that operational monitoring systems will be available to alert the operator to take remedial action. For example, strict time constraints are placed on certain phases of the fabrication process, e.g., the solution annealing phase of the waste package outer corrosion barrier heat treatment, to prevent the development of undesirable phases in the outer corrosion barrier material during cool-down (SNL 2007 [DIRS 179394], Table 4-1, Item 03-20). Imposing limits on the minimum outer corrosion barrier temperature allowable to begin the quench process implies that the outer corrosion barrier must be transferred to the quench facility within a prescribed time period. Exceeding the prescribed transfer period could result in an inadequate heat treatment process. A monitoring system would alert the operator to take remedial action, minimizing the likelihood that a process malfunction is undetected. For this analysis, some type of alarm system serves as a surrogate for such a monitoring system.

This assumption, which is used in Sections 6.3.3 and 6.3.5, requires confirmation that will be accomplished when the fabrication procedures are finalized.

5.6 QUENCHING OF WASTE PACKAGE OUTER CORROSION BARRIER

It is assumed that the waste package outer corrosion barrier quench operation will be performed with the outer corrosion barrier in an inverted axial position.

The rationale for this assumption is that an inverted position with the open end down provides the best arrangement for maintaining a relatively uniform through-wall metal temperature distribution during the rapid cool-down (SNL 2007 [DIRS 179394], Table 4-1, Item 03-20) since both inside and outside surfaces are quenched simultaneously. This arrangement is amenable to pool and/or spray quenching methods. Performing the quenching process with the outer corrosion barrier inverted also prevents any excess water from accumulating in the outer corrosion barrier.

This assumption is used in Section 6.3.3 and requires confirmation that it will be accomplished when the fabrication procedures are finalized.

5.7 PROBABILITY FOR MECHANICAL MALFUNCTIONING OF LIFTING AND MOVING EQUIPMENT

It is assumed that a value of 3×10^{-3} per event is an upper bound for the median probability of having a mechanical malfunction of moving equipment such as cranes and trolleys.

The rationale for this bounding assumption is that equipment malfunctions that could cause a failure of the heat treatment processes are much less severe but more likely than major failures for equipment. Data for major equipment failures (e.g., load drops) that cause damage to the objects being handled were used to develop the probability of damage to fuel assemblies due to equipment failure. This probability was estimated as 1.9×10^{-5} per event (BSC 2001 [DIRS 157560], Table 4). The probability of heavy load drops at reactor power facilities has been estimated as approximately 5.6×10^{-5} per event (Lloyd 2003 [DIRS 174757], Section 3.7.1). The equipment malfunctions that could cause a failure of the heat-treatment processes are much less severe but more likely. These malfunctions could be caused by such

events as degradation of the supply power or cable entanglement, which slow but do not halt the operation. However, these types of malfunction could cause the transfer operation to exceed the time specified for the operation. Thus, a mechanical malfunctioning probability that was more than two orders of magnitude above the probability for damage due to major failure of equipment was selected for these less severe events. The cause of a significant number of crane failures (not necessarily heavy load drops) was identified as a failure to follow or properly implement procedures. The probability for this type of failures was estimated as 3×10^{-3} per event (Lloyd 2003 [DIRS 174757], Section 3.7.1), which is consistent with this assumption. Assigning an error factor of 3 to this median probability value (Assumption 5.3) results in a mean value of 3.75×10^{-3} per event (Equation 4).

This assumption is conservatively two orders of magnitude above the major failure likelihood and does not require confirmation. This assumption was used in Sections 6.3.3 and 6.3.4.

5.8 FLUID MAKEUP SYSTEM FOR THE HEAT-TREATMENT QUENCHING PROCESS

It is assumed that a recirculation or makeup system will be used to maintain an adequate water supply for quenching the waste package outer corrosion barrier in order to maintain the minimum required cooling rate for all surfaces of the waste package outer corrosion barrier.

The rationale for this assumption is that a high volume of quench water must be applied to all waste package outer corrosion barrier surfaces to provide a rapid, even cooling of the outer corrosion barrier. This can be accomplished with either a tank immersion requiring a snorkel to vent trapped gases or a powered spray system. In either case, a recirculation or makeup pumping system will be needed to assure that adequate quench water is available.

This assumption was used in Section 6.3.4 and requires confirmation that it will be accomplished when the fabrication procedures are finalized.

5.9 INDEPENDENT CHECKS OF MECHANICAL AND OPERATIONAL PROCESSES ASSOCIATED WITH WASTE PACKAGES AND DRIP SHIELDS

It is assumed that independent checks will be made on the mechanical and operational processes associated with fabrication, handling, and emplacement of waste packages and drip shields with documentation logs maintained.

The rationale for this assumption is that any repository operation including component fabrication is under strict QA control requirements derived from 10 CFR Part 63 ([DIRS 180319], Subpart 142) (BSC 2005 [DIRS 175539], Section 2). Independent checking and documentation is an important aspect of such QA requirements for traceability and verification.

This assumption was used in Sections 6.3.2 and 6.4.4 and does not require confirmation, as such checks are normal procedures.

5.10 AUTOMATED SYSTEMS USED FOR FABRICATION PROCESSES ASSOCIATED WITH WASTE PACKAGES AND DRIP SHIELDS

It is assumed that fabrication of waste packages and drip shields will be performed in facilities using equipment operated with self-contained control systems (i.e., generalized systems independent of objects being fabricated).

The rationale for this assumption is that manufacturing activities for waste packages and drip shields are to be performed in accordance with a QA or quality control program (SNL 2007 [DIRS 179394], Table 4-1, Item 03-16). Industrial equipment with self-contained control systems for handling such objects under strict quality assurance requirements are commonly available and routinely used.

This assumption was used in Sections 6.3.3, 6.3.4, and 6.4.2 and does not require confirmation.

INTENTIONALLY LEFT BLANK

6. DISCUSSION OF EARLY FAILURE PROBABILITY CALCULATIONS

6.1 REVIEW OF DEFECT-RELATED FAILURES OF CONTAINERS IN VARIOUS INDUSTRIES

This section presents the results of a literature review performed to determine rates of manufacturing defect-related failure for various types of containers. In addition to providing examples of the rates at which defective containers occur, this information provides insight into the various types of defects that can occur and the mechanisms that cause defects to propagate to failure.

6.1.1 Boilers and Pressure Vessels

Waste packages are similar to pressure vessels in the sense that they are welded, metallic components of similar thickness that are typically fabricated in accordance with accepted standards and inspected prior to entering service. In addition, there are several sources of statistics on the numbers and types of failures that have occurred in large populations.

One study (Doubt 1984 [DIRS 100441], p. 7) examined data on 229 failures of pressure vessels constructed to Class I requirements of design codes recognized in the United Kingdom. The failures had occurred in a population of 20,000 vessels (Smith and Warwick 1978 [DIRS 107783]). The vessels were all welded or forged unfired pressure vessels with wall thicknesses greater than 9.5 mm and working pressures in excess of 725 kPa. The vessels included in the study were less than 40 years old as of 1976 (Smith and Warwick 1978 [DIRS 107783], p. 22). Doubt (1984 [DIRS 100441], p. 7) identified 17 instances of external leakage or in-service rupture that were caused by preexisting defects in weld or base metal or by incorrect material. Failures that were due to thermal or mechanical fatigue, corrosion, internal leaks, and part-through cracks found by visual examination or NDE were excluded. This yielded an estimated failure rate due to manufacturing defects of 8.5×10^{-4} per vessel.

Further examination of the data (Smith and Warwick 1978 [DIRS 107783], pp. 37 to 52) indicated that four of the failures were attributed to use of incorrect material in the weld, one to improper heat treatment, one to improper joint design, and the rest to weld flaws. In all cases involving weld flaws, the vessels were in service for several years prior to failure, which suggests that fatigue also contributed to the propagation of the flaws through the walls of the vessels. In some cases, failures that were attributed to fatigue, and thus not included in the evaluation of the previous failure rate, involved propagation of preexisting defects. Overall, approximately 29% of the failures appear to have involved a preexisting defect of some kind. The original source of the failure data (Smith and Warwick 1978 [DIRS 107783], p. 24) indicates that many of the defects occurred in areas where it was not the practice at the time of construction, even with Class I Standard vessels, for NDE to be performed. Because waste packages are not subject to cyclic stresses (which is necessary for fatigue) and will be nondestructively examined, application of the historical failure data for pressure vessels to estimate an early failure rate for waste packages would be inappropriate and extremely conservative.

Another source of information on failures is available from the National Board of Boiler and Pressure Vessel Inspectors (NBBPVI) (1999 [DIRS 107765]). The NBBPVI maintain records on all boilers and pressure vessels that carry a National Board-registered stamping. For the period of 1919 through 1997, a total of 27,618,733 registrations were filed (NBBPVI 1999 [DIRS 107765]). For the period of 1992 to 1997, incident reports indicate the number of failures that occurred as a result of various causes. For the category of "Faulty Design or Fabrication," the average incident rate is 83 per year. Assuming that this rate is constant over the 79 years in which vessels were registered, a point estimate probability of 2.4×10^{-4} per vessel for failure due to fabrication or design defects can be calculated. The NBBPVI report does not contain information on the cause of failure, and thus, its utility for this analysis is limited.

Data from the previous sources and from similar databases in Germany have been used in various studies to calculate the annual probability of vessel failure for use in risk assessments. The expected value for disruptive failure rates ranges from 2×10^{-6} to 4×10^{-5} per vessel-year, and the upper limit of the 99% confidence interval ranges from 5×10^{-6} to 8×10^{-5} per vessel-year (Tschoepe et al. 1994 [DIRS 107789], pp. 2-9 to 2-11). In general, these rates were not based on actual failures that had occurred but on reports of the size of the weld defects observed during inspection and the perceived consequences had the vessel been returned to service without repair of the defect. Because these rates involve significant interpretation as to the effect of weld flaws on component life under specific operating conditions, they cannot be directly used to determine the early failure rate of a waste package.

Finally, two instances were also found in the literature where cracking of stainless steel cladding on the interior surface of reactor coolant system components occurred as a result of defects that occurred during fabrication or transport. In one case, during a visual examination following a hot functional test that was conducted in March 1975, Indian Point 3 personnel noted rust-colored deposits in the primary-water boxes of all four steam generators (S.M. Stoller and Company 1976 [DIRS 107766], p. 44). A detailed chemical and metallurgical analysis of cladding samples was performed, and three distinct types of cracking were identified: (1) longitudinal interbead cracks in the upper parts of the heads that propagated along grain boundaries, (2) transverse cracks adjacent to repair welds, and (3) extensive cracking in the lower half of the heads. Studies of the cladding samples identified stress corrosion and dilution of the clad deposit with base metal as possible causes for the imperfections. The supposition of stress corrosion was supported by the fact that the channel heads were accidentally exposed to seawater during shipment.

In a second instance, microfissures were found in the cladding of two straight and two elbow sections of reactor coolant system piping during construction of Oconee 1 (Babcock & Wilcox 1970 [DIRS 107504], 1970 [DIRS 107509]). The fissures were found during a routine dye-penetrant exam while they were being reworked to accommodate the installation of new Westinghouse reactor coolant pumps. They would likely not have been found before operation if the original Bingham pumps had been re-installed. The cracks in the straight sections were caused by use of an improperly manufactured batch of flux in welding these sections. The cracking that occurred on the two elbow sections was attributed to the improper use of acidic cleaning agents. The Indian Point 3 and Oconee 1 cases were the only examples of contamination-related failures found in the nuclear-industry literature, and no efforts to determine their frequency of occurrence have been made.

While this review has provided general information on the reliability of large, welded, pressure-retaining components, the failure rate data cannot be directly applied to waste packages due to significant differences in operational conditions and degree of inspection performed prior to service. However, this review has identified several types of manufacturing defects that may be applicable to waste packages:

- Weld flaws
- Base metal flaws
- Use of improper material in welds
- Improper heat treatment of welded or cold-worked areas
- Improper weld flux material
- Poor joint design
- Contaminants.

The applicability of these types of defects to waste packages and their potential consequences to postclosure performance are discussed in Section 6.2.

6.1.2 Nuclear Fuel Rods

Nuclear fuel rods are conceptually similar to waste packages in the sense that they are manufactured in large numbers, are subjected to rigorous quality controls and inspections, and have radionuclide containment as one of their primary functions. As such, it is useful to review the reliability of these components and the rate at which manufacturing-induced defects occur. However, they are also simple, single-barrier components with a very small wall thickness compared to waste packages and are subjected to significantly different operating conditions over a much shorter period of operation. Thus, the failure rate information presented here cannot be directly used to estimate a waste package early failure rate.

Because a significant amount of scrutiny by utilities, vendors, and the NRC follows any report of failure in nuclear fuel, there is a large database on the number and causes of fuel-rod failures. The fuel-rod failure rate for both pressurized water reactor (PWR) and boiling water reactor (BWR) fuel through 1985 ranged from 2×10^{-4} to 7×10^{-4} per rod (EPRI 1997 [DIRS 100444], p. 4-1). As a result of vendor efforts to develop improved fuel designs to address some of the causes of failure, the current range of failure rates is from 6×10^{-5} to 3×10^{-4} per rod (EPRI 1997 [DIRS 100444], p. 4-2). The failures of fuel rods have been caused by a variety of mechanisms (Yang 1997 [DIRS 102049], p. 10; Framatome Cogema Fuels 1996 [DIRS 107754], pp. 4-2 to 4-7), among which two are applicable to waste packages. These are handling damage and manufacturing defects. Handling damage represents a small number of the fuel failures. It can occur during fabrication if loaded fuel rods are subjected to excessive flexing that causes defects, which lead to in-core failure or as a result of drops or other handling accidents that could occur at the utility. During the period from 1989 through 1995, there were 10 handling-damage failures in a population of 21,810 PWR discharged assemblies (Yang 1997 [DIRS 102049], p. 10), yielding a rate of 4.6×10^{-4} per discharged assembly. In each case, only a few rods in each assembly were actually damaged.

Manufacturing defects also represent a small fraction of fuel failures. Types of manufacturing defects associated with the cladding include contamination by solvents, oils, or filings; flawed or missing seal welds; flawed, missing, or mislocated endcap welds; base metal flaws (stringers, inclusions); and out-of-specification weld material (Framatome Cogema Fuels 1996 [DIRS 107754], Section 5). General Electric reports only 47 manufacturing defect-related failures in 4,734,412 rods fabricated between 1974 and 1993 (Potts and Proebstle 1994 [DIRS 107774], p. 92), which yields a rate of 9.9×10^{-6} per rod. As of October 1990, Advanced Nuclear Fuels had experienced seven BWR fuel rod failures and nine PWR fuel rod failures related to manufacturing defects out of 570,200 BWR fuel rods and 1,391,740 PWR fuel rods placed into service (Tschoepe et al. 1994 [DIRS 107789], p. 2-4). The resulting rates are 1.2×10^{-5} , 6.5×10^{-6} , and 8.2×10^{-6} for BWRs, PWRs, and combined failures, respectively. In addition to the previously mentioned defects, one occurrence of a rod that failed in service due to a missing seal weld was reported in *Fuel Integrity* (Framatome Cogema Fuels 1996 [DIRS 107754], p. 5-1). The rod had not passed the inspection process but had been inadvertently left with the accepted rods. Because this was an isolated event, it can be expected that the corresponding occurrence rate would be much lower than the reported global failure rate, excluding debris and fretting, of $1/200,000 = 5 \times 10^{-6}$ per rod (Framatome Cogema Fuels 1996 [DIRS 107754], p. 3-1).

While this review has provided general information on the reliability of fuel rods, the failure rate data cannot be directly applied to waste packages due to significant differences in construction and operational conditions. However, general types of manufacturing defects were identified in the review that may be applicable to waste packages:

- Weld flaws
- Base metal flaws
- Mislocated welds
- Contamination
- Missing welds
- Improper weld material
- Handling damage.

The applicability of these types of defects to waste packages and their potential consequences to postclosure performance are discussed in Section 6.2.

6.1.3 Underground Storage Tanks

A substantial amount of information is available on causes of early failure for underground storage-tank systems. The most extensive data source, which was compiled by the U.S. Environmental Protection Agency, provides data on a large population of bare-steel, clad- or coated-steel, and fiberglass-reinforced-plastic tank systems through 1987 (EPA 1987 [DIRS 107749], 1987 [DIRS 107751]). While overfilling and leakage of attached piping are dominant contributors to leakage from underground storage tank systems, failure of the tank itself is also a significant contributor. The majority of the tanks in service during the period covered by the study were bare-steel tanks, and 95% of those failures were caused by corrosion (EPA 1987 [DIRS 107749], p. 7). One interesting observation was that many bare-steel tanks

that have been unearthed were found to have corrosion holes that were plugged with corrosion product and showed no signs of leakage (EPA 1987 [DIRS 107749], p. 6).

The study also indicates that 5% to 7% of bare-steel tanks leaked when they were tested for the first time due to manufacturing or installation defects (EPA 1987 [DIRS 107749], p. 6). However, failures found during such a leak test would generally be repaired, and the fraction of the total population failed by unidentified defects would be much lower. The study indicates that 4% out of a population of 980 in-situ tanks were found to be leaking, and 0.9% of 24,452 leaking tanks were found to be leaking within 0 to 5 years (i.e., the early life of the underground storage tank) of being placed into service (EPA 1987 [DIRS 107749], p. 8). This suggests an upper bound of approximately 0.04% ($4\% \times 0.9\%$) on the fraction of a total population failing early in the service life by an unidentified defect. Additional information provided by the Steel Tank Institute indicates that the fraction of the population failed by unidentified manufacturing defects is closer to 3×10^{-4} percent (Grainawi 1999 [DIRS 107755]). Types of noncorrosion-based defects identified as causing failure include installation damage (EPA 1987 [DIRS 107749], p. 10) and failure of weld seams (EPA 1987 [DIRS 107751], p. 82).

While this review has provided general information on the fraction of the total population of underground storage tanks that fail due to any cause, rates of early failure by defects are generally obscured by the high rate of early corrosion failures. The information obtained is not directly applicable to waste packages because an underground storage tank made of bare steel is basically a single, less robust, noncorrosion-resistant barrier. However, it still indicates that even commercial-grade quality controls can produce components that have a relatively low rate of unidentified failures upon entering service. In addition, general types of manufacturing defects that may be applicable to waste packages were identified in the review as follows:

- Weld flaws
- Handling or installation damage.

The applicability of these types of defects to waste packages and their potential consequences to postclosure performance are discussed in Section 6.2.

6.1.4 Radioactive Cesium Capsules

During the period between 1974 and 1983, 1,600 radioactive cesium capsules were fabricated at the DOE Hanford facility. These capsules were double-walled cylinders initially designed and tested to be stored in storage pools at Hanford that were later used by commercial companies as radiation sources (Tschoepe et al. 1994 [DIRS 107789], p. 2-7). One of these capsules failed during 1988 as a result of its use in environmental conditions that were drastically different from those for which the capsules were designed and from the development test conditions. An investigation into this failure concluded that, despite other deficiencies that were found, the capsule would not have failed if it had operated in the environment for which it was designed. The remaining capsules were recalled to Hanford after this incident, and there have been no other failures to date. Thus, the failure rate to date is 6.3×10^{-4} per capsule.

While this type of administrative or operational error does not represent an actual defect in the fabrication of the component, nonetheless, it caused an early failure. The applicability of this type of defect to waste packages and its potential consequences to postclosure performance are discussed in Section 6.2.

6.1.5 Dry Storage Casks for Spent Nuclear Fuel

Dry storage casks that are sealed with a closure weld (as opposed to bolting) represent a close analog to waste packages. Examples include the dry-shielded canister that is part of the NUHOMS system by TransNuclear and the VSC-24 dry-storage cask fabricated by the Sierra Nuclear Corporation (Hodges 1998 [DIRS 107767]). While there have been no recorded cases of closure welds failing after casks were placed into service, there have been four cases where cracks in closure welds have been identified during postweld inspection of the cask (Hodges 1998 [DIRS 107767]). All of these cases have been associated with the VSC-24, of which there were 19 in service through July 1998. Table 6-1 summarizes relevant information on each of the cracking events. Figure 6-1 provides an illustration of the VSC-24 closure welds. A VSC-24 Owners Group weld review team, composed of industry experts in metallurgy, welding, and NDE, evaluated each of the four weld-cracking events to identify the root causes.

The team concluded that the Palisades weld crack was caused by an existing condition in the rolling plane of the shell material that was opened up by the process of making the shield lid weld (Hodges 1998 [DIRS 107767]). Metallographic analysis revealed a crack that propagated along prior austenitic grain boundaries of a preexisting weld of unknown origin (the weld had not been documented during fabrication). This base metal defect may have resulted from improper repair or incomplete removal of temporary low-quality welds used to facilitate the fabrication process (i.e., attachment of strong backs to assist in the rolling of plate material).

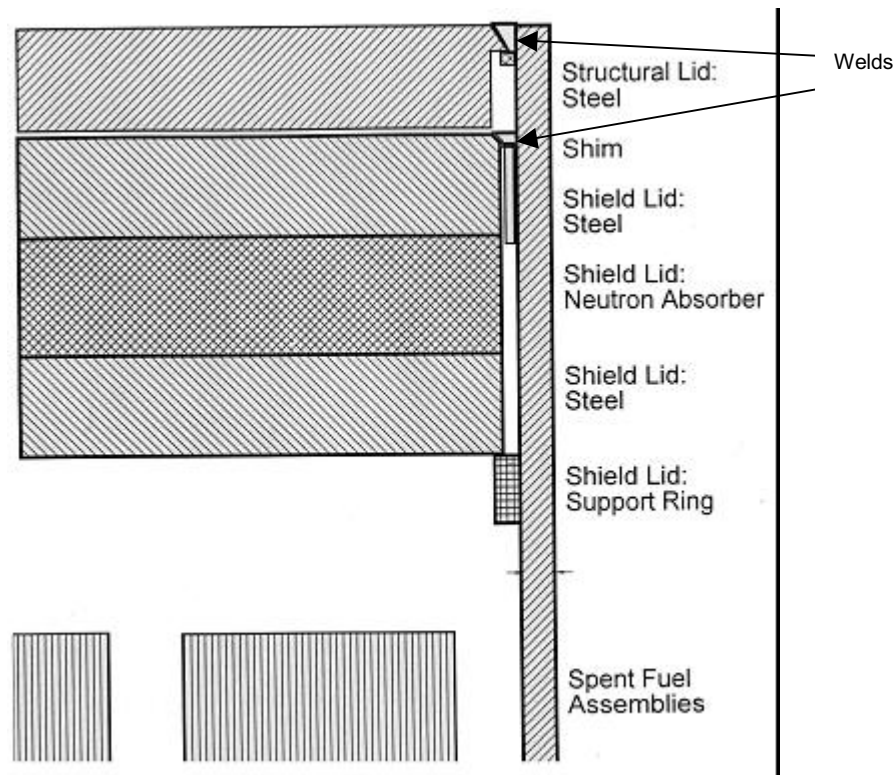
Table 6-1. Summary of VSC-24 Weld Cracking Events

Facility	Date	Detection	Location	Crack Description
Palisades	3/95	Helium leak test	Shield lid-to-shell weld	About 6 in long by 1/8 in deep that extended from about 1/8 in above the shield lid-to-shell weld fusion line into the shell base metal
Point Beach	5/96	Dye-penetrant test	Structural lid-to-shell weld Structural lid-to-shield lid weld	Three cracks, each less than 1 in long, located along the center of the root pass at locations where the fit-up gap between the lid and the backing ring was widest. In addition, cracking and weld porosity were found in the structural lid-to-shield lid seal weld (fillet weld associated with the vent port covers)
Arkansas Nuclear One	12/96	Helium leak test	Shield lid-to-shell weld	About 4 in long located along the weld fusion line
Arkansas Nuclear One	3/97	Dye-penetrant test	Shield lid-to-shell weld	About 18 in long located along the weld fusion line of the root pass

Source: Hodges 1998 [DIRS 107767].

The causes of the weld cracks at Point Beach were found to be associated with weld flaws caused by poor welding technique and moisture contamination (Hodges 1998 [DIRS 107767]). The cracks on the root pass of the structural lid-to-shell weld were caused by wide fit-up gaps that were not properly filled by the welding technique. The cracking and weld porosity found in the structural lid-to-shield lid seal weld were caused by moisture contamination of the weld. The moisture came from water forced out of the drain line during cask loading. The team concluded that none of the cracks at Point Beach was caused by the mechanism that produced the Palisades cracks.

The crack in the shield lid-to-shell weld for the first cask loaded at Arkansas Nuclear One was initially attributed to lamellar tearing based on visual observations of the crack by the welders before it was repaired (Hodges 1998 [DIRS 107767]). However, it was later shown that this crack was similar in appearance to the second crack that was discovered, which was attributed to hydrogen-induced cracking. The hydrogen-induced cracking was attributed to (1) the high hydrogen content of the weld wire, (2) susceptible microstructure of the steel welded, and (3) a highly restrained weld joint configuration leading to residual stresses at or near the yield level.



Source: Hodges 1998 [DIRS 107767].

Figure 6-1. Illustration of Closure Welds for the VSC-24 Dry Storage Cask

General types of manufacturing defects were identified in the review that may be applicable to waste packages. These types of defects are:

- Weld flaws
- Base metal flaws
- Contamination.

The applicability of these types of defects to waste packages and their potential consequences to postclosure performance are discussed in Section 6.2.

6.1.6 Summary

Table 6-2 briefly summarizes the information obtained from the literature search on the rate and causes of manufacturing defects in welded metallic containers. Eleven generic types of defects were identified:

- Weld flaws
- Base metal flaws
- Improper weld material
- Improper heat treatment
- Improper weld-flux material
- Poor weld-joint design
- Contaminants
- Mislocated welds
- Missing welds
- Handling or installation damage
- Administrative or operational error.

Table 6-2. Summary of Defect-Related Failures in Various Welded Metallic Containers

Container Type	Information on Failure	Types of Defects Leading to Early Failure
Boilers and pressure vessels	Seventeen out of 20,000 pressure vessels fabricated less than 40 years previous to 1976 failed due to manufacturing defects (dominant cause was fatigue growth of weld flaws). Stainless steel cladding on some reactor coolant system components for two nuclear units (different fabricators) cracked due to surface contamination remaining from transport or fabrication.	- Weld flaws - Base-metal flaws - Improper weld material - Improper heat treatment - Improper weld flux - Poor weld-joint design - Contaminants
Nuclear fuel rods (PWR and BWR)	Undetected manufacturing defect-related failure rate approximately one rod per 100,000. Overall failure rates in the range of 2 to 7 rods per 10,000 before 1985, 0.6 to 3 rods per 10,000 from 1985 to 1997.	- Weld flaws - Base-metal flaws - Mislocated welds - Contamination - Missing welds - Improper weld material - Handling damage
Underground storage tanks	Fraction of population in the range of 3×10^{-4} % to 4×10^{-2} % failed early in service life due to manufacturing or handling defects.	- Handling or installation damage - Weld flaws

Table 6-2. Summary of Defect-Related Failures in Various Welded Metallic Containers (Continued)

Container Type	Information on Failure	Types of Defects Leading to Early Failure
Radioactive cesium capsules	One failure out of 1,600 capsules.	- Administrative error resulting in unanticipated operating environment
Dry-storage casks for spent nuclear fuel	Four out of 19 Sierra Nuclear VSC-24 casks found to have cracked closure welds during postweld inspection (dye-penetrant and helium leak test only).	- Weld flaws - Base metal flaws - Contamination

Source: Summary of results of literature search presented in Sections 6.1.1 through 6.1.5.

A complementary type of defect is added to the previous list: out-of-specification (improper) base metal. This type of defect was not identified in the literature search; only instances of improper weld material were found. However, it is reasonable to consider the possibility that base metal, as well as weld material, might be out of specification. This particular defect mode is combined with those associated with base-metal flaws for the rest of this report. Planned repository design and operations (DOE 2006 [DIRS 176937]) indicate that the generic list should also include defects introduced by stress relief heat treatment of the waste package closure weld with a low-plasticity burnishing process and recognizing that the drip shield or waste packages might be improperly installed. Thus, 13 processes or conditions are evaluated in this analysis. These processes are listed below:

- Weld flaws
- Base metal flaws
- Improper weld filler material
- Improper stress relief for lid (low plasticity burnishing)
- Improper heat treatment of outer corrosion barrier and closure lid
- Improper weld-flux material
- Poor weld-joint design
- Contaminants
- Improperly located welds
- Missing welds
- Handling-induced defects
- Emplacement errors
- Administrative or operational errors.

The 13 types of defects were reviewed for their applicability to waste packages and results discussed in Section 6.2.3. Of these 13 flaws or processes, seven were identified as significant for the waste package outer corrosion barrier, requiring further analysis (Section 6.3). The remaining six processes were screened from further analysis on the basis of either very low likelihood of occurrence or low consequences. The seven processes retained for further analyses with respect to mechanisms for potential early failures of a waste package outer corrosion barrier are as follows¹:

¹ Heat treatment of the outer corrosion barrier involves two processes.

- Weld flaws
- Improper heat treatment of outer corrosion barrier
- Improper heat treatment of outer corrosion barrier lid
- Improper stress relief of outer corrosion barrier lid (low plasticity burnishing)
- Waste package mishandling damage
- Improper base metal selection
- Improper weld filler material.

The same 13 processes identified above were reviewed for potentially leading to early failure of a drip shield, and four were identified as significant, requiring further analysis (Section 6.4). The four processes retained for further analyses with respect to mechanisms for potential early failures of a drip shield are as follows:

- Improper heat treatment
- Base metal selection flaws
- Improper weld filler material
- Emplacement errors.

The probability of occurrence and consequences for postclosure performance of the package and drip shield were assessed for the applicable defects.

Weld flaws (e.g., slag inclusions, porosity, lack of fusion, or hydrogen-induced cracking) were a dominant contributor to early failure but usually required an external stimulus (e.g., cyclic fatigue) or environmental conditions to cause the flaw to propagate to failure. In many cases, components with unidentified defects entered service, not because the defect was missed by an inspection, but because no inspection for that type of defect was required at the time they were fabricated. For dry-storage casks, all of the defects were identified by postweld inspection prior to commencement of the storage phase and thus do not represent early failure as it is defined for this analysis.

As indicated previously, many of the defects require an external stimulus or the component was not subjected to inspections that would have identified the defect. There is likewise insufficient information available to defensibly relate the cumulative effect of the environment or stresses to which the component was subjected to that of the waste package or drip shields (e.g., whether the cumulative effects of the stresses and environmental conditions experienced by a pressure vessel in a 40- to 60-year life are relevant to 100, 1,000, or 10,000 years of waste package lifetime). Because the development of early failure modes from material defects is closely connected to the long-term environmental conditions, this analysis addresses the probability that such defects exist, not the likelihood of failures due to defects. Accordingly, the information on the fraction of components that experienced defect-related failure during their intended lifetime is not directly applicable to waste packages or drip shields. In addition, these population-based failure rates do not provide any insight into the time distribution of early failures. However, in some cases, information on the occurrence rate of particular types of defects was obtained from the literature search.

6.2 FABRICATION AND HANDLING PROCESSES RELEVANT TO EARLY FAILURE OF ENGINEERED BARRIER COMPONENTS

6.2.1 Waste Package Fabrication and Handling Processes

The overall dimensions of the TAD canister waste package outer corrosion barrier, a cylinder having a diameter of approximately 1.96 m and a length of approximately 5.85 m, have been developed and documented (SNL 2007 [DIRS 179394], Table 4-6). The processes for the fabrication and handling of the waste package outer corrosion barrier have conceptually been developed. The exact processes will be dependent on the approach of the vendor to meeting the specifications of the YMP. The specifications for the waste package fabrication can be found in *Total System Performance Assessment Data Input Package for Requirements Analysis for TAD Canister and Related Waste Package Overpack Physical Attributes Basis for Performance Assessment* (SNL 2007 [DIRS 179394]).

The fabrication process begins with the procurement of the plates that form the right circular cylinders comprising the waste package outer corrosion barrier. There are two primary elements: the inner structural vessel made of Stainless Steel Type 316 (UNS S31600); and the outer corrosion resistant barrier made of Alloy 22 (UNS N06022), a nickel-based chromium/molybdenum alloy (SNL 2007 [DIRS 179394], Table 4-1, Item 03-04). The inner vessel fits within the outer corrosion barrier with a maximum diametral clearance of 10 mm (SNL 2007 [DIRS 179394], Table 4-1, Item 03-06). Each vessel has lower and upper lids. Spacer rings are located within the bottom of the waste package outer corrosion barrier so that the inner lid does not touch the outer lid. The lower lids are welded in place at the fabrication site, while the upper lids are welded in place at the repository after the spent nuclear fuel or defense high-level waste canisters are placed within a waste package. The outer waste package barrier also has external sleeves on either end, 304.8 mm in length (SNL 2007 [DIRS 179394], Table 4-3), that assist in handling operations.

Both vessels are made from rolled and welded plates to form the right circular cylinders. The structural vessel is 50.8 mm thick, while the outer corrosion barrier is 25.4 mm thick (SNL 2007 [DIRS 179394], Table 4-3). The number of segments needed for each right circular cylinder depends directly on the mass of material of a particular heat that can be poured to form an ingot and then worked to form the plate segment. This usually requires the cast material to be, perhaps, forged, then rolled to the required thickness, cut to the required size, and followed by welding and a nondestructive inspection. Ideally, if the smelter could produce an ingot large enough for each vessel, the welding of segments would not be necessary. This is not now the case, and multiple plate segments may be necessary for each vessel. The segments would be welded together by gas tungsten arc welding or another acceptable process, then subjected to intensive NDE to ensure that weld flaws above the acceptable threshold are not present (SNL 2007 [DIRS 179394], Table 4-1, Items 03-16 through 03-19).

After the assembled and welded plates have passed inspection, the edges are machined as needed, then rolled into a cylinder of the required dimension (approximately 1.8 m in diameter) and a longitudinal weld is performed. The likely method would have two or three sections of cylinders fabricated by this method with their longitudinal welds offset, so that cracks in a longitudinal weld could not propagate along the entire length of the vessel. The sections would

then be welded circumferentially to complete the vessel, whose overall length is approximately 5.7 m (SNL 2007 [DIRS 179394], Table 4-3). After being inspected and undergoing the threshold flaw testing, the lower lid would be welded in place. The lids, basically large discs, are fabricated separately of the same alloy material as the body of the vessels. The lid thicknesses are 25.4 mm and 50.8 mm, respectively, for the outer corrosion barrier and inner vessel (SNL 2007 [DIRS 179394], Table 4-3). The lower lid welds will also be subjected to detailed NDE (SNL 2007 [DIRS 179394], Table 4-1, Item 03-17). The outer corrosion barrier and its lids are solution-annealed (SNL 2007 [DIRS 179394], Table 4-1, Item 03-20) to preserve their corrosion properties. The inner vessel does not require a heat treatment, since it serves primarily as a support structure. Following heat treatment of the outer corrosion barrier and machining of the weld preparations, the inner vessel is placed within the outer corrosion barrier. The lids are shipped along with the assembled waste package.

The dimensions of the completed vessels will be confirmed to ensure that the inner liner can be inserted into the outer corrosion barrier without interactions. Here, dimensions and ovality are important. The inner liner will then be inserted into the outer corrosion barrier and the completed unit packaged for transport to the repository. The waste package pieces will contain impressed inventory numbers so that each package can be followed through subsequent handling. The empty waste packages will be received and inspected at the repository and placed into temporary storage. When needed, the empty waste packages will be moved to the appropriate building where the TAD or defense high-level waste canister will be inserted in the vertical position. After waste insertion and placement of a Stainless Steel Type 316 spread ring, the inner lid will be welded in place. Following nondestructive inspection, the outer lid will be welded in place. This weld will undergo residual stress mitigation by means of low-plasticity burnishing, followed by detailed NDE (SNL 2007 [DIRS 179394], Table 4-1, Item 03-21). The loaded waste packages will then be rotated vertically and readied for movement by the fuel transporter into the repository position established for that package. The transporter is remotely operated and places the waste package and its pallet in the required position using location sensors.

6.2.2 Drip Shield Fabrication and Handling Processes

Conceptually the drip shield looks like an inverted “U” or mailbox. The overall dimensions of the drip shield, about 2.4 meters across and about 5.8 meters in length including the overlap section, have been developed and documented. These dimensions can be found in *Total System Performance Assessment Data Input Package for Requirements Analysis for EBS In-Drift Configuration* (SNL 2007 [DIRS 179354], Table 4-2, Item 07-01). The processes for the fabrication and handling of the drip shield have conceptually been developed. The exact processes will be dependent on the approach of the vendor to meeting the specifications of the YMP. The requirements and specifications for the drip shield can be found in *Total System Performance Assessment Data Input Package for Requirements Analysis for EBS In-Drift Configuration* (SNL 2007 [DIRS 179354], Table 4-2).

The fabrication process begins with the procurement of the plates and structural support beams that form the drip shield. The body of the drip shield and the connector plate are constructed of Titanium Grade 7 (R52400), an alpha-phase titanium alloy with approximately 0.15 wt % palladium added to increase corrosion resistance (SAE 1993 [DIRS 119579], Reactive and

Refractory Metals and Alloys). The support beams, added to increase stiffness of the drip shield, are constructed of Titanium Grade 29 (R56404), an alpha-beta-phase titanium alloy with about 6 wt % aluminum, 4 wt % vanadium, and 0.1 wt % ruthenium (SAE 1993 [DIRS 119579], Reactive and Refractory Metals and Alloys). The side support beams also contain a lifting feature that will permit the drip shield to be lifted whenever it is necessary to do so. The support beams will be welded to the body using an intermediate alloy composition, Titanium Grade 28. The base of the drip shield (its “feet”) is fabricated from Alloy 22. These support feet are attached with pins that do not require welding to attach them to the titanium material. These provide additional corrosion protection in that they eliminate the potential for the titanium drip shields to contact the iron in the invert structure. These elements together make up the drip shield. There will be two drip shield segments; a long one and a shorter one that is designed to overlap and attach two long sections together while assuring that the joint between them does not leak water while in service.

The drip shield is made from rolled and welded plates to form the required inverted “U” shape. The vendor may choose to form a larger rectangular structure, which could be rolled into the required shape, or to have three sections, two flat sides and one rolled roof member, which are then welded together. The number of plates needed will be dependent on the choice the vendor makes to fabricate the drip shield. The former method would likely require several small plates that would be welded together. The latter method may only require three plates. In all cases, the plates are produced by melting and casting. The cast billet is then forged, rolled to the required thickness, and cut to the required size. The segments are welded together, by gas tungsten arc welding or another acceptable process, then subjected to intensive NDE to ensure that weld flaws above the acceptable threshold are not present. The choice of welding processes is governed by the requirement that the weld be performed in an atmosphere that has an absolute minimum amount of hydrogen, which causes degradation of the weld.

After the drip-shield body has passed inspection, the connector plate will be welded into position. Four support beams will then be welded to each side of the structure, and two lifting assemblies will be welded to each side. An additional four support beams are welded onto the top of the drip shield and to the side beams. After the drip shield body has been completely fabricated, the entire drip shield will be stress-relieved (in air) at a temperature that will allow about 50% of the stresses to be removed from the welds. It is probable that the stress relief will be performed on a large fixture that will provide assurance that the shape is preserved during the heating and cooling required for stress relief.

The angle-bracket Alloy 22 base is pinned into position, and then the pins are welded to Alloy 22 washers. The drip shields will be suitably packaged in protective wrappings and shipped to the repository, where they will be thoroughly inspected again. Prior to permanent closure of the repository, the drip shields will be placed over the array of waste packages within an emplacement drift by the use of a drip shield emplacement device. This device will locate each drip shield using sensors that confirm that each section is appropriately aligned.

6.2.3 Disposition of Possible Engineered Barrier Component Fabrication or Handling Processes That Could Lead to Defects

Eleven generic types of defects or processes that could lead to defects were summarized in Section 6.1.6 as potential causes for early failure of metallic containers. Many of these types of defects could also be introduced to a waste package or drip shield during fabrication, transport to the repository, storage, loading, or emplacement. In addition to these 11, two more defect modes have been identified as applicable to waste package and/or drip shield: (1) improper stress relief of waste package closure lid weld, and (2) emplacement error. All 13 possible defects or processes that could lead to defects are discussed below, and some are screened from further evaluation.

- *Weld flaws:* Tensile hoop stresses in the metal will tend to propagate any perpendicular flaws in the welds. Thus, flaws that are oriented approximately perpendicular to the waste package hoop stress and sufficiently near the surface, are recognized and quantified as being capable of propagating. Low-plasticity burnishing is a stress mitigation process in which the metal surface is compressed over a few millimeters depth providing causes plastic deformation in the material beneath the tool. The deformed region is thus constrained by surrounding, undeformed material leaving the treated region in a state of compressive residual stress to counter any residual tensile stresses. Weld flaws in the waste package outer corrosion barrier closure weld are stress-mitigated through a low-plasticity burnishing process. Thus, flaws that are oriented approximately perpendicular to the waste package hoop stress and sufficiently near the surface are recognized and quantified as being capable of causing early failure. All welds in the waste package canister will be inspected with multiple NDEs as described in *Total System Performance Assessment Data Input Package for Requirements Analysis for TAD Canister and Related Waste Package Overpack Physical Attributes Basis for Performance Assessment* (SNL 2007 [DIRS 179394], Table 4-1, Item 03-17); thus, any large flaws will be detected and repaired. Because all welds in the waste package outer corrosion barrier and lid, except those created during final closure of the package, are annealed (as was discussed in Section 6.2.1), any residual flaws are not susceptible to propagation and are screened from early-failure analyses. The evaluation of flaws in the closure welds for outer corrosion barrier lid is documented in Section 6.3.1.

As part of the fabrication process, all drip shield welds will be inspected using a variety of examinations as discussed in *Total System Performance Assessment Data Input Package for Requirements Analysis for EBS In-Drift Configuration* (SNL 2007 [DIRS 179354], Table 4-2, Item 07-10). All welds in the drip shield will be stress-relieved through heat treatment as described in Section 6.2.2, so any flaws remaining after the inspections will not be sources for propagation of cracks. Thus, weld flaws in the drip shield are screened from further evaluation.

- *Base-metal flaws or out-of-specification base metal:* It is conceivable that an out-of-specification base metal could be selected for use in fabricating drip shields or waste packages. The defects could result from having the wrong material alloy or having a base metal delivered to the fabrication operation with undetected flaws that would not be found during subsequent processes. While no documented cases of this type were

found in case studies, an analogue was found: the use of improper weld material, as discussed in *Records Investigation Report Related to Off-Chemistry Welds in Material Surveillance Specimens and Response to IE Bulletins 78-12 and 78-12A - Supplement* (Babcock & Wilcox 1979 [DIRS 108219], Table I of Part II). The potential for a defective waste package outer corrosion barrier to result from this scenario is quantified in Section 6.3.2 and for the drip shield in Section 6.4.1.

- *Improper weld filler material:* The use of improper weld material is noted in *Records Investigation Report Related to Off-Chemistry Welds in Material Surveillance Specimens and Response to IE Bulletins 78-12 and 78-12A - Supplement* (Babcock & Wilcox 1979 [DIRS 108219], Table I of Part II). The potential for a defective waste package outer corrosion barrier to result from this scenario is quantified in Section 6.3.7 and for the drip shield in Section 6.4.3.
- *Improper heat treatment:* As discussed previously in Section 6.1, improper heat treatment has been documented as a contributor to flawed pressure vessels. As discussed below, heat treatment procedures for Alloy 22 waste packages are complex and are expected to be susceptible to mistakes that could conceivably go undetected. Similar challenges will exist for heat treatment of the titanium drip shields. For these reasons, this scenario is recognized, and the potential for a defective waste package outer corrosion barrier to result from this scenario is quantified in Section 6.3.3, for the outer corrosion barrier lid in Section 6.3.4, and for the drip shield in Section 6.4.2.
- *Improper stress relief in the waste package closure weld:* Weld flaws in the waste package closure weld will be stress relieved at the weld surface through a low-plasticity burnishing process as discussed in Section 6.2.1. This process could be improperly implemented as a result of either machine malfunction or operator error and through failure of post-fabrication inspections. For this reason, this scenario is recognized, and the potential for a defective waste package outer corrosion barrier lid to result from this scenario is quantified in Section 6.3.5. A comparable process for the drip shield will not be applied and thus is screened from further evaluation.
- *Improper weld-flux material:* Welds in waste package outer corrosion barriers and drip shields will employ a welding method (such as tungsten inert gas or metal inert gas) that does not use weld-flux material. Thus, use of improper weld-flux material is screened from further evaluation.
- *Poor joint design:* A significant development and testing effort will have gone into the design of the final closure joint. Lessons learned from the types of closure weld problems experienced in the dry-storage cask systems (Section 6.1.5) are expected to be incorporated into the design of closure welds for waste packages and drip shield welds. Therefore, problems with the design of the weld joint for the waste package outer corrosion barriers and drip shields are not expected, and this scenario is screened from further evaluation. This does not exclude weld flaws or other types of weld-related defects that could occur during the waste package closure process.

- *Missing welds:* Data on the occurrence of this type of defect in fuel rods (presented in Section 6.1.2) indicated that it would occur at a rate much lower than 5×10^{-6} per rod. A missing weld on a waste package or drip shield would be easier to identify than one on a fuel rod and would have a noticeable effect on the configuration of the waste package (e.g., a missing closure weld could cause the lid to fall off when the waste package is tilted to a horizontal position) or drip shield. Therefore, it is expected that the occurrence rate of this defect for a waste package or drip shield would be significantly less than a more-dominant failure mechanism such as improper heat treatment, and this scenario is screened from further evaluation.
- *Contaminants:* The possibility exists that the outer surfaces of a waste package outer corrosion barrier or drip shield could become contaminated with some corrosion-enhancing material. However, fabrication and handling requirements for the waste package outer corrosion barrier (SNL 2007 [DIRS 179394], Table 4-1, Item 03-25) and drip shield (SNL 2007 [DIRS 179354], Table 4-2, Item 07-14) state that operations must be conducted in a manner conducive to minimizing surface contamination. In addition, multiple inspections of the waste package outer corrosion barrier and drip shield are required prior to emplacement (SNL 2007 [DIRS 179394], Table 4-1; 2007 [DIRS 179354], Table 4-2). Therefore, it is expected that the likelihood of this type of defect for a waste package outer corrosion barrier or drip shield being undetected prior to emplacement would be significantly less than the more-dominant failure mechanisms, and, thus, contaminants are screened from further evaluation.
- *Mislocated welds:* This defect is mainly applicable to very small, single-pass welds (e.g., fuel rod end caps). For larger multipass welds, such as those on the waste package or drip shield, any significant mislocation of the electrode would cause the weld arc not to strike. This would be immediately obvious to both the operator and the control system for the automated welder. This is much less likely than a more-dominant failure mechanism such as improper heat treatment and, thus, mislocated welds are screened from further evaluation.
- *Handling or installation damage:* A typical waste package containing a loaded TAD canister will have a mass of approximately 162,000 pounds as shown in *Total System Performance Assessment Data Input Package for Requirements Analysis for TAD Canister and Related Waste Package Overpack Physical Attributes Basis for Performance Assessment* (SNL 2007 [DIRS 179394], Table 4-3). The outer corrosion barrier of the waste package will be susceptible to denting or gouging during handling due to its large inertial mass. It is conceivable that dents or gouges could occur and not be detected during subsequent inspections. For this reason, this scenario is considered, and the potential for a defective waste package outer corrosion barrier to result from this scenario is quantified in Section 6.3.6. However, because the strength-to-mass ratio of the drip shield is much higher and the drip shields will be resilient to impacts incurred during handling and emplacement, this mode of defect is not considered further for the drip shields.

- *Emplacement error*: Emplacement of waste packages and drip shields will be performed under a quality control program, and emplacement of drip shields will be monitored remotely by cameras and other mechanical sensory equipment (SNL 2007 [DIRS 179354], Table 4-4, Item 05-01 and Table 4-2, Item 07-14). Minor deviations in the waste package-to-pallet positions or the improper location of waste packages relative to other waste packages is conceivable; however, the consequences of this would be negligible, as long as the packages are protected by the drip shield from rockfall and seepage. Major deviations in these components are considered sufficiently unlikely that they are not considered further because inspections will detect the deviations, which will be fixed. It is conceivable, however, that drip shields could be improperly joined to adjacent drip shields, rather than correctly as described in *Total System Performance Assessment Data Input Package for Requirements Analysis for EBS In-Drift Configuration* (SNL 2007 [DIRS 179354], Table 4-2, Items 07-02 and 07-02B), and that subsequent inspections would fail to identify the problem. For this reason, this mode of introducing defects to the repository configuration is recognized, and the potential for an improper drip shield emplacement to result from this scenario is quantified in Section 6.4.4.
- *Administrative or operational error*: Administrative and operational errors are expected, and provisions in drip shield and waste package fabrication and handling procedures and equipment will be made to reduce these errors to acceptable levels. Even after taking the planned precautions, these types of errors are still recognized as likely, and the associated rates and consequences are included in the evaluations documented in Sections 6.3 and 6.4. Therefore, these types of errors are not considered to be separate defect modes.

6.3 WASTE PACKAGE POTENTIAL DEFECTS

Of the 13 defect modes or processes identified above, six were identified as applicable to fabrication and handling of waste packages. The remaining seven were screened from further analysis on the basis of either very low likelihood of occurrence or low consequences. The six processes² retained for further analyses with respect to mechanisms for early waste package failure are as follows:

- Weld flaws
- Improper heat treatment of outer corrosion barrier
- Improper heat treatment of outer corrosion barrier lid
- Improper stress relief of outer corrosion barrier lid (low plasticity burnishing)
- Waste package mishandling damage
- Improper base metal selection
- Improper weld filler material.

² One process, heat treatment, is duplicated since it occurs twice (once for the waste package out corrosion barrier and once for the closure lid). Hence the list actually contains seven processes.

Implementation of the waste package weld flaw analysis is discussed in Section 6.3.1. The remaining six processes are analyzed using an event tree/fault tree approach where the basic event tree for evaluating these processes is shown in Figure 6-2. The branches, labeled from 2 through 7, are transferred to the individual trees for each defect type. The event trees and probabilities associated with these mechanisms are provided in Sections 6.3.2 through 6.3.7. All of the event trees and fault trees used in the analysis of early failure mechanisms of waste packages are provided in Appendix B.

The quantification of events using the event tree approach and, in particular, uncertainty analyses incorporates the premise that the events are independent (i.e., that events are not correlated by common causes) (Apostolakis and Kaplan 1981 [DIRS 160971], pp. 136 to 139). However, the probabilities of nominally identical events (i.e., those that are distinct (independent) but for which the state of knowledge for determining their distributions is identical) have been correlated together. This is accomplished in the SAPHIRE computations by assigning the same correlation class to nominally identical events. The net effect on the analysis results of assigning correlation classes is to somewhat broaden the uncertainty distributions.

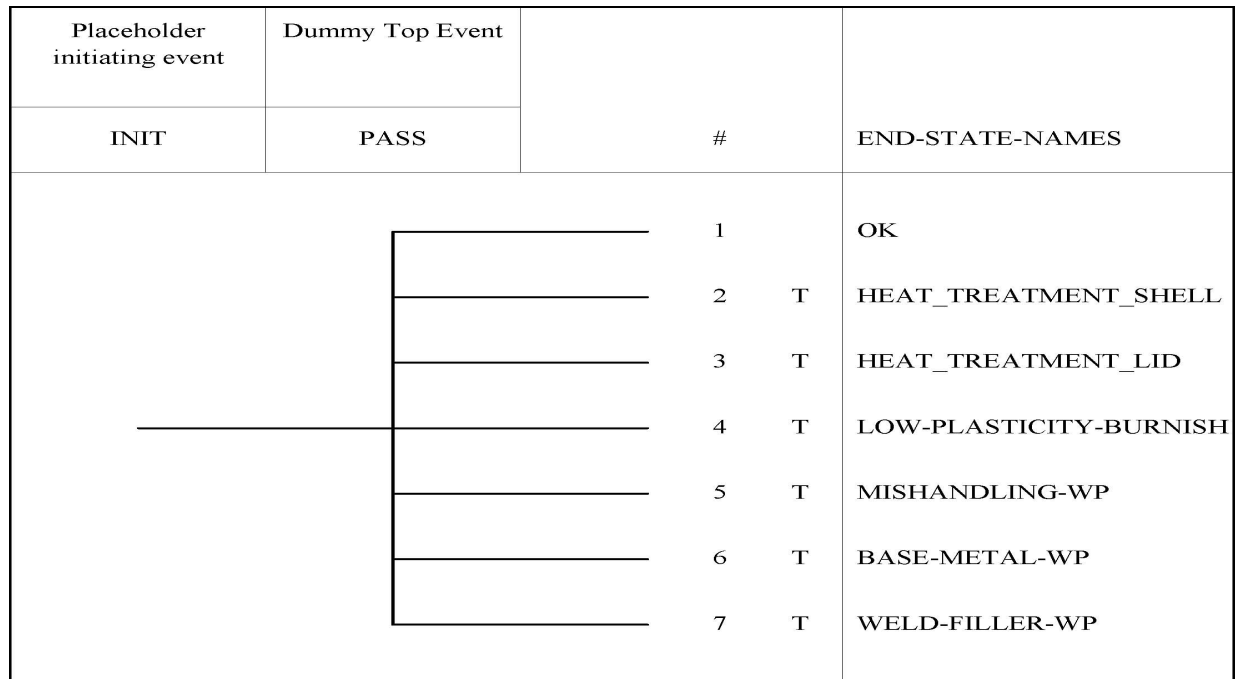


Figure 6-2. Basic Waste Package Defect Event Tree

6.3.1 Evaluation of Weld Flaws in Waste Package Outer Lid Weld

Weld flaws are among the most extensively studied types of defects that can affect the performance of metallic components used in the nuclear industry. Much of the weld-flaw research has been directed toward estimating the number and depth of flaws in welds to support probabilistic structural mechanics models for predicting the reliability of piping and reactor vessel. For example, Khaleel et al. (1999 [DIRS 107764]) developed weld-simulation software to simulate the weld manufacture, the errors that lead to different types of flaws, and the

reliability of various inspection methods, but this software was developed for stainless steel and not Alloy 22.

Work has been performed directly on the welding of Alloy 22 specimen rings (Smith 2003 [DIRS 163114]; SNL 2007 [DIRS 179394]) that duplicate closely the actual outer lid weld of a waste package. Although the design of the outer lid has been modified since that work was performed, the modifications do not impact the validity of the results obtained here. Only the closure weld configuration was modeled in the specimen ring testing and, although diameters are different, the general form and size of the weld remains the same, as shown in “Detail D” of the drawing cited in *Total System Performance Assessment Data Input Package for Requirements Analysis for TAD Canister and Related Waste Package Overpack Physical Attributes Basis for Performance Assessment* (SNL 2007 [DIRS 179394], Section 4.1.2.3). Therefore, the weld flaw inspection results are used as a surrogate to represent the expected weld flaws in the closure lid of the waste package outer corrosion barrier.

Sixteen specimen rings were welded employing procedures, processes, and equipment similar to that expected to be used for the closure of the waste package (Smith 2003 [DIRS 163114], Section 2.3). Nondestructive examinations were performed to accumulate significant information on the weld flaws and included ultrasonic and radiographic testing, which was followed by metallographic examination. This information consists of weld flaw location, size and shape. Based on this information, summarized in Section 4.1.2.2, several distributions are developed here to characterize the size of the flaws in the through-wall extent of the weld (Y direction on Figure 4-1), their density (mean number of flaws per volume of weld) and their depth (distance between the outer surface of the weld and the onset of the flaw in the Y direction).

Metallographic inspections were performed on the specimen rings at the sites where imperfections were indicated by ultrasonic testing and/or radiographic testing as discussed in Section 4.1.2.2. Three flaws were not observed in the follow-up metallographic inspection and are not included in this analysis. Based on all the testing results, it was determined that, “UT [ultrasonic testing] and RT [radiographic testing] are capable of detecting volumetric flaws as small as 1 millimeter in size...” from “Study Summary” in the drawing cited in *Total System Performance Assessment Data Input Package for Requirements Analysis for TAD Canister and Related Waste Package Overpack Physical Attributes Basis for Performance Assessment* (SNL 2007 [DIRS 179394], Section 4.1.2.3). Of course, it was not possible to perform metallographic examination on the entire specimen rings since it is a very time-consuming process; instead, metallographic inspections (up to six per ring) were performed at randomly selected locations in the areas where no flaw had been detected through ultrasonic testing inspection. None of these metallographic inspections revealed a flaw of size larger than the estimated ultrasonic testing detection threshold of 1 mm. This strongly suggests that the majority, if not all, of the flaws greater than 1 mm were detected, as noted in “Study Summary” from the drawing cited in *Total System Performance Assessment Data Input Package for Requirements Analysis for TAD Canister and Related Waste Package Overpack Physical Attributes Basis for Performance Assessment* (SNL 2007 [DIRS 179394], Section 4.1.2.3).

The imperfections found through metallographic examinations that were not detected by the ultrasonic/radiographic testing inspections were gas pores, and the majority of them were less than 3×10^{-3} inch (around 8×10^{-2} mm) in diameter. Gas pores are spherical in shape when the gas is in thermal equilibrium with its surrounding liquid (Holman 1997 [DIRS 101978], Section 9-5), in this case metal, and have no orientation. Therefore, they are not part of those flaws that are radially oriented. Gas pores are treated the same as spherical porosity in *Stress Corrosion Cracking of the Drip Shield and the Waste Package Outer Barrier* (SNL 2007 [DIRS 177417], Section 6.3.4.1). In other words, they will not induce propagation of cracks via SCC. Thus, they are unlikely to affect the performance of the waste package and are discarded from further consideration.

The same type of ultrasonic testing inspections will be performed on the welds of the waste package (SNL 2007 [DIRS 179394], Table 4-1, Item 03-17) to identify those flaws that may jeopardize its performance so that these flaws can be removed. Based on the design requirement that specifies the detection criterion of weld flaws to be equal to or greater than 1/16 in (SNL 2007 [DIRS 179394], Section 4.1.2.3) and on the improved ultrasonic testing detection results, the characteristic flaw size is set at 1/16 in (1.5875 mm). This value reasonably represents that only half of the flaws of this size will actually be detected. Thus, while the ultrasonic testing detection limit appears better than this size, the 1/16-in flaw size is deemed the appropriate size at which weld repair should be performed and where ultrasonic detection capability is more reliable.

The characteristics of the flaws that may remain in the waste package closure welds can be calculated from the distributions by knowing the per waste package closure weld volume and weld thickness. The TSPA can utilize these results, with the critical flaw orientation probability and an applicable depth factor, to model where undetected flaws remain and might result in SCC that can penetrate the waste package closure weld. The following subsections will each describe a portion of the analysis that is then usable, either in part or entirely, by TSPA to determine the potentially adverse weld-flaw population that survives to repository service. The computations were carried out in Appendix A using MathCAD[®] (output DTN: MO0701PASHIELD.000). The results of the analysis are shown with rounded values. If it is necessary to redo the analysis, the computations should be carried out from the input values given in Section 4.1.2; the intermediate values should not be used, unless otherwise stated.

6.3.1.1 Analysis Input Descriptions

The direct inputs described in Section 4.1.2 are used in the MathCAD[®] evaluation of weld flaw distributions. The following briefly describes those preliminary input operations as contained in Appendix A, Section A.1.

For purposes of calculating the volume of the 16 specimen-ring welds used in Section 6.3.1.3, the diameter of the weld centerline is needed. Table 4-2 yields a weld length of around 4.85 m for a specimen ring. This is multiplied by the cross-sectional area, which is calculated in Appendix A, Section A.1 (variable cross section) based upon the weld geometry descriptions in Table 4-2. The 16 rings therefore contain an estimated total weld volume of, $V_f = 1.656 \cdot 10^{-2} \text{ m}^3$.

The extent of the ultrasonic testing indications in the radial direction (width, or Z direction), their length in the direction of the weld (length, or X direction), and along the weld thickness (Y direction) are given in Table 4-3. The largest flaw in the X direction is around 3.5 cm, and, because this is small compared to the radius of the specimen ring (around 77 cm; see Section 4.1.2.1), the effect of the curvature in the direction of the weld is small. Therefore, the angle θ of a flaw can be closely calculated by taking the arctangent of the ratio of its extent in the Z direction over its extent in the X direction. Notice that the inputs given in Section 4.1.2.2 make it possible to evaluate only the absolute value of θ , not its sign. This angle information is calculated in Appendix A, Section A.4 and used in Section 6.3.1.4.

6.3.1.2 Flaw Size Distribution in the Y-Direction

The flaw size distribution in the Y direction (see Figure 4-1 for conventions on orientation) is estimated using the Bayesian approach with a noninformative prior. Information on the Bayesian approach in the evaluation of parameters is given in *PRA Procedures Guide, A Guide to the Performance of Probabilistic Risk Assessments for Nuclear Power Plants* (NRC 1983 [DIRS 106591], Section 5.5.2). Briefly stated, the Bayesian estimation consists of updating the belief of the analyst about the parameter (embodied in a prior distribution) with evidence from observation (quantified in a likelihood function) to obtain a posterior distribution.

The reason for using the Bayesian approach, rather than the classical (also called “frequentist”) approach, is that it utilizes a probability distribution on the parameter to be estimated in order to express confidence. As mentioned in *PRA Procedures Guide, A Guide to the Performance of Probabilistic Risk Assessments for Nuclear Power Plants* (NRC 1983 [DIRS 106591], p. 12-16), this has been a common way of representing uncertainty since the publication of *Reactor Safety Study: An Assessment of Accident Risks in U.S. Commercial Nuclear Power Plants* (NRC 1975 [DIRS 107799]). Expressing uncertainty around a parameter in terms of a probability distribution is also adequate for subsequent performance assessments of the waste package.

The reason for using a noninformative prior distribution is that in generating the posterior estimate, this minimizes the relative importance of the prior distribution compared to the data (NRC 1983 [DIRS 106591], p. 5-34). This is appropriate here because there is very little generic information on flaws in Alloy 22 welds.

A modeling decision was made to represent the weld flaw sizes in the Y direction as an exponential distribution. The reasons for this choice are that an exponential distribution is widely used and determined by a single parameter. The single parameter characteristic is an important aspect of this distribution since the number of data points is limited. Notice that the exponential distribution is a particular case of the more general Weibull distribution, which has also been employed to characterize flaw-size distributions (Schuster et al. 1998 [DIRS 160078], p. 8.2). Weibull distributions are determined with two parameters; this method allows for more flexibility in the shape of the distribution. However, an exponential distribution is sufficient to fit the ultrasonic testing indication dimensions in the Y direction accrued on the specimen ring welds.

The cumulative exponential distribution for the flaw size s (in mm) in the Y direction of the weld has the form shown in Equation 5 (Martz and Waller 1991 [DIRS 160924], p. 330):

$$P_s(s) = 1 - e^{-\lambda_s \cdot s} \quad (\text{Eq. 5})$$

where λ_s is the parameter (in mm^{-1}) that is to be determined. It will be referred to as the flaw-size parameter in the following. Note that s is always positive.

In order to calculate the probability density function (PDF) related to the flaw-size parameter, it is first necessary to determine which sampling scheme was employed to get the flaw-size information. The information presented in Section 4.1.2.2 can be viewed as a fixed number of flaws n_f ($n_f = 7$) to which correspond random flaw sizes. A sampling scheme characterized by a fixed number of items (namely, the number of flaws) to which is associated a random variable (namely, the size of the flaws) is referred to as gamma sampling (Martz and Waller 1991 [DIRS 160924], pp. 330 and 331). Based on the same reference, for this kind of sampling, a sufficient statistic for estimating λ_s is s_t , the sum of all flaw sizes, which has been evaluated at 31.75 mm.

According to Martz and Waller (1991 [DIRS 160924], p. 336), the noninformative prior distribution for λ_s based on gamma sampling is proportional to $1/\lambda_s$. The resulting posterior PDF p_{λ_s} (termed $f_s(x)$ in computations presented in Appendix A, Section A.2) of the flaw-size parameter λ_s is given in Equation 6:

$$p_{\lambda_s}(\lambda_s) = \frac{s_t^{n_f}}{\Gamma(n_f)} \cdot \lambda_s^{n_f-1} \cdot e^{-\lambda_s \cdot s_t} \quad (\text{Eq. 6})$$

where Γ is the gamma function.

Statistics and quantile values for the flaw-size parameter (gamma) distribution are calculated in MathCAD[®] and presented in Appendix A, Section A.2. The results give a mean value of $2.2 \times 10^{-1} \text{ mm}^{-1}$, with a standard deviation of $8.3 \times 10^{-2} \text{ mm}^{-1}$.

The size distribution of the weld flaws in the Y direction follows an exponential distribution of parameter λ_s , with λ_s having a PDF given by Equation 6. Because it is desirable to have a flaw-size distribution that could be applicable for different weld thicknesses, a modified version of the exponential distribution is used that includes an additional parameter, namely the thickness t of the weld. The cumulative flaw size distribution $P_{sg}(s, \lambda_s, t)$ for a flaw of s mm in the Y direction of a weld of thickness t mm with the flaw-size parameter λ_s (in mm^{-1}) is shown in Equation 7:

$$P_{sg}(s, \lambda_s, t) = \frac{1 - e^{-\lambda_s \cdot s}}{1 - e^{-\lambda_s \cdot t}} \quad \text{with } 0 \leq s \leq t \quad (\text{Eq. 7})$$

As a reminder, in Equation 7 the variable of interest is the flaw size s , while λ_s and t are parameters. In order to be consistent with MathCAD[®] notations used in Appendix A, λ_s and t are shown on the left side of the equation along with s .

It is worth noting that in the case of the specimen rings, most of the ultrasonic testing indications report flaws that are much smaller than the weld thickness. Therefore, Equation 7 presents a modified flaw-size distribution that is, numerically, only slightly different from the pure exponential distribution.

The form of Equation 7 is not the only one possible. For example, an alternative choice would be to discard the denominator and introduce t inside the exponential term of the numerator (as in $t - s$). This case is examined in Appendix A, Section A.2 and shown to produce results almost identical to Equation 7 results (also see Figure 6-3). Based on this comparison and the need to select only one distribution, only the modified exponential distribution given in Equation 7 is considered in the following.

The PDF p_{sg} (termed $p_{sg}(x,\lambda)$ in the Appendix A, Section A.2 computation) for the flaw-size distribution based on Equation 7 is given by Equation 8:

$$p_{sg}(s, \lambda_s, t) = \frac{\lambda_s \cdot e^{-\lambda_s \cdot s}}{1 - e^{-\lambda_s \cdot t}} \quad \text{with } 0 \leq s \leq t \quad (\text{Eq. 8})$$

As a reminder, in Equation 8 the variable of interest is the flaw size s , while λ_s and t are parameters.

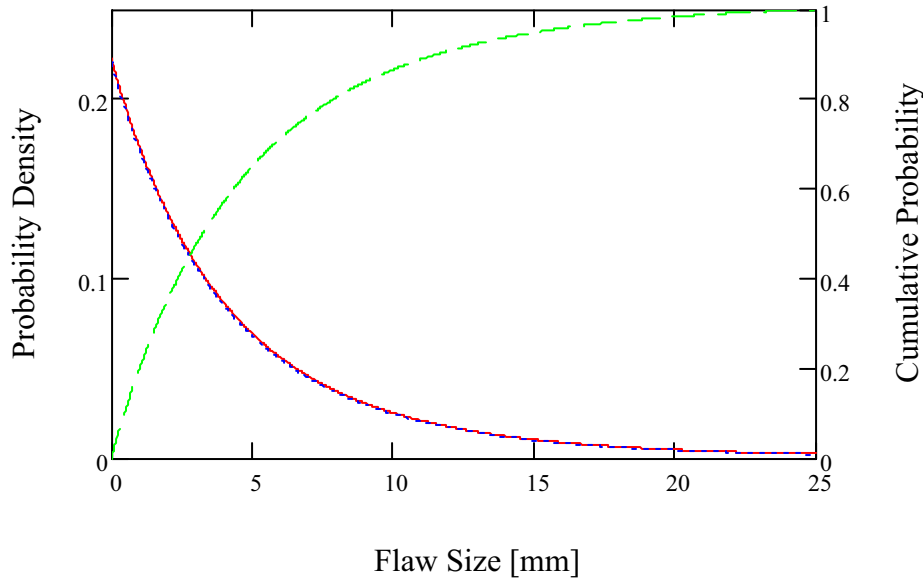
As complementary information, the PDF p_{msg} accounting for all possible values of λ_s , weighted by their probability, is calculated. The PDF p_{msg} (termed $p1(x)$ in Appendix A, Section A.2 computation) is a function of s , with parameter t , and is evaluated using Equation 9:

$$p_{msg}(s, t) = \int_0^{\infty} \frac{\lambda_s \cdot e^{-\lambda_s \cdot s}}{1 - e^{-\lambda_s \cdot t}} \cdot p_{\lambda_s}(\lambda_s) d\lambda_s \quad (\text{Eq. 9})$$

The associated CDF, P_{msg} (termed $P1(x)$ in Appendix A, Section A.2 computation), for the flaw size s (t being a parameter) is determined by Equation 10:

$$P_{msg}(s, t) = \int_0^s p_{msg}(u, t) du \quad (\text{Eq. 10})$$

Figure 6-3 shows P_{msg} for the outer lid weld ($t = 25$ mm).



Source: Computation, Appendix A, Section A.2.

NOTE: Initial flaw-size PDF is shown by the red line, its CDF by the green dashed line, and the alternate distribution by the blue dashed line.

Figure 6-3. Initial Flaw Size PDF and Its CDF Compared with the Alternate Distribution

In conclusion, the size s (in mm) of the flaws in the Y direction of a weld of thickness t (in mm) can be evaluated using the cumulative distribution $P_{sg}(s, \lambda_s, t)$ given in Equation 7. The flaw-size parameter λ_s has the PDF defined in Equation 6. The resulting mean flaw size is about 4.8 mm; quantile values of the flaw-size distribution are given in Appendix A, Section A.2.

6.3.1.3 Flaw Density

The flaw density is the mean number of flaws per volume of weld. The flaw density is investigated because it will enable prediction of the distribution of the number of flaws expected in each of the waste package closure welds. Appendix A, Section A.3 contains the numerical analyses discussed here in two parts: flaw-density parameter development and the marginal number of flaws per weld specimen.

Information on ultrasonic testing indications presented in Section 4.1.2.2 is used to characterize the flaw density of the significant flaws in the closure welds. In the total weld volume of the 16 specimen rings, $n_f = 7$ flaws were detected. Here, n_f is random while the volume of weld is fixed (V_f). This corresponds to Poisson sampling (Martz and Waller 1991 [DIRS 160924], pp. 254 and 255). According to Martz and Waller (1991 [DIRS 160924], p. 286), the noninformative prior distribution for λ_d (termed “x” in Appendix A, Section A.3) based on Poisson sampling is proportional to $\lambda_d^{-1/2}$. The resulting posterior PDF p_{λ_d} (termed $g_d(x)$ in Appendix A, Section A.3) of the flaw-density parameter λ_d is given in the same reference and presented here as Equation 11:

$$p_{\lambda_d}(\lambda_d) = \frac{V_f^{n_f+0.5}}{\Gamma(n_f+0.5)} \cdot \lambda_d^{n_f-0.5} \cdot e^{-\lambda_d \cdot V_f} \quad (\text{Eq. 11})$$

where V_f is the total specimen ring weld volume examined as described in Section 6.3.1.1.

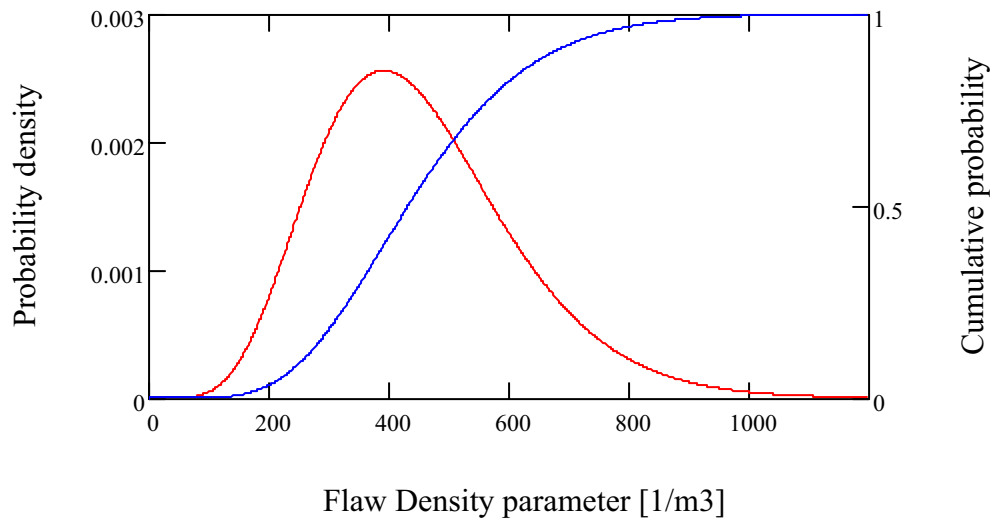
The associated CDF (termed $G_d(x)$ in Appendix A, Section A.3) is plotted with the probability density, given by Equation 11, in Figure 6-4.

A mean of 453 flaws per cubic meter of weld is determined (Appendix A, Section A.3). Quantile values of the flaw density distribution are also given in Appendix A, Section A.3.

In the second part, the marginal number of welds per weld specimen, a distribution was found that could adequately describe the number of flaws in any one closure weld (which takes discrete values); the Poisson distribution was chosen because it is a discrete distribution that is used for characterizing many processes. Given the total specimen ring weld volume, V_{sw} (in m^3), and a flaw-density parameter λ_d (termed as λ in Appendix A, Section A.3), the Poisson distribution characterizing the probability on the number of flaws n has the form shown in Equation 12 (Martz and Waller 1991 [DIRS 160924], pp. 254 and 255):

$$P_n(n, \lambda_d, V_{sw}) = e^{-\lambda_d \cdot V_{sw}} \times \frac{(\lambda_d \times V_{sw})^n}{n!} \quad (\text{Eq. 12})$$

The mean of this distribution is $\lambda_d \times V_{sw}$ (Martz and Waller 1991 [DIRS 160924], p. 17).



Source: Computation, Appendix A, Section A.3.

Figure 6-4. PDF and CDF for Flaw-Density Parameter before Ultrasonic Inspection

The volume of weld in a waste package is determined by using the same cross-sectional geometry as the specimen rings; therefore, the number of flaws to be expected will be governed by λ_d . The Bayesian approach with a noninformative prior is used for the PDF determination for the same reasons as those presented in Section 6.3.1.2.

Based on previous parameters, the number of flaws in the weld follows a Poisson distribution $P_n(n, \lambda_d, V_f)$ (Equation 12), with λ_d having the PDF given in Equation 11.

In conclusion, the probability on the number of flaws n in a volume of weld V_f can be evaluated using the Poisson distribution $P_n(n, \lambda_d, V_f)$ given in Equation 12. The flaw-density parameter λ_d has the PDF defined in Equation 11. Applying these equations to the current waste package design results in the flaw-expectation probabilities shown in Table 6-3.

Table 6-3. Expected Distribution of As-Welded Waste Package Weld Flaws (informational only)

Number of Weld Flaws	Probability
0	0.585
1	0.303
2	0.089
3	0.019
4	0.004

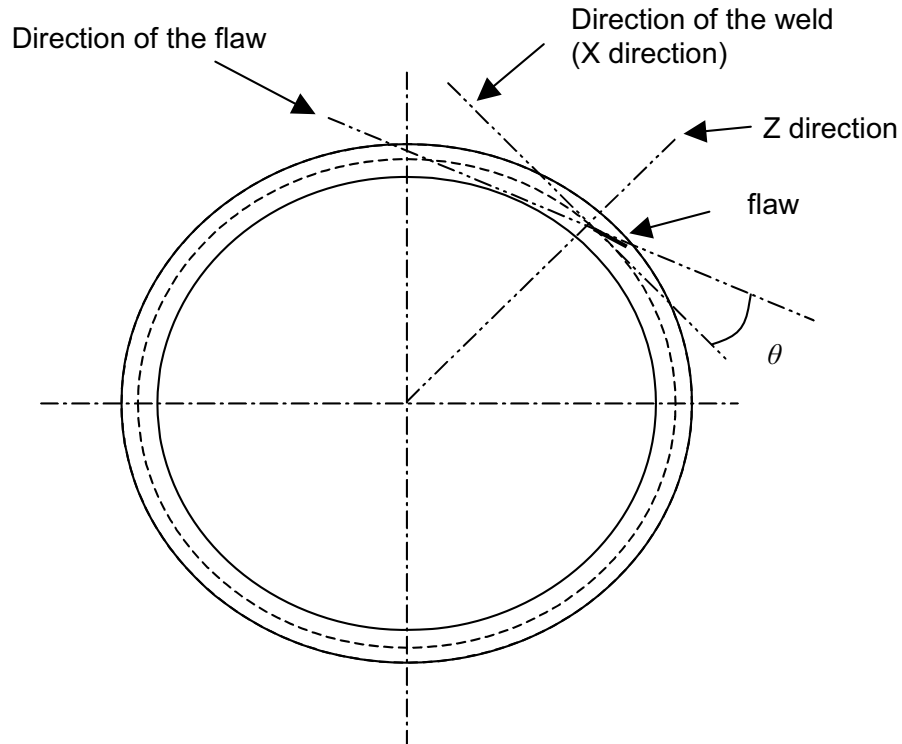
Source: Computation, Appendix A, Section A.3.

6.3.1.4 Flaw Depth

The flaw depth is the distance between the outer surface of the weld and the onset of the flaw in the Y direction (see Figure 4-1 for orientation of the Y direction). A uniform distribution is chosen to represent the flaw depth. Ultrasonic testing indications shown in Table 4-3 seem to indicate that flaws are scattered over the entire extent of the Y direction (0.97 in), but, with only seven data points, it is difficult to demonstrate this statistically. The welding process itself is comprised of multiple welding passes; this provides a mechanistic reason for a uniform distribution of flaws, since any particular layer of welding may contain a flaw.

6.3.1.5 Flaw Orientation

The orientation of the flaws is investigated in the plane of the specimen rings. The objective is to investigate the angle θ that the flaws make with the direction of the weld (see Figure 6-5 for a schematic representation). This is important in trying to determine an estimate of the flaws that have mostly a radial orientation (a broad definition of radially orientated flaws is those flaws that have an angle θ greater than 45°). These radially oriented flaws are able to propagate through-weld, being driven by the hoop stress. However, the more abundant circumferential flaws are less impacted by this driving hoop stress and are also unlikely to reorient (SNL 2007 [DIRS 177417], Section 6.3.4.3).



Source: For illustration only, to accompany analyses in Appendix A.

Figure 6-5. Schematic Representation of Flaw Orientation on Specimen Ring

Orientation of defects in welds has been investigated by Shcherbinskii and Myakishev (1970 [DIRS 149953]). They report that the angle between a defect and the direction of the weld can be fit to a centered normal distribution with a standard deviation of around 5° . Based on this information, the present analysis considers a centered normal distribution in trying to fit the Alloy 22 weld data available.

The fact that the distribution is chosen to be centered (i.e., with a mean of 0°) is logical since most of the defects observed are lack-of-fusion flaws, which typically are in the direction of the weld. The standard deviation of 5° is discarded from further consideration since the available data report a flaw with an angle of approximately 27° , which suggests a larger standard deviation. The flaw with an angle of approximately 27° is not a lack-of-fusion defect but results from a poor weld preparation (a flaw found on ring K (see Section 4.1.2.2) and angle values calculated in Appendix A, Section A.1 per Section 6.3.1.1). In a conservative approach, this flaw was kept in the analysis, though it is not representative of the highly controlled conditions under which operations will be conducted on the waste package, and in fact this specimen ring leads to a change in the weld geometry to a wider mouth opening. The standard deviation, σ , of the normal distribution is evaluated using the Bayesian approach with a noninformative prior. A noninformative prior is selected to put maximum emphasis on the information provided by the data.

Only the absolute values for θ are available, not their signs. Therefore, the distribution for θ is not normal by definition, since it is defined only by positive values. In fact, there are two possible initial angle values (one positive, one negative) that correspond to a single value of θ . Therefore, the actual PDF p_θ for θ is equal to twice the PDF of the centered normal distribution, with standard deviation σ . The PDF of a normal distribution is found in the study by Martz and Waller (1991 [DIRS 160924], p. 49), and the resulting PDF for θ is given in Equation 13:

$$p_\theta(\theta, \sigma) = 2 \cdot \frac{1}{\sigma \cdot \sqrt{2\pi}} \cdot \exp\left[-\frac{1}{2} \cdot \left(\frac{\theta}{\sigma}\right)^2\right] \text{ for } \theta \geq 0 \quad (\text{Eq. 13})$$

The corresponding CDF P_θ is given in Equation 14:

$$P_\theta(\theta, \sigma) = 2 \cdot \int_0^\theta \frac{1}{\sigma \cdot \sqrt{2\pi}} \cdot \exp\left[-\frac{1}{2} \cdot \left(\frac{u}{\sigma}\right)^2\right] du \quad (\text{Eq. 14})$$

Based on the work of Martz and Waller (1991 [DIRS 160924], pp. 225 and 226), a noninformative prior for σ when considering the quasi-normal PDF $p_\theta(\theta, \sigma)$ is $1/\sigma$.

Applying Bayes' theorem leads to the expression shown in Equation 15 for the posterior PDF p_σ of σ (Martz and Waller 1991 [DIRS 160924], pp. 174 and 175):

$$p_\sigma(\sigma) = \frac{L_\theta(\sigma)}{\int_0^\infty \frac{L_\theta(u)}{u} du} \quad (\text{Eq. 15})$$

where $L_\theta(\sigma) = \prod_{i=1}^{n_f} p_\theta(\theta_i, \sigma)$ is the likelihood function related to the $n_f = 7$ observed angles θ_i .

Based on the posterior PDF, the mean value of σ_m is calculated to be around 13.9° . The 5th and 95th percentiles are around 8.7° and 21.6° , respectively.

Based on the previous developments, the expected fraction of flaws, F_θ , that have an angle θ greater than 45° is calculated using the following formula:

$$F_\theta = \int_0^\infty [1 - P_\theta(45, \sigma)] \cdot p_\sigma(\sigma) d\sigma \quad (\text{Eq. 16})$$

This yields $F_\theta = 0.008$ (Appendix A, Section A.4). Therefore, around 0.8% of the weld flaws will have an angle greater than 45° .

In conclusion, investigation of flaw orientation has shown that almost all of the specimen-ring flaws are in the direction of the weld, in agreement with literature information. The fraction of flaws that are radially oriented (i.e., making an angle of 45° or more with respect to the direction of the weld) is 0.8% of the flaws.

6.3.1.6 Ultrasonic Inspection Characterization

This section investigates the PND of a flaw of size s in the Y direction using ultrasonic testing. The corresponding PND curve was not developed during the ultrasonic testing inspection of the specimen rings. Nevertheless, information from the literature and available results from ultrasonic testing inspection capability on the specimen rings were combined to elaborate a conservative ultrasonic testing PND curve that should overestimate the number of undetected closure-weld flaws. The analyses corresponding to this section are in Appendix A, Section A.5. A comparison of several PND curves for weld flaws using parameters identified in the literature and resulting in a conservative estimate is given in Figure 6-6.

Bush (1983 [DIRS 107696], pp. 13A.5.6 and 13A.5.7) summarizes the results of previous studies on ultrasonic testing reliability and provides parameter values for a PND curve (termed $P_{nd}(x, s_0, \nu)$ in Appendix A.5) defined in Equation 17:

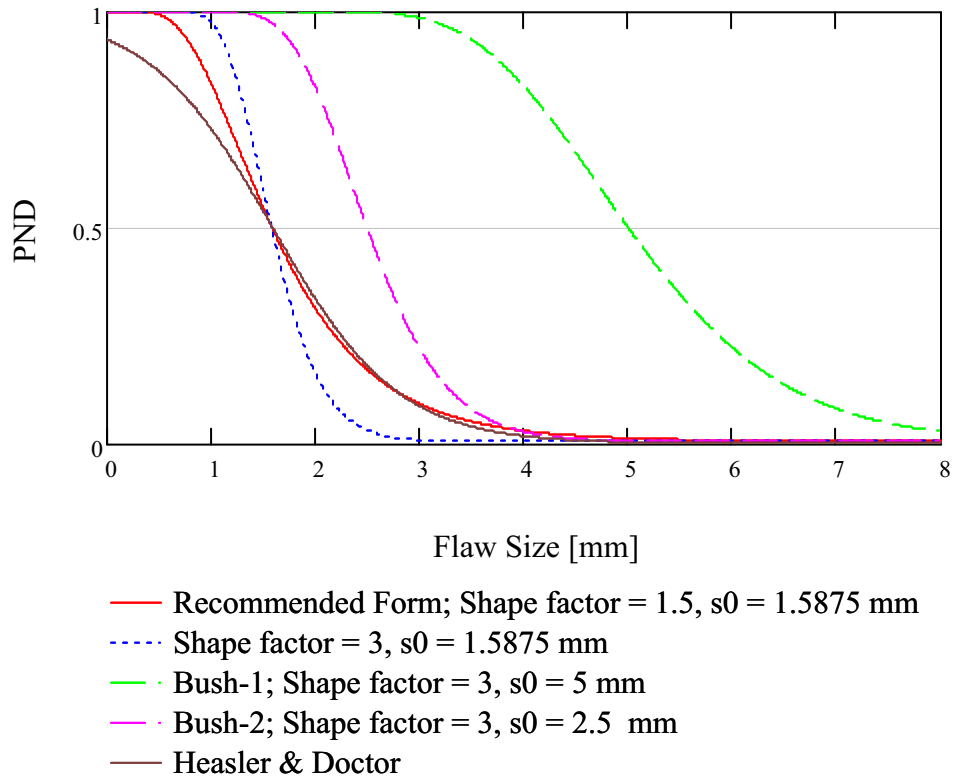
$$P_{ND}(s, \varepsilon_1, s_0, \nu) = \varepsilon_1 + \frac{1}{2} \cdot (1 - \varepsilon_1) \cdot \operatorname{erfc} \left[\nu \cdot \ln \left(\frac{s}{s_0} \right) \right] \quad (\text{Eq. 17})$$

where

- s = size of the flaw (in mm)
- ε_1 = lower limit of P_{ND}
- ν = shape factor
- s_0 = characteristic flaw size, in mm, which is the flaw size at the median of the P_{ND} distribution
- erfc = complementary error function.

In Equation 17, s is the variable while ε , ν , and s_0 are parameters.

Focusing on detection of intergranular SCC in austenitic piping, Bush (1983 [DIRS 107696], p. 13A.5.7) suggested the following parameter values: $\varepsilon_1 = 5 \times 10^{-3}$, $\nu = 3$, and $s_0 = 5$ mm or 2.5 mm (curves labeled respectively “Bush-1” and “Bush-2” in Figure 6-6). Because these results are based on experiments performed in the late 1970s, they reflect detection capabilities that have been significantly surpassed.



Source: Computation, Appendix A, Section A.5.

NOTE: See text for descriptions of curves; the red curve is recommended.

Figure 6-6. Comparison of Several Ultrasonic PND Curves

A more recent study on the use of ultrasonic testing to detect intergranular SCC in stainless steel, reported by Heasler and Doctor (1996 [DIRS 107758]), shows significantly improved reliability. This reference provides the parameters for a logistic function giving the probability of detection as a function of flaw size (s) for nearside access (i.e., the defect is located on the accessible side of the weld centerline). The PND curve based on the study by Heasler and Doctor (1996 [DIRS 107758], p. 5.1) has the form shown in Equation 18 (from Appendix A.5 and labeled as “Heasler & Doctor” in Figure 6-6):

$$P_{nd2}(s, \beta_1, \beta_2) = 1 - \frac{1}{1 + \exp(-\beta_1 - \beta_2 \times s)} \quad (\text{Eq. 18})$$

where

- s = flaw size in mm
- β_1 = -2.67 (based on Heasler and Doctor 1996 [DIRS 107758], p. 5.9)
- β_2 = $1.6709/\text{mm}$ (based on Heasler and Doctor 1996 [DIRS 107758], p. 5.9).

The median value for the Heasler and Doctor distribution (Equation 18) with the given parameters is

$$P_{nd2}(0.5, \beta_1, \beta_s) = \frac{-\beta_1}{\beta_2} = 1.598.$$

A weld-flaw detection criterion equal to or greater than 1/16 in (1.5875 mm) has been assumed for the fabrication of waste packages (Assumption 5.1, Section 5). This detection criterion specifies that the ultrasonic testing inspection method employed will therefore be able to detect all weld flaws equal to or greater than approximately 1.6 mm (i.e., a PND = 0.0 at this size and larger). A way to account for finer detection requirement and capability and to obtain a reasonable level of uncertainty in the ultrasonic testing inspection process is to reduce the value of s_0 in Equation 17. Based on the design assumption (Assumption 5.1, Section 5) specifying the detection of weld flaws at 1/16 in (1.5875 mm) or greater, and on the improved ultrasonic testing detection results shown by Equation 18, s_0 is set at 1/16 in (1.5875 mm). This value is the median of the PND uncertainty distribution and represents that, for postclosure analysis purposes, half of the flaws of this size will be detected.

The other two parameters implemented to determine PND of weld flaws are: (1) the lower limit of PND from *Reliability of Nondestructive Examination* (Bush 1983 [DIRS 107696], p. 13A.5.7) taken directly from the recommendation in that study ($\varepsilon_l = 5 \times 10^{-3}$, used in Equation 17), and (2) the shape factor (ν) modified as follows. The shape factor of 3, as determined by Bush (1983 [DIRS 107696]), is tailored to the less-sensitive detection techniques of that time. A smaller shape factor is more appropriate for use with a smaller s_0 ; the larger value gives a very steep PND response (labeled “Shape factor = 3” in Figure 6-6), and a smaller value provides for a more uncertain distribution. A shape value of $\nu = 1.5$ is specifically chosen because it then follows the tail of the more recent results from *Piping Inspection Round Robin* (Heasler and Doctor 1996 [DIRS 107758]) represented in Equation 18 (red curve labeled as “Recommended Form” in Figure 6-6). All PND curves discussed are shown in Figure 6-6. The equation from *Piping Inspection Round Robin* (Heasler and Doctor 1996 [DIRS 107758]) is not deemed appropriate for direct use because its PND does not approach 1.0 (no detection possible) as the flaw size approaches zero; therefore, it is not physically realistic.

As mentioned in Section 4.1.2.2, the ultrasonic testing inspection threshold employed in the examination of the specimen rings had a sensitivity of 1 mm, which calls for detection of flaws of this size or larger. This was confirmed by metallographic examination of the specimen rings: no flaws larger than 1 mm were found by metallographic testing that had not already been detected through the ultrasonic testing inspections. Therefore, any of the ultrasonic testing PND curves shown in Figure 6-6 appear to display less detection capability than what is attainable on waste package closure welds using current industry equipment.

Based on the information given previously, an acceptable ultrasonic testing PND curve, applicable to the waste package closure weld, is given in Equation 17 with the following parameter values: $\varepsilon_l = 5 \times 10^{-3}$, $\nu = 1.5$, and $s_0 = 1/16$ in (1.5875 mm). This ultrasonic testing PND curve is used in the following sections to develop the flaw density and size distributions of the flaws remaining in the weld after inspection and repair.

6.3.1.7 Undetected Flaw Size Distribution in the Y-Direction

The flaws that are detected during ultrasonic testing inspection will be evaluated in accordance with the ASME code. In the event that a flaw is identified, it will be evaluated to determine whether it meets code requirements. If any flaw does not meet code requirements, it will be removed by repair welding. Additionally, a YMP criterion of 1/16 in is applied for determining the minimum flaw-detection size (Assumption 5.1, Section 5).

The repair of weld flaws may affect the results for flaw-depth distribution and flaw orientation of Sections 6.3.1.4 and 6.3.1.5. This means that the flaw-depth distribution will no longer be uniform but may result in fewer flaws at or near the weld surface. Nevertheless, following an approach to preserve the greatest number of weld flaws, the results of Sections 6.3.1.4 and 6.3.1.5 are considered adequate to characterize the flaw-depth distribution and the flaw orientation in the closure welds that have been inspected and repaired.

For those flaws that go undetected, Equation 8 in Section 6.3.1.2 gives the PDF for the flaw-size distribution (p_{sg}) of flaws of size s in the Y direction based on welds of thickness t prior to ultrasonic testing inspection. It is a function of the random parameter λ_s whose PDF is given by Equation 6.

The ultrasonic testing inspection and subsequent weld repair are characterized by the ultrasonic testing PND curve P_{NDI} given in Equation 17 with the parameter values: $\varepsilon_l = 5 \times 10^{-3}$, $\nu = 1.5$ and $s_0 = 1.5875$ mm.

Using the calculated value of λ_s , the fraction of flaws that remain in the closure weld after ultrasonic testing inspection and weld repair is calculated with the convolution equation shown in Equation 19 (termed $F_{nd}(x)$ in Appendix A.6):

$$F_{ND}(t, \lambda_s, \varepsilon_1, s_0, \nu) = \int_0^t p_{sg}(s, \lambda_s, t) \cdot P_{NDI}(s, \varepsilon_1, s_0, \nu) ds \quad (\text{Eq. 19})$$

Equation 19 is sampled in the final determination of the postinspection weld-flaw density (given as Equation 23) in the following section. None of the following PDF or CDF equations are propagated forward; they are used here only as a check for a sample flaw-size distribution.

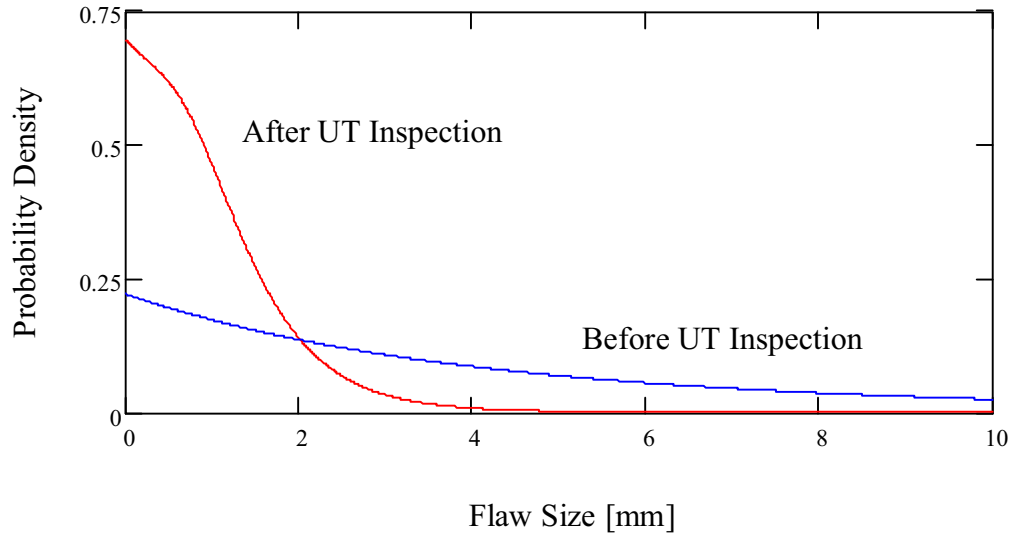
As complementary information and as a check on the reasonableness of the results, p_{sgUT} , the PDF for the size of the remaining flaws accounting for all possible values of λ_s (f_s in Appendix A, Section A.2), weighted by their probability, can be calculated using Equation 20 (termed $p_{sgUT}(s)$ in Appendix A, Section A.6):

$$p_{sgUT}(s, t, \varepsilon_1, s_0, \nu) = \int_0^\infty \frac{p_{sg}(s, \lambda_s, t) \cdot P_{NDI}(s, \varepsilon_1, s_0, \nu)}{F_{ND}(t, \lambda_s, \varepsilon_1, s_0, \nu)} \cdot p_{\lambda_s}(\lambda_s) d\lambda_s \quad (\text{Eq. 20})$$

The corresponding CDF is given as Equation 21 (termed $P_{sgUT}(x)$ in Appendix A, Section A.6):

$$P_{sgUT}(s, t, \varepsilon, s_0, \nu) = \int_0^s p_{sgUT}(u, t, \varepsilon, s_0, \nu) du \quad (\text{Eq. 21})$$

Figure 6-7 shows $p_{sgUT}(s, t, \varepsilon_1, s_0, \nu)$ for $t = 25$ mm, which corresponds to the size distribution of the flaws remaining in the specimen ring weld (or the similar outer-lid weld of the waste package) after ultrasonic testing inspection and repair. Note that the PDF and CDF, Equations 20 and 21, respectively, do account for all possible values of λ_s , weighted by their probability. Because the quantity of computational results is quite extensive for graphical purposes, the CDF has not been included in Figure 6-7.



Source: Appendix A, Section A.6.

Figure 6-7. PDF for Flaw Size before and after Ultrasonic Inspection and Repair in 25-mm-Thick Weld

The corresponding mean size for the flaws remaining in the 25-mm-thick weld is given by Equation 22:

$$s_{mgUT}(t, \varepsilon_1, s_0, \nu) = \int_0^t p_{sgUT}(u, t, \varepsilon_1, s_0, \nu) \cdot u \, du \quad (\text{Eq. 22})$$

Results yield a mean value of 1.0 mm, with the 5th and 95th percentiles calculated from Equation 21 yielding, respectively, 7×10^{-2} and 2.6 mm (Appendix A, Section A.6). After inspection, about 19% of the remaining weld flaws are equal to or greater than 1/16 in (1.5875 mm) in size.

6.3.1.8 Inspected Flaw Density

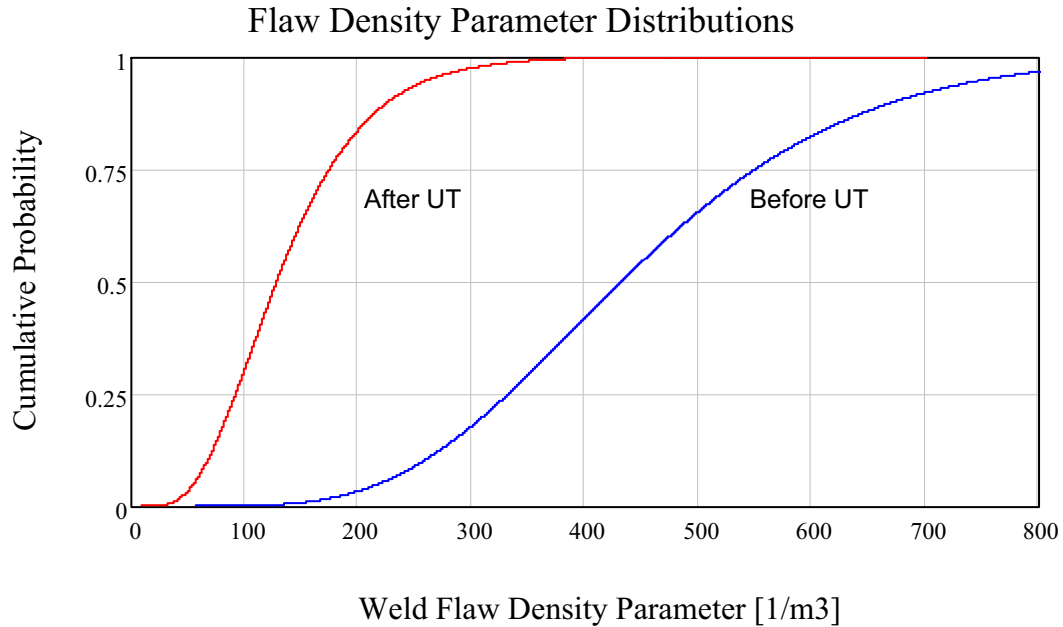
As discussed in Section 6.3.1.3, before ultrasonic testing inspection, the mean number of flaws per volume of weld is given by the flaw-density parameter λ_d , whose PDF is shown in Equation 11. After ultrasonic testing inspection and repair, the mean number of remaining flaws per cubic meter of weld, λ_{dPR} , will be equal to λ_d , adjusted by the fraction F_{ND} of flaws that will not be detected. This corresponds to Equation 23:

$$\lambda_{dPR}(\lambda_d, \lambda_s, t, \varepsilon_1, s_0, \nu) = \lambda_d \cdot F_{ND}(t, \lambda_s, \varepsilon_1, s_0, \nu) \quad (\text{Eq. 23})$$

where F_{ND} is evaluated with Equation 19.

In Equation 23, λ_{dPR} is a function of two independent random parameters (λ_d and λ_s), and four fixed parameters (t , ε_I , s_0 , and ν).

As complementary information, the CDF of λ_{dPR} , accounting for all possible values of λ_s and λ_d , weighted by their probability, is calculated using a Monte-Carlo random sampling. Figure 6-8 shows the resulting CDF curve from 50,000 samples (Appendix A, Section A.7) as compared to the pre-inspection weld-flaw density.



Source: Computation, Appendix A, Section A.7.

NOTE: The blue line is the weld-flaw density before ultrasonic testing and repair; the red line is the density after ultrasonic testing and repair.

Figure 6-8. CDF of Weld-Flaw Density before and after Ultrasonic Inspection and Repair in 25 mm-Thick Weld

In conclusion, the probability of the number of flaws n remaining in a weld of volume V (in m^3) after ultrasonic testing inspection and repair is calculated using the Poisson distribution given in Equation 24 (used in Appendix A, Section A.7):

$$P_{mut}(n, \lambda_{dPR}, V) = e^{-\lambda_{dPR} \cdot V} \cdot \frac{(\lambda_{dPR} \cdot V)^n}{n!} \tag{Eq. 24}$$

where λ_{dPR} is estimated based on Equation 23. The probabilities of having various numbers of undetected weld flaws in a waste package outer closure weld volume are given in Section 6.3.1.9.

6.3.1.9 Summary of Results and Comparison

In this section, the information needed to calculate the characteristics of the flaws expected in the waste package welds is summarized in Tables 6-4 and 6-5. Example results are summarized in Table 6-6, based upon the current TAD canister-containing waste-package design (see Appendix A, Section A.7 for the computations).

Table 6-4. Parameters Needed for Calculating Weld-Flaw Characteristics

Type of Parameter	Symbol	Description	Numerical Value or Related Equation	See Notes
Random variable	s	Flaw size in the Y direction	See Table 6-5	
	n	Number of flaws in the weld	See Table 6-5	
Fixed parameter	t	Thickness of the weld, representative for specimen rings and waste package closure welds	25 mm (rounded value)	a
	n_f	Number of ultrasonic testing indications in specimen rings	7	b
	s_t	Sum of ultrasonic testing indication sizes in the Y direction	31.75 mm	c
	V_f	Total volume of welds examined in specimen rings	$1.656 \times 10^{-2} \text{ m}^3$	c
	ϵ_l	Lower limit for ultrasonic testing PND	0.005	d
	s_0	Characteristic flaw size for ultrasonic testing PND	1.5875 mm	e
	ν	Shape factor for ultrasonic testing PND	1.5	e
Random parameter	λ_s	Flaw size parameter in the Y direction (in mm^{-1})	PDF: Equation 6	
	λ_d	Flaw density parameter (flaws per cubic meter of weld)	PDF: Equation 11	

NOTES: a. See Table 4-2, distance OC.
 b. See Table 4-3.
 c. See Appendix A, Section A.1.
 d. See Table 4-4.
 e. See Section 6.3.1.6.

Table 6-5. Parameter Summary for Evaluating Flaw Characteristics

Flaw Characteristic	Before Ultrasonic Inspection	After Ultrasonic Inspection and Weld Repair
Flaw size (s, in mm)	CDF P_{sg} given in Equation 7 Secondary equation: Equation 2 Parameters: λ_s, t, n_f, s_t	CDF P_{sgut} given in Equation 21 Secondary equations: Equations 6, 8, 17, 19 Parameters: $\lambda_s, t, n_f, s_t, \epsilon_1, s_0, v$
Flaw number (n)	Poisson distribution: Equation 12 Secondary equation: Equation 11 Parameters: λ_d, V, n_f, V_f	Poisson distribution: Equation 24 Secondary equations: Equations 6, 8, 11, 17, 19, 23 Parameters: $\lambda_d, V, n_f, V_f, \lambda_s, t, \epsilon_1, s_0, v, s_t$
Flaw orientation ^a	Of the flaws, 0.8% are radially oriented	Of the flaws, 0.8% are radially oriented
Flaw depth ^b	Uniform distribution on weld thickness	Uniform distribution on weld thickness

^a Calculated in Section 6.3.1.5.

^b Discussed in Section 6.3.1.4.

Table 6-6 shows the mean, the 5th, and the 95th percentiles of the predicted flaw sizes, before ultrasonic inspection (Equation 10) and after ultrasonic inspection and weld repair (Equation 21). These values are calculated based on the distribution of the flaw size, weighted with the probability values assumed by λ_s .

Table 6-6 also shows the probability of having zero, one, and two or more flaws in the welds of the waste package before ultrasonic inspection, and after ultrasonic inspection and weld repair. The results in this table are only an example determination, and TSPA will determine these results as needed for its use.

Table 6-6. Main Characteristics of Flaws in Welds of Waste Package (informational only)

	Weld Flaw Size ^a (mm)			Probability of Number of Flaws ^b		
	Mean	5th percentile	95th percentile	0	1	2 or more
Before ultrasonic inspection	4.8	0.23	15.2	0.585	0.303	0.112
After ultrasonic inspection and weld repair	1.0	0.072	2.6	0.844	0.140	0.015

^a Flaw sizes are given with two significant figures. MathCAD® results in Appendix A, Sections A.2 and A.6.

^b Probability values on number of flaws are the rounded MathCAD® results in Appendix A, Sections A.3 and A.7.

6.3.2 Improper Base-Metal Selection for Waste Package Outer Corrosion Barrier

In the absence of data on the likelihood of making improper material selections, the basis for the probability distribution associated with this type of event is the similarity between the operations of selecting materials for fabrication and selecting weld filler material. The improper selection of weld material affecting a significant weld population is documented in response to NRC Bulletin 78-12 (NRC 1978 [DIRS 165403]), which was prompted by the discovery that the weld chemistry of a portion of the Crystal River 3 surveillance-block weld did not meet the specification requirements. In the preparation of a response to the bulletin, Babcock & Wilcox (1979 [DIRS 108219]) investigated their records to determine the extent to which out-of-specification weld wire may have been used in the fabrication of reactor vessels. Their findings showed that, out of 1,706,556 pounds of weld wire (Babcock & Wilcox 1979 [DIRS 108219],

p. I-6) (rounded to 1,707,000 pounds) used to make 43 reactor vessels for the American market (Babcock & Wilcox 1979 [DIRS 108219], Table 1 of Part II), an estimated 65 to 350 pounds of weld wire were out of specification (Babcock & Wilcox 1979 [DIRS 108219], pp. 2 and I-4). From this estimate, the range for the probability of using improper welding material is estimated to be from 3.81×10^{-5} (65/1,707,000) to 2.05×10^{-4} (350/1,707,000) per selection event.

The information provided in *Records Investigation Report Related to Off-Chemistry Welds in Material Surveillance Specimens and Response to IE Bulletins 78-12 and 78-12A – Supplement* (Babcock & Wilcox 1979 [DIRS 108219]) is not sufficient in itself to draw conclusions about the shape of the distribution for the probability of using improper welding material. However, it is assumed that this type of error can be represented by an HEP (Assumption 5.2, Section 5). Thus, based on Assumption 5.2, the lower and upper bounds for the probability range associated with an improper choice of material, as discussed, are assigned as the 5th and the 95th percentiles, respectively. HEPs used in this analysis are summarized in Table 4-1. From Equations 1 through 4, the median value is 8.84×10^{-5} with an error factor of 2.32 yielding a mean value of 1.01×10^{-4} for improper material selection errors.

Babcock & Wilcox (1979 [DIRS 108219]) concluded that the evolution of shop practices as of 1979 had virtually eliminated the possibility that improper weld material would be used in the fabrication of a reactor vessel. New instrumentation, such as portable X-ray spectroscopy equipment, makes it possible to perform quick field measurements of material compositions (ASM International 1990 [DIRS 106780], pp. 1,030 to 1,032). However, there is still the possibility that the technician in charge of this work could fail to perform the operation correctly. This HEP is represented by the probability (distributed lognormally) of improperly reading and recording a digital display (Item 2 of Table 4-1), which has a median of 1×10^{-3} and an error factor of 3, providing a mean value of 1.25×10^{-3} from Equation 4.

Thus, the likelihood of selecting improper base metal material in the fabrication of the outer corrosion barrier of the waste package (BM_FLAW) follows a lognormal distribution having a mean value rounded to 1.0×10^{-4} and an error factor rounded up to 3. The probability that the error is not detected (CHECK_BM_FLAW) has a mean value of 1.25×10^{-3} and an error factor of 3.

The event tree for evaluating an improper base metal selection process is shown in Figure 6-9. Sequence branch #2 represents the detection of the use of improper base metal and leads to rejection of the item.

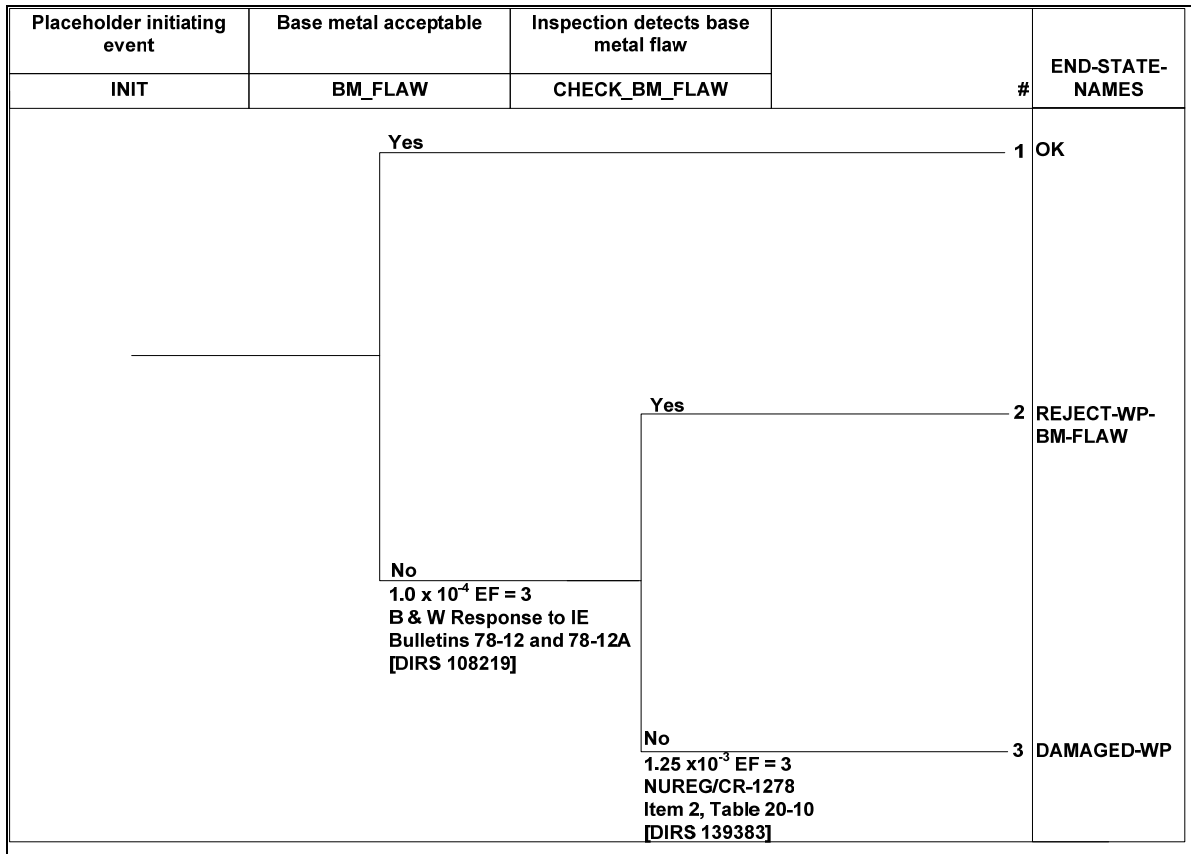


Figure 6-9. Event Tree for Evaluating Improper Base Metal Selection for Waste Package Outer Corrosion Barrier

6.3.3 Improper Heat-Treatment Implementation for Waste Package Outer Corrosion Barrier

Heat treatment of the outer corrosion barrier of the waste package can be controlled by any suitable method of heating and cooling, provided the required heating and cooling rates, metal temperature uniformity, and temperature control are maintained (SNL 2007 [DIRS 179394], Table 4-1, Item 03-20). Such controls are assumed to be integrated into the heat treatment facility independent of the objects being processed (Assumption 5.10, Section 5). The heat treatment, however, must provide for heating of the entire outer corrosion barrier with the exception of the closure lid as a single application. Quenching in a water bath to achieve the minimum quenching rate for the outer corrosion barrier (SNL 2007 [DIRS 179394], Table 4-1, Item 03-20) is evaluated in this report. Auxiliary instrumentation associated with the heat treatment of the outer corrosion barrier uses calibrated thermocouples in contact with the material while protecting them from direct contact with water. These thermocouples monitor the operation and provide a record of the heat treatment and solution annealing process. Such records are maintained for the quality assurance documentation and can be inspected as a check that the annealing process followed the procedures correctly. The solution-annealing operation following the heat treatment is a time-sensitive operation, and particular attention must be paid to this part of the process in order to achieve proper annealing. The final machining of the inner diameter of the outer corrosion barrier, if required, and of the final closure weld area will be performed after the solution-annealing process is complete.

The outer corrosion barrier is to be furnace-heated at a temperature of 2,050°F + 50°F/−0°F for a minimum of 20 minutes (no maximum specified) and then quenched. Cooling will be achieved by immersion in water or spray quenching with water. The cooling rate for the entire outer corrosion barrier will be greater than 275°F/min from soak temperature to less than 700°F (SNL 2007 [DIRS 179394], Table 4-1, Item 03-20 and Section 4.1.2.2) to avoid a phase transition during cooling. The quench delay (time from removal from furnace to start of quench) needs to be sufficiently limited to assure that the quench initiation starts at 2,020°F or higher. Since it is expected that the outer corrosion barrier will be quenched in an inverted position (Assumption 5.6, Section 5), a snorkel must be installed on the interior of the outer corrosion barrier to permit the interior to fill rapidly if immersion quenching is selected. The quench rate is specified to be greater than 275°F/min, and, based on a rate that is on the order of 300°F/min, the quenching operation will require approximately four minutes to complete. Thus, it is reasonable that the makeup water system must operate for at least six minutes to be at capacity when needed. It is assumed that this last phase of the heat treatment of the waste package outer corrosion barrier (i.e., removal from the furnace and quenching) is the critical part of the process (Assumption 5.4, Section 5), and the analysis of the heat treatment process focuses on this phase. It is expected that the outer corrosion barrier will be moved into the heat treatment facility and then to the quench chamber by a crane, since this type of handling equipment is the most suitable for such large and non-compact objects as the outer corrosion barrier.

While fabrication processes for the waste package outer corrosion barrier have not been finalized (Section 5), prototypes have been fabricated that provide collaborative support for the assumptions concerning fabrication processes. In particular, a full-sized Alloy 22 prototype outer corrosion barrier was furnace-heated in an inverted position and subsequently tank-quenched on both sides using two pipes for purging internal gases. Figure C-1 in Appendix C shows the outer corrosion barrier being lowered by a crane into the quench tank. Figure C-2 in Appendix C shows the postannealed outer corrosion barrier with the purge piping still attached.

The probability that the waste package outer corrosion barrier will be subjected to an improper heat treatment, without the error being detected prior to emplacement in the repository, is a combination of human error and process failure probabilities where the HEPs follow lognormal distributions, and the process failure probabilities are point values. It is assumed that process failure probabilities, usually given as point or rate values, can be represented as the mean value of a distribution assumed to be lognormal (Assumption 5.3, Section 5). Error factors were thus assigned to point values to provide a range for uncertainty in the values. Heat treatment of the waste package inner vessel is not evaluated, since no special heat-treatment process is specified for the inner vessel, except that maximum temperatures associated with welding have been specified (BSC 2006 [DIRS 180190], Section 5.5.1.3A); these maximum temperatures are cited in *Total System Performance Assessment Data Input Package for Requirements Analysis for TAD Canister and Related Waste Package Overpack Physical Attributes Basis for Performance Assessment* (SNL 2007 [DIRS 179394], Section 4.1.2.2).

The event tree for evaluating an improper heat treatment for the waste package outer corrosion barrier is shown in Figure 6-10. Five events in the heat treatment process that could lead to an improper heat treatment combined into event sequences are considered in this evaluation. These events are as follows:

- The first top event (Figure 6-10, HT_SHELL_MOVE_WP) tests whether or not the outer corrosion barrier is moved from the heat treatment facility to the quench facility within the time constraint necessary to maintain the outer corrosion barrier temperature \geq the 2,020°F quench initiation temperature. The top branch represents success and the lower branch failure. This event is evaluated through a fault tree containing two basic events, CRANE_MALFUNCTION and CRANE_OPERATOR_ERROR as shown in Figure B-4 in Appendix B.

Complete failure of the crane system (e.g., stops for some extended period) would be readily apparent and the heat treatment operation repeated. Thus, a crane malfunction is identified as an undetected equipment-operating problem where the crane fails to move the outer corrosion barrier from the heat treatment facility to the quench tank within the required time limit such that the outer corrosion barrier temperature drops below the specified quench initiation temperature. This could be caused by degradation of the supply power, cable entanglement, etc. that slows, but does not halt the operation. The crane malfunctioning probability is represented by a median value of 3×10^{-3} (Assumption 5.7, Section 5) with an error factor of 3 that is assumed to provide an upper bound on the probability of mechanical malfunctions of moving equipment. Using Equation 4 results in a mean value for the probability distribution of 3.75×10^{-3} per event.

The crane operator error is identified as the failure to recognize or respond to the crane malfunction while the operation is in progress. This error would result in delay in moving the outer corrosion barrier from the heat treatment facility to the quench tank and allowing the process to continue. This event is represented by the HEP “failure to complete a change of state...” (Item 7 of Table 4-1) that has a median value of 3×10^{-3} , a mean value of 3.75×10^{-3} , and an error factor of 3.

- As stated in the description of the top event (HT_SHELL_MOVE_WP), it is expected that travel time between the furnace and the quench facility must be sufficiently short to maintain the temperature above the minimum quench initiation temperature (set at 2,020°F). It is expected that the maximum time allowable for the move, adjusted for local conditions, will be monitored with a timer system equipped with recording capability and an alarm. The top event (Figure 6-10, HT_SHELL_MOVE_CHECK_WP) tests whether or not the outer corrosion barrier movement from the heat treatment facility to the quench facility within the specified time constraint is successful and properly monitored. The top branch represents success and the lower branch failure. While this check is normally operative for all moves, a failure of the check process only has consequences for outer corrosion barrier move failures. This event is evaluated through a fault tree containing two basic events, TIMER_FAILURE and HT_OPERATOR_ERROR, as shown in Figure B-5 in Appendix B.

The timer error (TIMER_FAILURE) is identified as a failure of alarm to operate, which could be due either to improper operation of the clock or the alarm not functioning; thus the operator is not alerted to the move error. The failure probability is represented by a mean value of 1.2×10^{-4} with an error factor of 10 derived from the item "I & C alarm fails to alarm" (Blanton and Eide 1993 [DIRS 141700], Table 6f), which lists the failure rate as 3×10^{-5} per hour. Since the change in temperature during the move is small, a duration time of two minutes is assumed for this operation. However, the alarm system is assumed to be in an operational state during the heat treatment process (Assumption 5.5, Section 5). Thus, based on having two such heat treatments scheduled per shift, the demand period for the alarm system is four hours. The probability of the alarm failure during the demand period is represented by a failure rate of 3×10^{-5} /hour and a mission time of four hours with an error factor of 10.

The operator error (HT_OPERATOR_ERROR) is identified as failure of the process operator to respond to the alarm signal that the process was not operating properly. This event is represented by the HEP "failure to respond to a compelling signal" (Benhardt et al. 1994 [DIRS 157684], Table 4, Item 2), a low-probability item with a median value of 1.1×10^{-3} , a mean value of 3×10^{-3} , and an error factor of 10.

- The top event (Figure 6-10, HT_SHELL_QUENCH_WP) tests whether the outer corrosion barrier is quenched according to the specifications for cooling, specifically that the cooling water is applied to all surfaces interior as well as exterior to the outer corrosion barrier and that the water supply is sufficient to maintain the minimum rate of cooling required; the top branch represents success and the lower branch failure. This event is evaluated through a fault tree containing two basic events, SNORKEL_ATTACHMENT_FAIL and MAKEUP_WATER_SYSTEM_FAIL as shown in Figure B-6, Appendix B.

The most likely failure mode for the snorkel is an improper attachment that does not allow gases to escape as the outer corrosion barrier is being immersed and cooled. Blockage of the snorkel is expected to be improbable, since any such object would necessarily be large. To assure that sufficient water is available during the quench period, it is assumed that a recirculation or makeup system will be used. While several potential failure mechanisms can be postulated, any failures of this system are expected to be dominated by a failure of the makeup valve to open; therefore, the failure of recirculation or makeup will be bounded by such a failure. This type of failure is represented in this analysis as a failure of the inlet valve to fully open or the recirculation system to be fully functional, i.e., at capacity. For example, a complete failure of the valve or recirculation system to operate would very likely be observed by the operator and the process terminated. The probability of a failure to properly attach the snorkel (SNORKEL_ATTACHMENT_FAIL) is represented by an HEP derived from the low-probability item "failure of administrative control" (Benhardt et al. 1994 [DIRS 157684], Table 4, Item 1) that has a median value of 1.9×10^{-4} , a mean value of 5×10^{-4} , and an error factor of 10.

The probability of a failure of the inlet valve or recirculation system to fully function (MAKEUP_WATER_SYSTEM_FAIL) is represented by a probability derived from the item, “motor operated valve fails to open” (Blanton and Eide 1993 [DIRS 141700], Table 6a), which lists the failure rate as 3×10^{-3} per demand. Thus, the partial failure of the makeup water system to operate is set to 3×10^{-3} with an error factor of 5, since the system is only required once during the heat-treatment process.

- The top event (Figure 6-10, HT_SHELL_QNCH_CHK_WP) tests whether or not the outer corrosion barrier quenching is properly monitored where the top branch represents success and the lower branch represents failure. Processes that could result in an incorrect monitoring of the outer corrosion barrier quench process include improperly installed thermocouples or operator failure to respond to a signal (alarm) that the monitoring system was not functioning correctly. While this check is normally operative for all quenching operations, its second purpose is as a check that the quench process was carried out correctly. A failure of the monitoring system only has consequences for barriers in the postclosure era for otherwise previously undetected failures of the outer corrosion barrier quench process. If this process check is not executed properly, the initial error will remain undetected. This event is evaluated through a fault tree containing three basic events, WP_SHELL_TC_INSTALL, WP_SHELL_TC_CHECK, and HT_OPERATOR_ERROR as shown in Figure B-7, where WP_SHELL_TC_INSTALL and WP_SHELL_TC_CHECK evaluate the thermocouple failure probability.

The basic event, WP_SHELL_TC_INSTALL, is represented by an HEP derived from “failure to use written test or calibration procedure” (Item 1 of Table 4-1) that has a median value of 5×10^{-2} , a mean (rounded) value of 8.1×10^{-2} , and an error factor of 5.

It is expected that the thermocouple installation will be independently checked. The checker error, WP_SHELL_TC_CHECK, is identified as a failure to detect the installer’s error. This event is represented by the HEP derived from “checker failure to detect an error made by others...” (Item 6 of Table 4-1) that has a median value of 1×10^{-1} , a mean value of 1.6×10^{-1} , and an error factor of 5.

The operator error, HT_OPERATOR_ERROR, is identified as failure of the process operator to respond to the alarm signal that the process was not operating properly. This event is represented by the HEP “failure to respond to a compelling signal” (Benhardt et al. 1994 [DIRS 157684], Table 4, Item 2) low type probability that has a median value of 1.1×10^{-3} , a mean value of 3×10^{-3} , and an error factor of 10.

- The top event (Figure 6-10, HT_INSPECT_WP) tests whether a postprocessing inspection of the log of the outer corrosion barrier heat-treatment process detects whether the process was performed correctly, where the top branch represents success and the lower branch failure. While this check is normally operative for all quenching operations for quality control documentation, its second purpose is as a check that the annealing process followed the procedures correctly. Thus, a failure of the thermocouple monitor only has barrier performance consequences for otherwise undetected outer corrosion barrier quench

process failures. If this process check is not executed properly, the initial error will remain undetected. This event is represented by the HEP derived from “checker failure to detect an error made by others ...” (Item 6 of Table 4-1) that has a median value of 1×10^{-1} per demand, a mean value of 1.6×10^{-1} , and an error factor of 5.

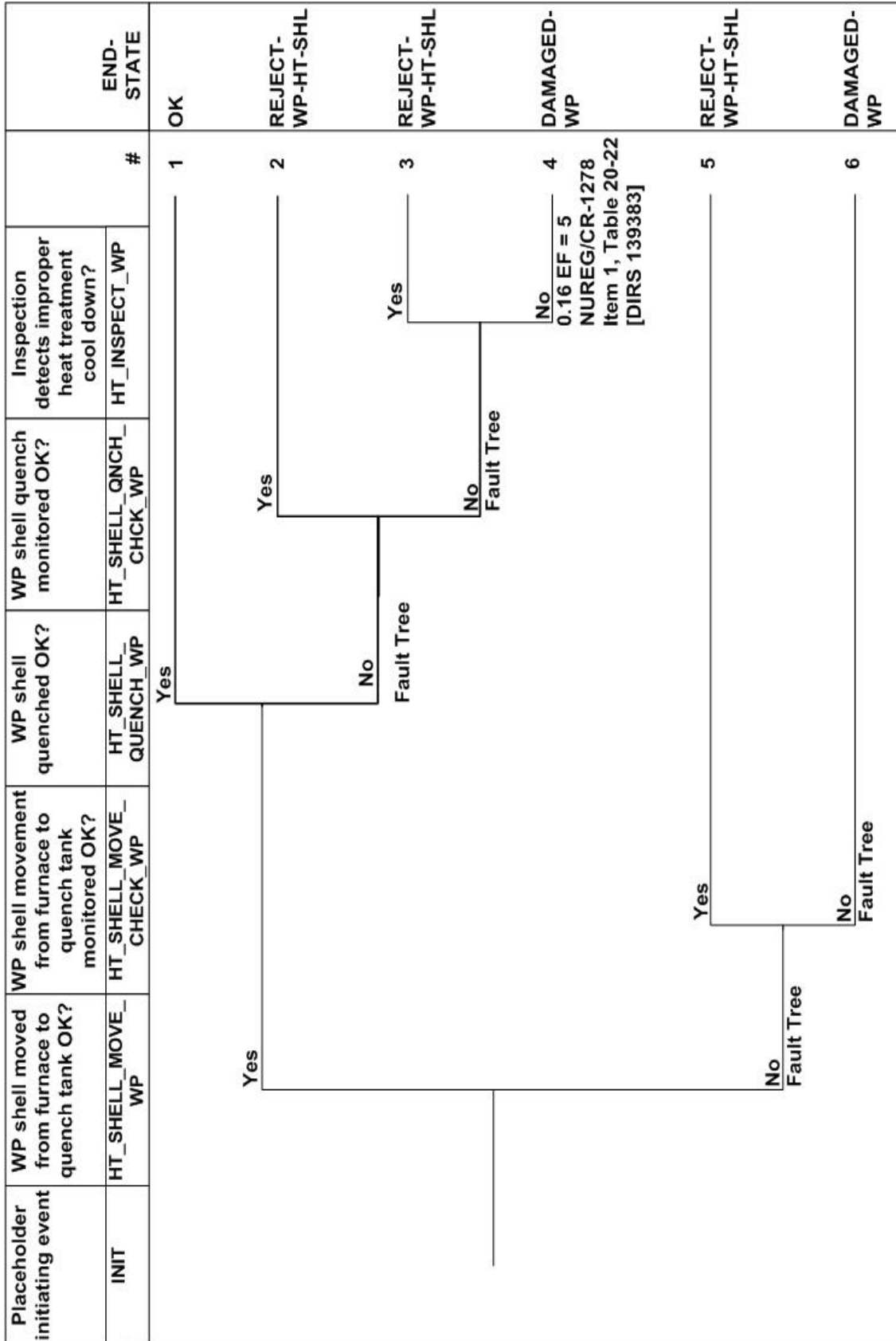


Figure 6-10. Event Tree for Evaluating Improper Heat Treatment of the Waste Package Outer Corrosion Barrier

6.3.4 Improper Heat-Treatment Implementation for Waste Package Outer Corrosion Barrier Lid

Heat treatment of the outer corrosion barrier lid of the waste package can be accomplished by any suitable method of heating and cooling, provided the required heating and cooling rates, metal temperature uniformity, and temperature control are maintained (SNL 2007 [DIRS 179394], Table 4-1, Item 03-20). Such controls are assumed to be integrated into the heat treatment facility independently of the objects being processed (Assumption 5.10, Section 5). Quenching in a water bath to achieve the minimum quenching rate for the lid (SNL 2007 [DIRS 179394], Table 4-1, Item 03-20) is evaluated in this report. Auxiliary instrumentation associated with the heat treatment of the outer corrosion barrier lid utilizes calibrated thermocouples in contact with the material while protecting them from direct contact with water. These thermocouples monitor the operation and provide a record of the heat-treatment/solution-annealing process as it evolves. Such records are important for the quality assurance documentation and as a check that the annealing process followed the procedures correctly. The solution-annealing operation following the heat treatment is a critical operation, and particular attention must be paid to this part of the process in order to achieve proper annealing.

The outer corrosion barrier lid is to be furnace heated at a temperature of $2,050^{\circ}\text{F} + 50^{\circ}\text{F}/-0^{\circ}\text{F}$ for 20 minutes minimum (no maximum specified) and then quenched. Cooling will be achieved by immersion in water or spray quenching with water. The cooling rate for the outer corrosion barrier lid shall be greater than $275^{\circ}\text{F}/\text{min}$ from soak temperature to less than 700°F (SNL 2007 [DIRS 179394], Section 4.1.2.2) to avoid a phase transition during cooling. The quench delay (time from removal from furnace to start of quench) needs to be sufficiently limited to assure that the quench initiation starts at 2020°F or higher. The quench rate is specified to be greater than $275^{\circ}\text{F}/\text{min}$, and, assuming the rate is on the order of $300^{\circ}\text{F}/\text{min}$, the quenching operation requires approximately four minutes. Thus, it is reasonable that the makeup water system must operate for at least six minutes to be at capacity when needed. It is assumed that this last phase of the heat treatment of the waste package outer corrosion barrier lid, removal from the furnace and quenching, is the critical part of the process (Assumption 5.4, Section 5), and the analysis of the heat treatment process focuses on this phase. It is expected that the outer corrosion barrier lid will be moved into the heat treatment facility and then to the quench chamber by either a trolley or a crane as these types of handling equipment are common for large objects, where a trolley is analyzed as the preferred method, since the lid is a regular plate.

The probability that the waste package outer corrosion barrier lid will be subjected to an improper heat treatment, without the error being detected prior to emplacement in the repository, is a combination of human error and process failure probabilities, where the HEPs follow lognormal distributions and the process failure probabilities are point values. It is assumed that process failure probabilities, usually given as point or rate values, can be represented as the mean value of a distribution assumed to be lognormal (Assumption 5.3, Section 5). Error factors were thus assigned to point values to provide a range for uncertainty in the values.

The event tree for evaluating an improper heat treatment for the waste package outer corrosion barrier lid is shown in Figure 6-11. Five events in the heat treatment process for the lid that could lead to an improper heat treatment combined into event sequences are considered in this evaluation. These events are as follows:

- The first top event (Figure 6-11, HT_LID_MOVE_WP) tests whether the outer corrosion barrier lid is moved from the heat treatment facility to the quench facility within the time constraint necessary to maintain the lid temperature \geq the 2,020°F quench initiation temperature or not where the top branch represents success and the lower branch failure. This event is evaluated through a fault tree containing two basic events, TROLLEY_MALFUNCTION and TROLLEY_OPERATOR_ERROR as shown in Appendix B, Figure B-9.

Complete failure of the trolley system (e.g., stops for some extended period) would be readily apparent and the heat treatment operation repeated. Thus, a trolley malfunction is identified as an equipment-operating problem where the trolley fails to move the lid from the heat treatment facility to the quench tank or spray system within the required time limit such that the lid temperature drops below the specified quench initiation temperature. This could be caused by events such as the degradation of the supply power or cable entanglement, which slow but do not halt the operation. However, this type of malfunction causes the transfer operation to exceed the time specified for the operation. The trolley-malfunctioning probability is represented by a median value of 3×10^{-3} (Assumption 5.7, Section 5) with an error factor of 3 that is assumed to provide an upper bound on the probability of mechanical malfunctions of moving equipment. Using Equation 4 results in a mean value for the probability distribution of 3.75×10^{-3} per event.

The trolley operator error is identified as the failure to recognize or respond to the trolley malfunction while the operation was in progress. This error would result in a delay in moving the corrosion barrier lid from the heat treatment facility to the quench tank and allowing the process to continue. This event is represented by the HEP “failure to complete a change of state...” (Item 7 of Table 4-1) that has a median value of 3×10^{-3} , a mean value of 3.75×10^{-3} , and an error factor of 3.

- As stated in the description of the top event (HT_LID_MOVE_WP), it is expected that travel time between the furnace and the quench facility must be sufficiently short to maintain the temperature above the minimum quench initiation temperature (set at 2,020°F). It is expected that the maximum time allowable for the move, adjusted for local conditions, will be monitored with a timer system equipped with recording capability and an alarm. The top event (Figure 6-11, HT_LID_MOVE_CHECK_WP) tests whether the outer corrosion barrier movement from the heat treatment facility to the quench facility within the specified time constraint is successful and properly monitored or not where the top branch represents success and the lower branch failure. While this check is normally operative for all moves, a failure of the check process only has consequences for outer corrosion barrier lid move failures. This event is evaluated through a fault tree containing two basic events, TIMER_FAILURE and HT_OPERATOR_ERROR as shown in Appendix B, Figure B-10.

The timer error (TIMER_FAILURE) is identified as a failure of an alarm to operate, which could be due either to improper operation of the clock or to a malfunctioning alarm; thus the operator is not alerted to the move error resulting from exceeding the specified time constraint. The failure probability is represented by a mean value of 1.2×10^{-4} derived from the item "I & C alarm fails to alarm" (Blanton and Eide 1993 [DIRS 141700], Table 6f), which lists the failure rate as 3×10^{-5} per hour with an error factor of 10. Since the change in temperature during the move is small, a duration time of two minutes is assumed for this operation. However, the alarm system is assumed to be in an operational state during the heat-treatment process. Assuming two such heat treatments per shift gives a demand period of four hours. The probability of the alarm failure during the demand period is represented by a failure rate of 3×10^{-5} /hour and a mission time of four hours with an error factor of 10.

The operator error (HT_OPERATOR_ERROR) is identified as the failure of the process operator to respond to the alarm signal that the process was not operating properly. This event is represented by the HEP "failure to respond to a compelling signal" (Benhardt et al. 1994 [DIRS 157684], Table 4, Item 2); it has a low probability, with a median value of 1.1×10^{-3} , a mean value of 3×10^{-3} , and an error factor of 10.

- The top event (Figure 6-11, HT_LID_QUENCH_WP) tests whether the outer corrosion barrier lid is quenched according to the specifications for cooling, specifically that the cooling water is applied to all surfaces of the outer corrosion barrier lid and that the water supply is sufficient to maintain the minimum rate of cooling required, where the top branch represents success and the lower branch failure. To assure that sufficient water is available during the quench period, it is assumed that a recirculation or makeup system will be used (Assumption 5.8, Section 5). While several potential failure mechanisms can be postulated, any failures of this system are expected to be dominated by a failure of the makeup valve to open; therefore, the failure of recirculation or makeup will be bounded by such a failure. This type of failure is represented in this analysis as a failure of the inlet valve to fully open or the recirculation system to be fully functional (i.e., at capacity). A complete failure of the valve or recirculation system to operate would very likely be observed by the operator and the process terminated. Since there are no cavities to trap gases, this event is evaluated as a failure of the makeup water system to function properly, which is identified as a failure of the quench tank inlet valve to completely open. This failure mode is represented by a mean value derived from the item "motor operated valve fails to open" (Blanton and Eide 1993 [DIRS 141700], Table 6a) which lists the failure probability as of 3×10^{-3} per demand. Thus, the failure of the makeup water system to operate is set to 3×10^{-3} with an error factor of 5, since the valve opens only once during the heat treatment process.
- The top event (Figure 6-11, HT_LID_QNCH_CHK_WP) tests whether the outer corrosion barrier lid quenching is properly monitored, where the top branch represents success and the lower branch failure. Processes that could result in an incorrect monitoring of the lid quench process include improperly installed thermocouples or the failure of the operator to respond to a signal (alarm) that the monitoring system was not functioning correctly. While this check is normally operative for all quenching

operations, a failure of the monitoring system only has consequences for barriers in the postclosure era for undetected failures of the lid quench process. This event is evaluated through a fault tree containing three basic events, WP_LID_TC_INSTALL, WP_LID_TC_CHECK, and HT_OPERATOR_ERROR as shown in Appendix B, Figure B-11, where WP_LID_TC_INSTALL and WP_LID_TC_CHECK evaluate the thermocouple failure probability.

The basic event, WP_LID_TC_INSTALL, is represented by an HEP derived from “failure to use written test or calibration procedure” (Item 1 of Table 4-1) that has a median value of 5×10^{-2} , a mean (rounded) value of 8.1×10^{-2} , and an error factor of 5.

It is expected that the thermocouple installation will be independently checked. The checker error, WP_LID_TC_CHECK, is identified as a failure to detect the installer’s error. This event is represented by the HEP derived from “checker failure to detect an error made by others...” (Item 6 of Table 4-1) that has a median value of 1×10^{-1} , a mean value of 1.6×10^{-1} , and an error factor of 5.

The operator error, HT_OPERATOR_ERROR, is identified as the failure of the process operator to respond to the alarm signal that the process was not operating properly. This event is represented by the HEP “failure to respond to a compelling signal” (Benhardt et al. 1994 [DIRS 157684], Table 4, Item 2) low type probability that has a median value of 1.1×10^{-3} , a mean value of 3×10^{-3} , and an error factor of 10.

- The top event (Figure 6-11, HT_INSPECT_WP) tests whether a postprocessing inspection of the log of the outer corrosion barrier heat treatment process detects whether the process was performed correctly, where the top branch represents success and the lower branch failure. While this check is normally operative for all quenching operations for quality assurance purposes, its second purpose, as stated, is as a check that the annealing process followed the procedures correctly. Thus, a failure of the thermocouple monitor only has barrier performance consequences for (at this point) undetected lid quench process failures. This event is represented by the HEP derived from “checker failure to detect an error made by others...” (Item 6 of Table 4-1), which has a median value of 1×10^{-1} per demand, a mean value of 1.6×10^{-1} , and an error factor of 5.

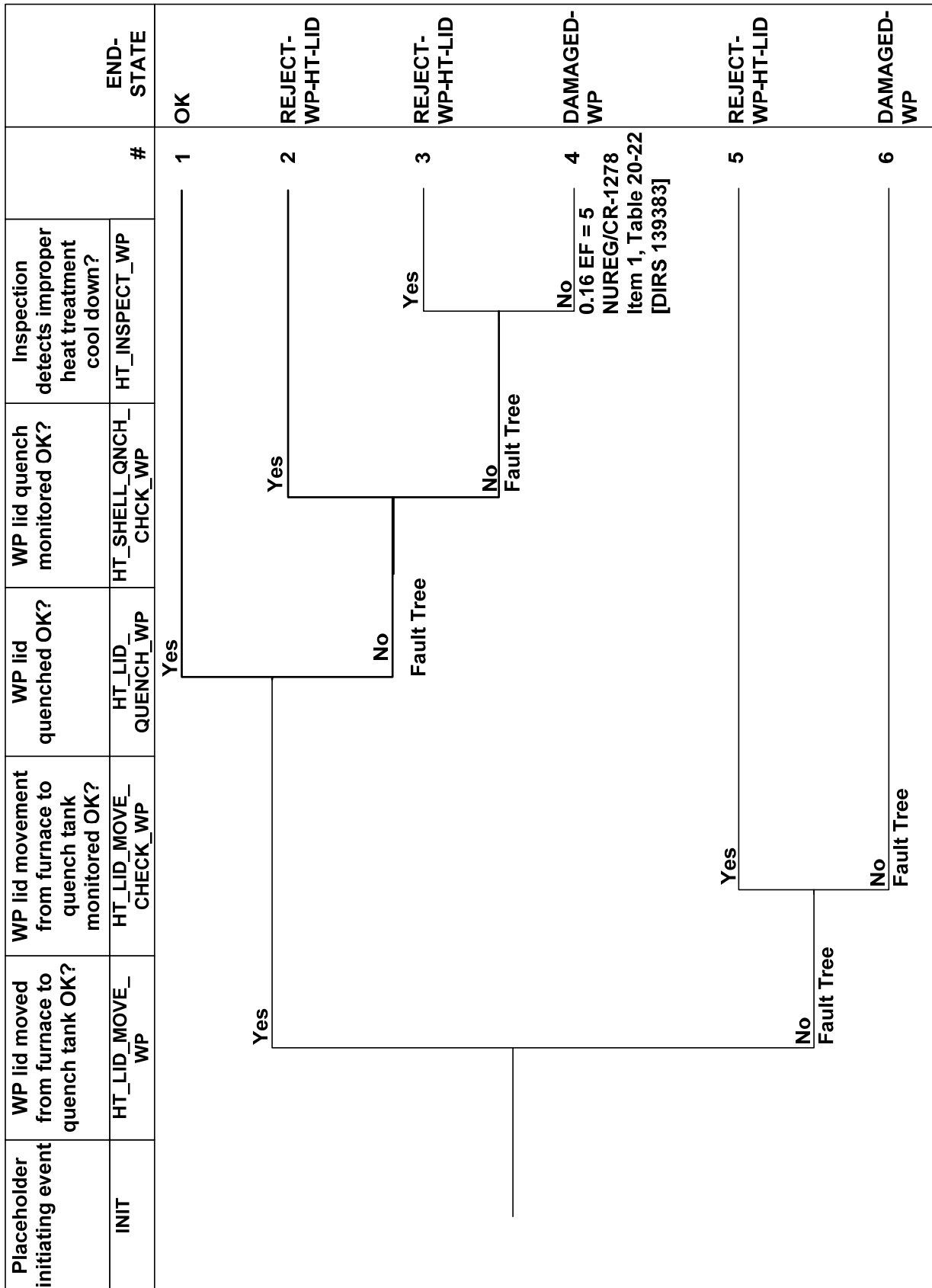


Figure 6-11. Event Tree for Evaluating Improper Heat Treatment of the Waste Package Outer Corrosion Barrier Lid

6.3.5 Low-Plasticity Burnishing Treatment Implementation

The low-plasticity burnishing process has been selected as the method to be used for the stress mitigation technique on the closure weld of the outer lid to waste package, since it is the method of choice from a value-engineering evaluation (SNL 2007 [DIRS 179394], Table 4-1, Item 03-21) and is also identified as the method of choice in *Yucca Mountain Project Conceptual Design Report* (BSC 2006 [DIRS 176937], Section 4.5.3.6).

The equipment that would likely be employed in the low-plasticity burnishing process for stress mitigation of the outer lid weld of the waste package is relatively simple mechanically and the process relatively fast. Therefore, in order to evaluate the probability that the outer lid weld of a given waste package will be subjected to an improper low-plasticity burnishing process, without being detected prior to emplacement in the repository, it is necessary to identify expected general elements of the process.

The low-plasticity burnishing hardware is expected to be a dedicated system with no requirements for an operator selection to be made from (possibly) a set of multiple operating modes; process malfunctions will be signaled to the operator via alarms (Assumption 5.5, Section 5). This expectation follows from the specification that the low-plasticity burnishing operation is designated only for stress mitigation of the final waste package lid welding operation. In proof of concept tests, the low-plasticity burnishing operation has been successfully performed with the tool attached to a commercial computer controlled machine. Thus, it is expected that only one operating setup would be necessary for this process. Such a system would likewise be expected to be amenable for continuous monitoring during the operation.

It is likewise expected that a record of the results of the post-operation inspection (e.g., visual, ultrasonic) parameters following the low-plasticity burnishing process will be maintained and that this record will be reviewed as a QA check performed by an individual other than the operator. This expectation is consistent with QA requirements that results of inspections must be preserved and thus are expected to be available for checking. It is conservative to combine inspections into one review (since it is expected that multiple inspection methods will be utilized), and thus the probability of a failure to observe from the record that a malfunction of the low-plasticity burnishing process occurred can be approximated by the human error probability of misreading a digital readout device (Item 2 of Table 4-1).

In addition to HEP failure modes, there exists the possibility of a process failure. It is assumed that process failure probabilities, usually given as point or rate values, represent the mean value of a distribution assumed to be lognormal (Assumption 5.3, Section 5). Error factors were thus assigned to point values to provide a range for uncertainty in the values. This failure mode is evaluated through a fault tree approach by assigning probability values to the mechanisms that lead to the occurrence of undetected process malfunctions during the low-plasticity burnishing of a waste package.

This information is developed as an event tree for the improper low-plasticity burnishing process of the outer lid weld of the waste package as shown in Figure 6-12. The probability values of the basic events involved in the improper low-plasticity burnishing process event tree are as follows:

- The top event (Figure 6-12, WP-LPB_PRCSS) tests whether the instrumentation operator detects and responds to any signals that the stress relief process was not successfully performed due to a process failure, where the top branch represents success (i.e., process performed according to specification or operator responded properly to out-of-specification performance) and the lower branch failure of the operator to respond properly. This event is evaluated through a fault tree containing three basic events, WP-LPB-SENSOR, WP-LPB-IC, and WP-LPB-OPERATOR as shown in Figure B-13, where WP-LPB-SENSOR and WP-LPB-IC evaluate the instrumentation failure probability.

The basic event, WP-LPB-SENSOR, tests whether the pressure monitor for the low-plasticity burnishing hydraulic system fails and is represented by a lognormal distribution that has mean of 1×10^{-6} per hour with an error factor of 3 derived from the item “Pressure Failure” (Blanton and Eide 1993 [DIRS 141700], Table 6f). The total process time for using one tool is estimated to be two hours; however, since the procedure has not been finalized, a duration time of 10 hours is used for this analysis, which gives a mean probability of 1×10^{-5} with an error factor of 3.

The basic event, WP-LPB-IC, tests whether the instrumentation and control system fails to alarm if the low-plasticity burnishing hydraulic system fails and is represented by a lognormal distribution that has a mean of 3×10^{-5} per hour with an error factor of 10 derived from the item “I & C Alarm Fails to alarm” (Blanton and Eide 1993 [DIRS 141700], Table 6f) that gives a mean probability of 3×10^{-4} with an error factor of 10.

The operator error, WP-LPB-OPERATOR, is identified as failure of the process operator to respond to the alarm signal. This event is represented by the HEP “failure to respond to a compelling signal” (Benhardt et al. 1994 [DIRS 157684], Table 4, Item 2); it is low-probability event, with a median value of 1.1×10^{-3} , a mean value of 3×10^{-3} , and an error factor of 10.

- The top event (Figure 6-12, WP-LPB_ACR) tests whether or not the checker detects the operator’s failure to respond properly to a process malfunction annunciator where the upper branch is a success and the lower branch is a failure. This event is represented by the HEP derived from “checking routine tasks with alerting factors” (Item 8 of Table 4-1), which has a median value of 5×10^{-2} per demand, a mean value of 8.1×10^{-2} , and an error factor of 5.
- The event of an alarm triggered during the low-plasticity burnishing process will be entered into the report generated by the computerized system. The top event (Figure 6–12, WP-LPB_CHECK) tests whether the QA checker, during a review of the log, observes that the operator and checker did or did not respond properly to an alarm generated by a process malfunction. A probability is derived from the HEP “checker

failure to detect errors made by others” (Item 6 of Table 4-1), with a median of 0.1 providing a mean value of 1.6×10^{-1} , with an error factor of 5.

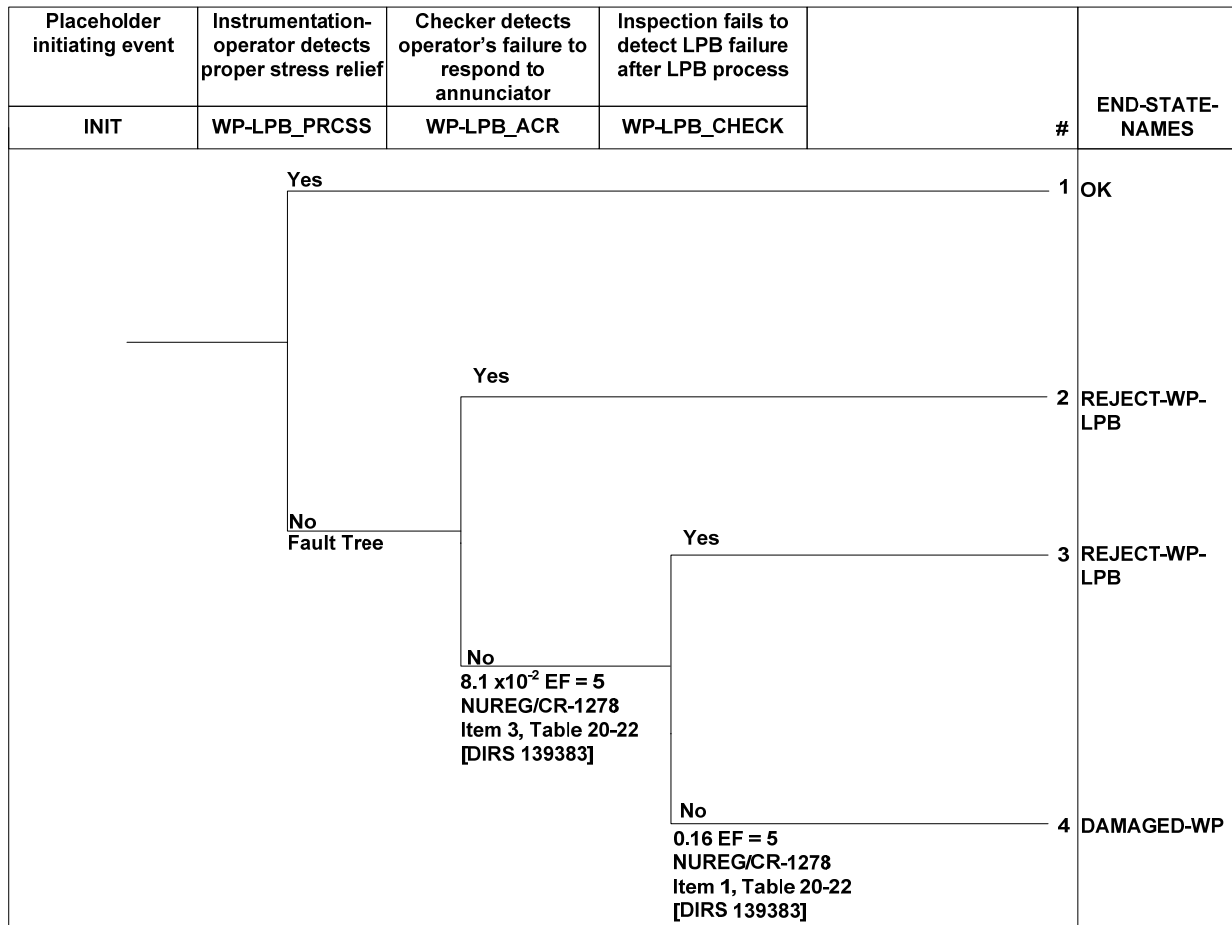


Figure 6-12. Event Tree for Evaluating Low-Plasticity Burnishing Treatment of the Waste Package Outer Corrosion Barrier Lid

6.3.6 Improper Handling of Waste Package

Handling damage is defined as any visible gouging or denting of the waste package surface that may jeopardize the performance of the Alloy 22 barrier. It is expected that inspections will be performed on the waste package outer corrosion barrier prior to emplacement to detect traces of damage to the waste package (SNL 2007 [DIRS 179394], Table 4-1, Items 03-26, 03-27, and 03-28). These inspections are expected to include a visual inspection of the waste package while in the surface facilities of the repository following receipt of the waste package and remote inspections (via camera) at various times prior to repository closure. The more difficult inspections are those requiring remote camera devices; this is the process focused upon for this analysis of the probability of undetected flaws. Since actual operating experience has yet not been accrued on the handling of the waste packages, information on reported instances of damage to nuclear fuel assemblies during their handling has been used as a surrogate to estimate that probability. These data were selected as fuel assembly-handling activities and are performed

in a nuclear environment representative of the highly controlled conditions under which handling of the waste package is expected to occur. Therefore, it is deemed appropriate to use this information for estimating the probability of damaging a waste package by mishandling.

The probability of fuel assembly damage was evaluated in *Waste Package Misload Probability* (BSC 2001 [DIRS 157560], Table 5) as a point value of 4.8×10^{-5} per moved fuel assembly. As was noted in *Waste Package Misload Probability* (BSC 2001 [DIRS 157560], Table 4), the sources of fuel assembly damage events included human errors, procedural errors, and equipment failure. Thus, associating this probability with an HEP and applying an error factor derived for HEPs for the uncertainty range is inappropriate.

There are multiple opportunities identified for mishandling and potentially damaging a waste package outer surface between the inspection of the waste package outer corrosion barrier at reception and the final inspection at the time of emplacement. The waste package might be mishandled and damaged by typical operations (e.g., being tilted in an upward position, being down-ended, being placed onto the waste package pallet, or being moved from the transporter vehicle to the emplacement vehicle). These operations involve a waste package directly, i.e., maneuvers to reposition a waste package, either empty or loaded, into a different position or orientation. Another potential source of damage prior to drip shield emplacement is from drift collapse. Although inspections of waste packages for damage will be required following observations of drift collapse (SNL 2007 [DIRS 179394], Table 4-1, Item 03-28), the possibility exists for nondetection of damage. Since these inspections will be performed remotely, the same probability of nondetection of damage by remote sensors is assigned to drift collapse damage. Other potential sources of minor surface defects, although they are outside the maximum size specified (SNL 2007 [DIRS 179394], Table 4-1, Item 03-27), include loading and closure operations. As stated above, these inspections will be performed remotely; therefore, the same probability of non-detection of damage by remote sensors is assigned to damage from these sources. The various types of operations that have been identified are the principal ones for which it is anticipated that the waste package surface will not be shielded by protective equipment but rather will be exposed. Mishandlings that could occur when loading the fuel assemblies into TAD canisters (or the waste package basket) are not considered because such mishandling will affect only the assembly basket or, at most, the inner surface of the stainless steel cylinder, which are not of concern for the performance of the Alloy 22 barrier and potential early failure mechanisms.

This information is developed in an event tree for the mishandling of the waste package, as shown in Figure 6-13. Since processing steps for the waste package (outer corrosion barrier and TAD canister) have not been finalized, the various operations that could lead to waste package surface damage were not analyzed in detail for each operation.

The top event (Figure 6-13, MISH-WP) is evaluated with a fault tree composed of eight generic basic events, as shown in Figure B-15, which act as surrogates for operations that could lead to potential waste package surface damage. Each of the basic events was assigned a probability value of 4.8×10^{-5} (BSC 2001 [DIRS 157560], Table 5) and an error factor of 10 to provide an uncertainty range.

The top event (Figure 6-13, CAM_DET) tests whether or not the QA checks are able to detect surface flawing of the waste package from any of the various mechanisms, where the upper branch is a success and the lower branch is a failure. This event is represented by the HEP derived from “error of commission in check-reading analog meter...” (Item 3 of Table 4-1) that has a median value of 2×10^{-3} , a mean value of 2.50×10^{-3} , and an error factor of 3.

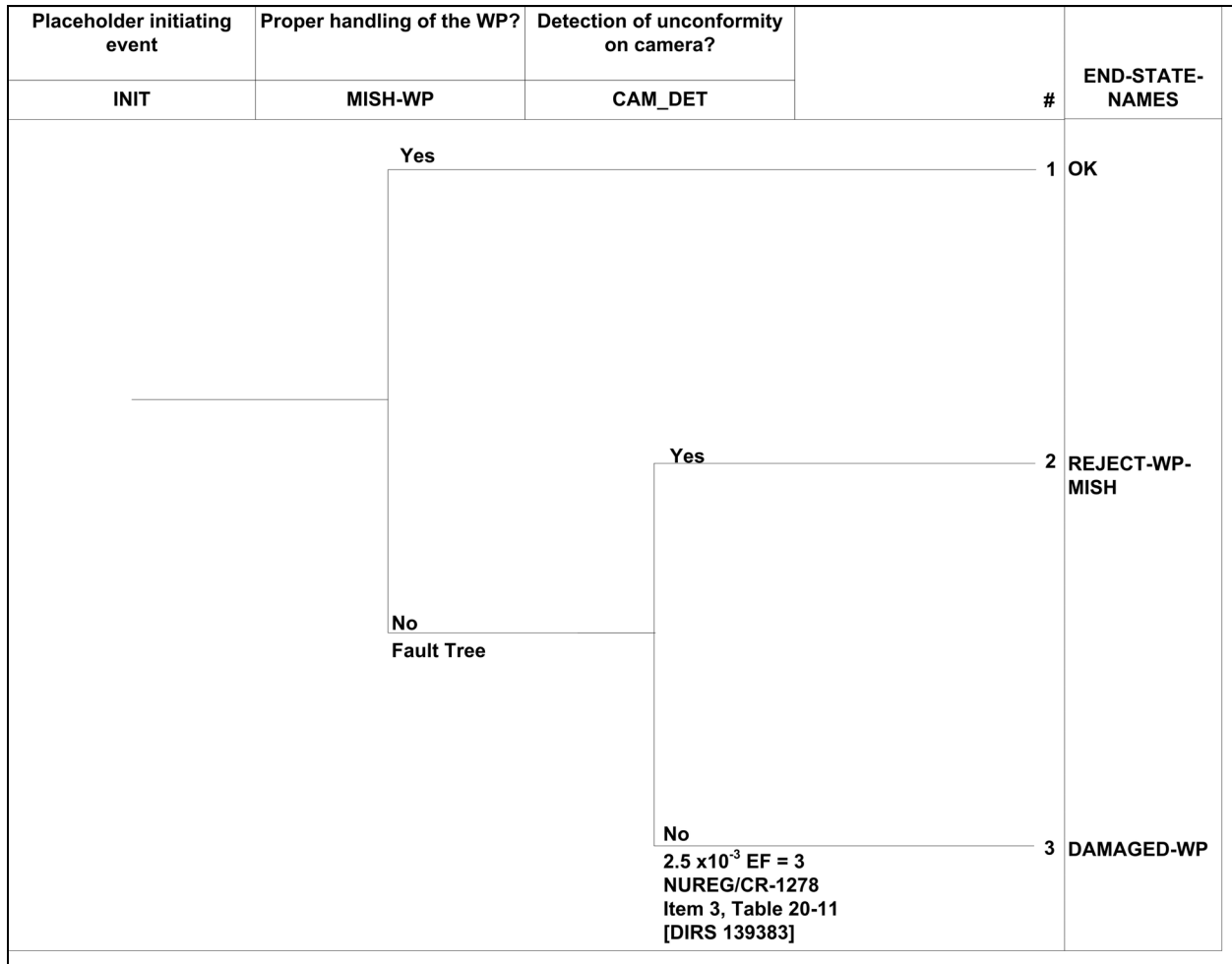


Figure 6-13. Event Tree for Evaluating Mishandling of the Waste Package Outer Corrosion Barrier

6.3.7 Improper Weld Filler Material Selection for Waste Package

The probability of selecting improper weld filler material for the waste package outer corrosion barrier is evaluated on the same basis as the likelihood of selecting improper base metal material in the fabrication of the outer barrier of the waste package (Section 6.3.2). Thus, the top event (Figure 6-14, WELD_FILLER_FLAW-WP) that tests whether or not such an error occurs has an uncertainty that follows a lognormal distribution having a mean value of 1.0×10^{-4} per demand and an error factor of 3. The top event (Figure 6-14, WELD_FILLER_ISP-WP) that tests whether or not an inspection detects the use of improper material is represented by the HEP

“error of commission in reading and recording quantitative information...” (Item 2 of Table 4-1), which has a mean value of 1.25×10^{-3} and an error factor of 3.

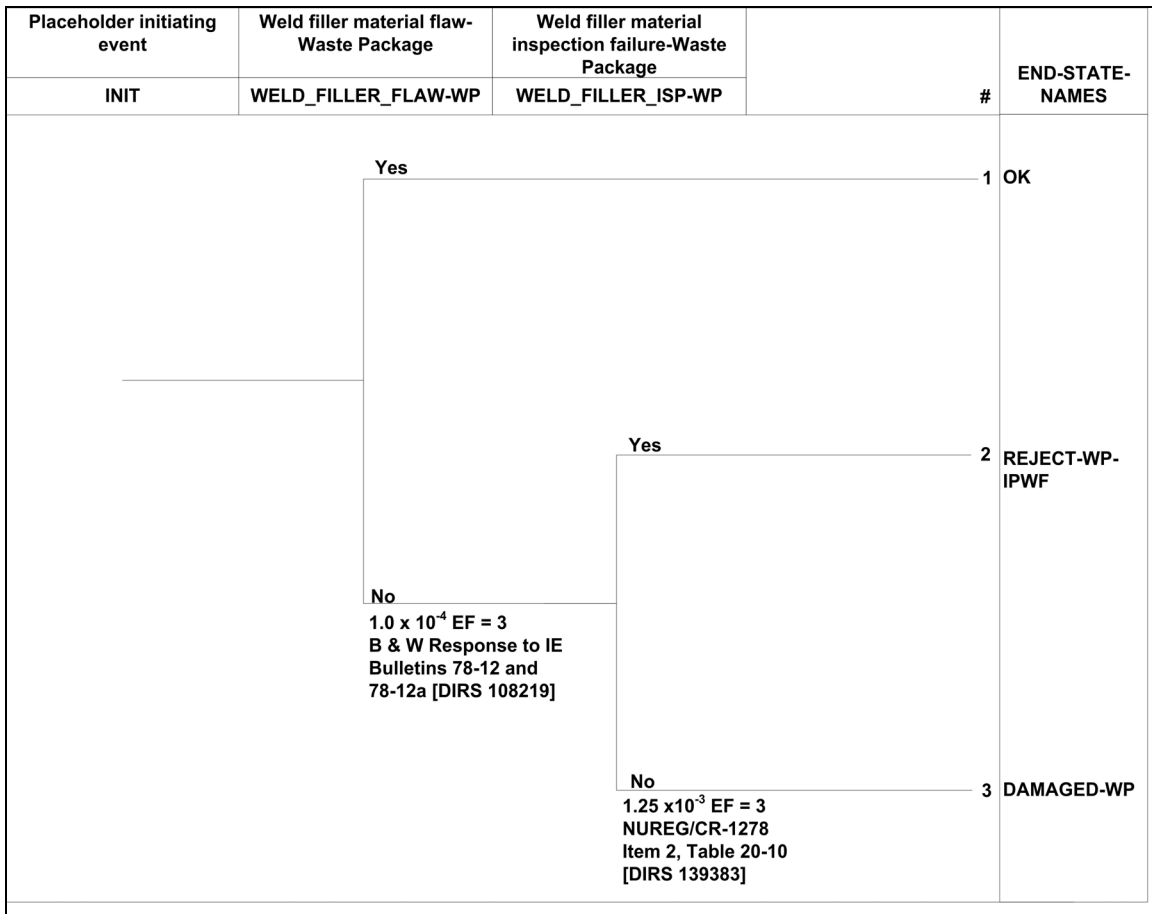


Figure 6-14. Event Tree for Evaluating Weld-Filler Material Defects in the Waste Package Outer Corrosion Barrier

6.4 DRIP SHIELD FABRICATION, HANDLING, AND POTENTIAL DEFECTS

The various processes (e.g., human errors, material defects, processes failures) identified in Section 6.1.6 that could potentially lead to early failure of a drip shield were reviewed; four were identified as significant (i.e., could not be a priori screened from consideration), thus requiring further analysis. The four processes retained for further analysis with respect to mechanisms leading to early drip shield failure are as follows:

- Improper heat treatment
- Base metal selection flaws
- Improper weld filler material
- Emplacement damage.

The basic event tree evaluating these processes is shown in Figure 6-15 where branches 2 through 5 provide transfers to the individual trees for each of the defect types identified. The event trees and probabilities associated with these mechanisms are provided in Sections 6.4.1 through 6.4.4. All of the event trees and fault trees used in the analysis of early failure mechanisms of drip shields are illustrated in Appendix B.

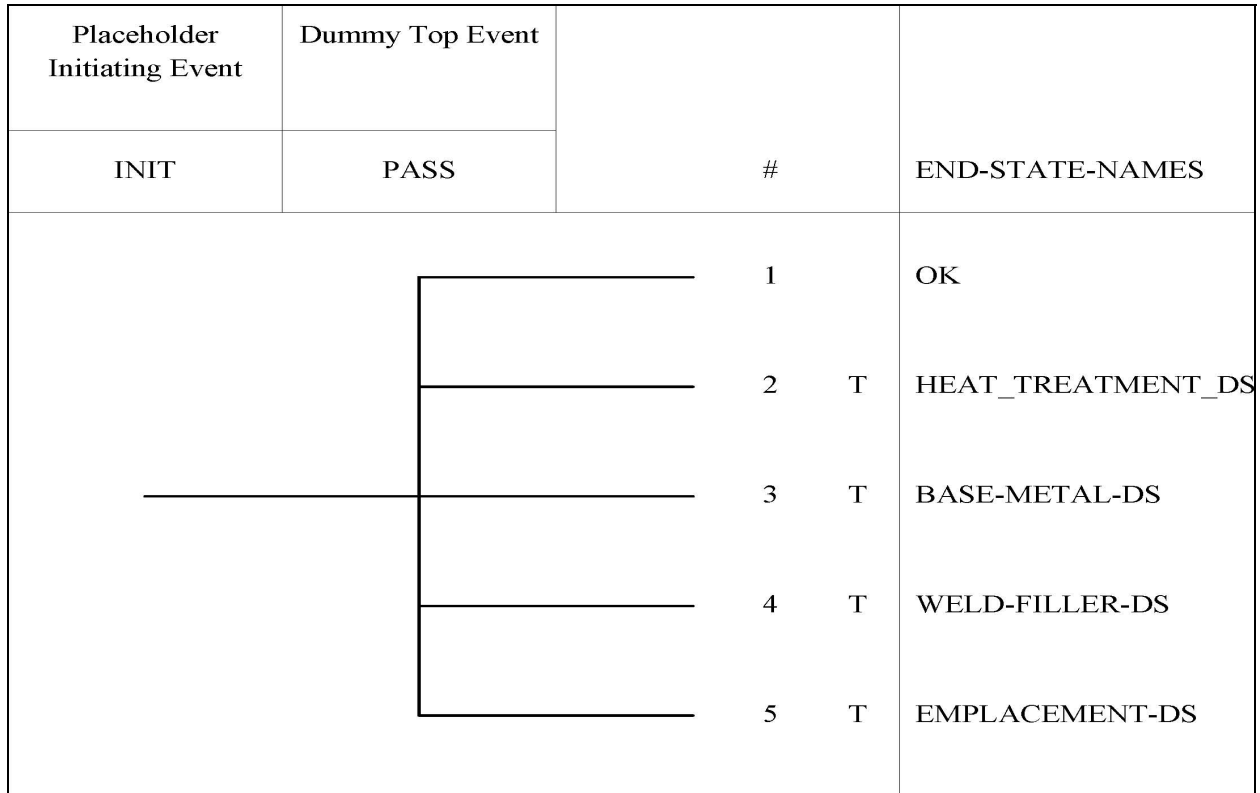


Figure 6-15. Basic Drip Shield Defect Event Tree

6.4.1 Drip Shield Base Metal Flaw Implementation

The event tree for evaluating an improper base metal selection process is shown in Figure 6-16. The probability of occurrence for introducing base metal flaws in the drip shield material is based on the same arguments as used for the waste package material (Section 6.3.2). Thus, the top event (Figure 6-16, BM_FLAW_DS) that tests whether or not such an error occurs follows a lognormal distribution having a mean value rounded to 1.0×10^{-4} and an error factor rounded up to 3. The top event (Figure 6-16, CHECK_BM_FLAW_DS) that tests whether or not inspection detects the use of improper material has a mean value of 1.25×10^{-3} and an error factor of 3.

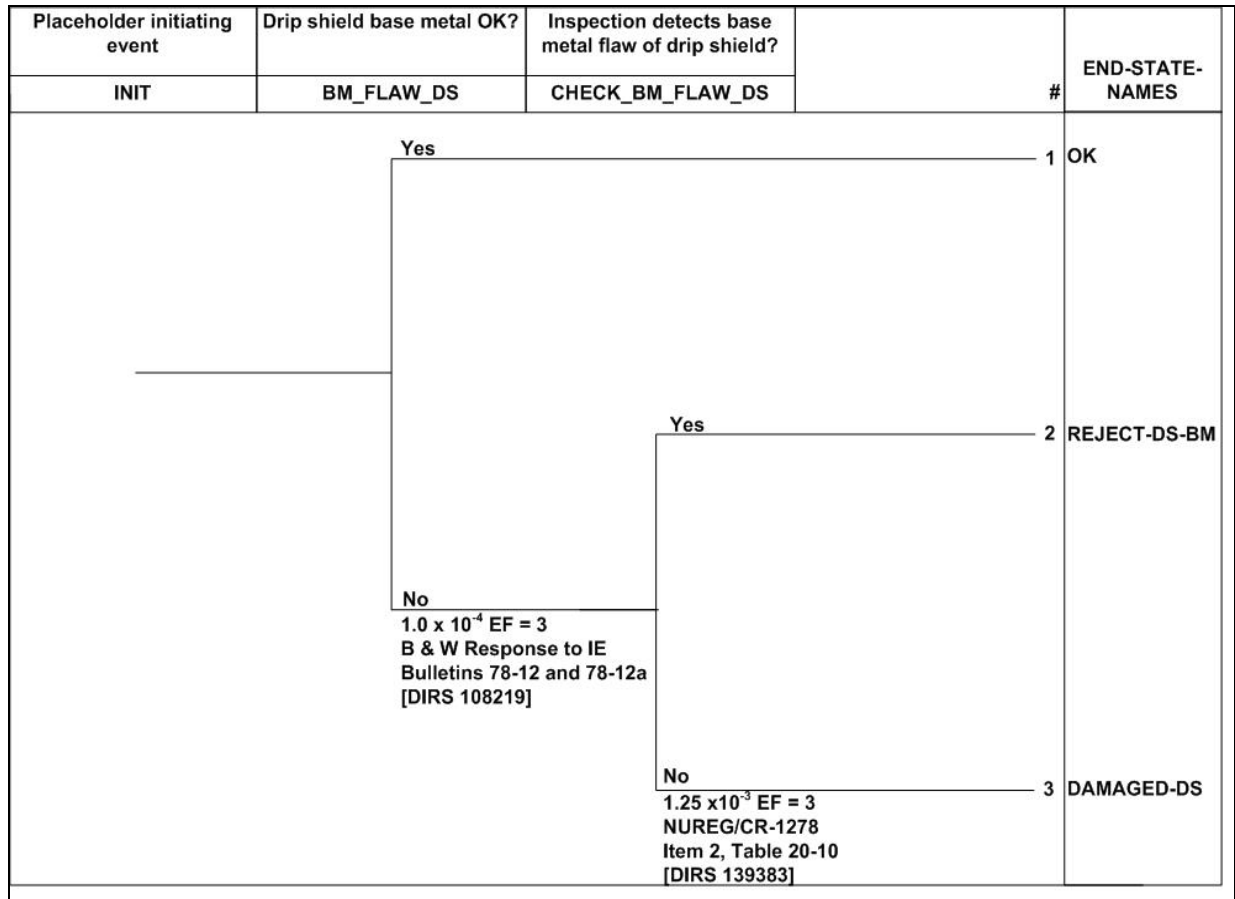


Figure 6-16. Event Tree for Evaluating Improper Base-Metal Selection for Drip Shield

6.4.2 Drip Shield Improper Heat-Treatment Implementation

Heat treatment of the drip shield can be accomplished by any suitable method of heating and cooling, provided the required heating and cooling rates, metal temperature uniformity, and temperature control are maintained (SNL 2007 [DIRS 179354], Table 4-2, Item 07-13). Such controls are assumed to be integrated into the heat treatment facility independently of the objects being processed (Assumption 5.10, Section 5). The heat treatment, however, must provide for heating of the entire drip shield as a single application. Air is the cooling fluid of choice for cool-down of the drip shield (SNL 2007 [DIRS 179354], Table 4-2, Item 07-13). Auxiliary instrumentation associated with the heat treatment of the drip shield utilizes calibrated thermocouples in contact with the material while protecting them from non-drip shield thermal sources. These thermocouples monitor the operation and provide a record of the heat treatment as it evolves. Such records are important for the QA documentation and as a check that the process followed the procedures correctly.

The purpose of the heat treatment process for the drip shield is stress relief as the final part of the fabrication process with no repairs performed on the drip shield after heat treatment. Particular attention must be paid to the procedure to achieve the stress relief that meets the requirements and to prevent distortion of the units. The entire drip shield is to be furnace-heated at a

temperature of $1,100^{\circ}\text{F} \pm 50^{\circ}\text{F}$ for a minimum of 120 min and then air cooled (SNL 2007 [DIRS 179354], Table 4-2, Item 07-13). Sufficient temperature recordings must be taken during this process to confirm time and temperatures within specified tolerances.

The probability that the drip shield components will be subjected to an improper heat treatment, without the error being detected prior to emplacement in the repository is a combination of human error and process failure probabilities where the HEPs follow lognormal distributions and the process failure probabilities are point values. It is assumed that process failure probabilities, usually given as point or rate values, represent the mean value of a lognormal distribution (Assumption 5.3, Section 5). Error factors were thus assigned to point values to provide a range for uncertainty in the values.

While process failures can occur, the drip shield stress relief heat treatment duration covers hours providing opportunity for correction. This type of review resulted in identification of three events with potential for nondetection that could lead to an improper heat treatment process for the drip shield. These events are combined into an event tree shown in Figure 6-17 that is evaluated as follows:

- The first top event (Figure 6-17, HT_DS) tests whether or not the drip shield heat treatment is performed properly (e.g., the drip shield is given sufficient stress relief), where the top branch represents success and the lower branch failure. The heat treatment process for a drip shield is expected to be a procedurally controlled type of process, since there are no critical moves or quench rates required. Thus, this event is represented by the HEP derived from the routine, repetitive circumstances evaluation for “failure of administrative control” (Benhardt et al. 1994 [DIRS 157684], Table 4, Item 1), which has a mean value of 5×10^{-4} and an error factor of 10.
- The top event (Figure 6-17, HT_CHECK_DS) tests whether the drip shield heat treatment is properly monitored or not, where the top branch represents success and the lower branch failure. Processes that could result in an incorrect monitoring of the heat treatment process include improperly installed thermocouples or failure of the operator to respond to a signal (alarm) that the monitoring system was not functioning correctly. While this check is normally operative for all heat treatment operations, a failure of the monitoring system only has consequences for barriers in the postclosure era for undetected failures of the drip shield heat treatment process. This event is evaluated through a fault tree containing three basic events, DS_TC_INSTALL, DS_TC_CHECK, and HT_OPERATOR_ERROR, as shown in Appendix B, Figure B-20, where DS_TC_INSTALL and DS_TC_CHECK evaluate the thermocouple failure probability.

The basic event, DS_TC_INSTALL, is represented by an HEP derived from “failure to use written test or calibration procedure” (Item 1 of Table 4-1), which has a median value of 5×10^{-2} , a mean (rounded) value of 8.1×10^{-2} , and an error factor of 5.

It is assumed that the thermocouple installation will be independently checked (Assumption 5.9, Section 5). The checker error, DS_TC_CHECK, is identified as a failure to detect the error of the installer. This event is represented by the HEP derived from “checker failure to detect an error made by others...” (Item 6 of Table 4-1), which has a median value of 1×10^{-1} , a mean value of 1.6×10^{-1} , and an error factor of 5.

The operator error, HT_OPERATOR_ERROR, is identified as a failure of the process operator to respond to the alarm signal that the process was not operating properly. This event is represented by the HEP “failure to respond to a compelling signal” (Benhardt et al. 1994 [DIRS 157684], Table 4, Item 2), a low-probability type that has a median value of 1.1×10^{-3} , a mean value of 3×10^{-3} , and an error factor of 10.

- The top event (Figure 6-17, HT_INSPECT_DS) tests whether a postprocessing inspection of the log of the drip shield heat treatment process detects whether the process was performed correctly, where the top branch represents success and the lower branch failure. While this check is normally operative for all heat-treatment operations for quality assurance purposes, its second purpose, as stated, is as a check that the stress relief process followed the procedures correctly. Thus, a failure of the thermocouple monitor only has barrier performance consequences for (at this point) undetected drip shield heat treatment process failures. This event is represented by the HEP derived from “checker failure to detect an error made by others...” (Item 6 of Table 4-1), which has a median value of 1×10^{-1} per demand, a mean value of 1.6×10^{-1} , and an error factor of 5.

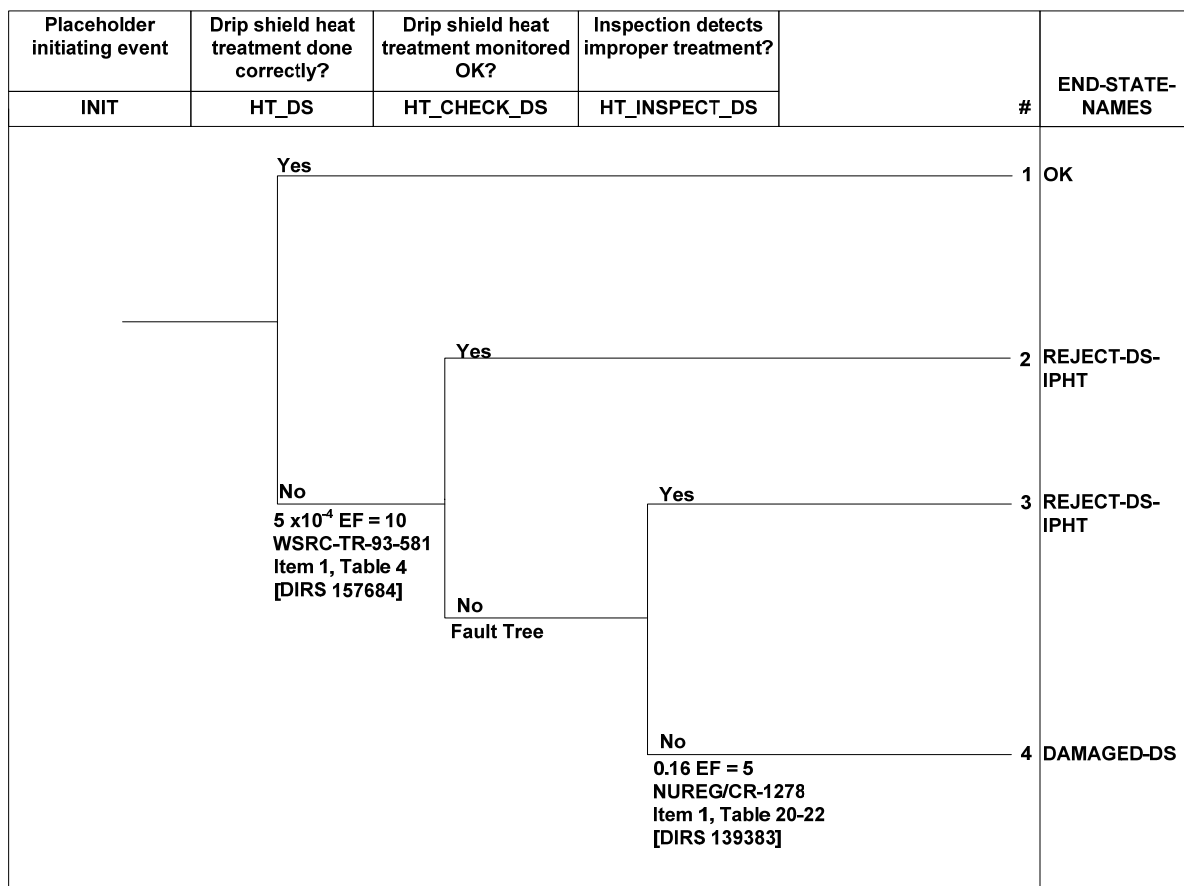


Figure 6-17. Event Tree for Evaluating Improper Heat Treatment of the Drip Shield

6.4.3 Drip Shield Weld-Filler Defects

Drip shield welds are of three types, Titanium Grade 7 to Titanium Grade 7 (plates), Titanium Grade 29 to Titanium Grade 29 (structural members), and Titanium Grade 7 to Titanium Grade 29 (structures to plates) (SNL 2007 [DIRS 179354], Table 4-2, Item 07-12). In the first two cases, where the welded materials are the same, that grade of titanium will be used as filler. For the third case where the grades are dissimilar, Titanium Grade 28 will be used as filler. The consequence of using incorrect weld filler material is the enhanced potential for weld cracking.

The probability of selecting improper weld-filler material for the drip shield is evaluated on the same basis as the likelihood of selecting improper base-metal material in the fabrication of the outer barrier of the waste package (Section 6.3.2). The event tree for evaluating an improper welding operation for the drip shield is shown in Figure 6-18. Thus, the top event (Figure 6-18, WELD_FILLER_FLAW-DS) that tests whether or not such an error occurs follows a lognormal distribution having a mean value of 1.0×10^{-4} per demand and an error factor of 3. The top event (Figure 6-18, WELD_FILLER_ISP-DS) that tests whether or not inspection detects the use of improper material has a mean value of 1.25×10^{-3} and an error factor of 3. The probability values are the same as those documented in Section 6.3.2.

The event tree for evaluating an improper welding operation for the drip shield is shown in Figure 6-18.

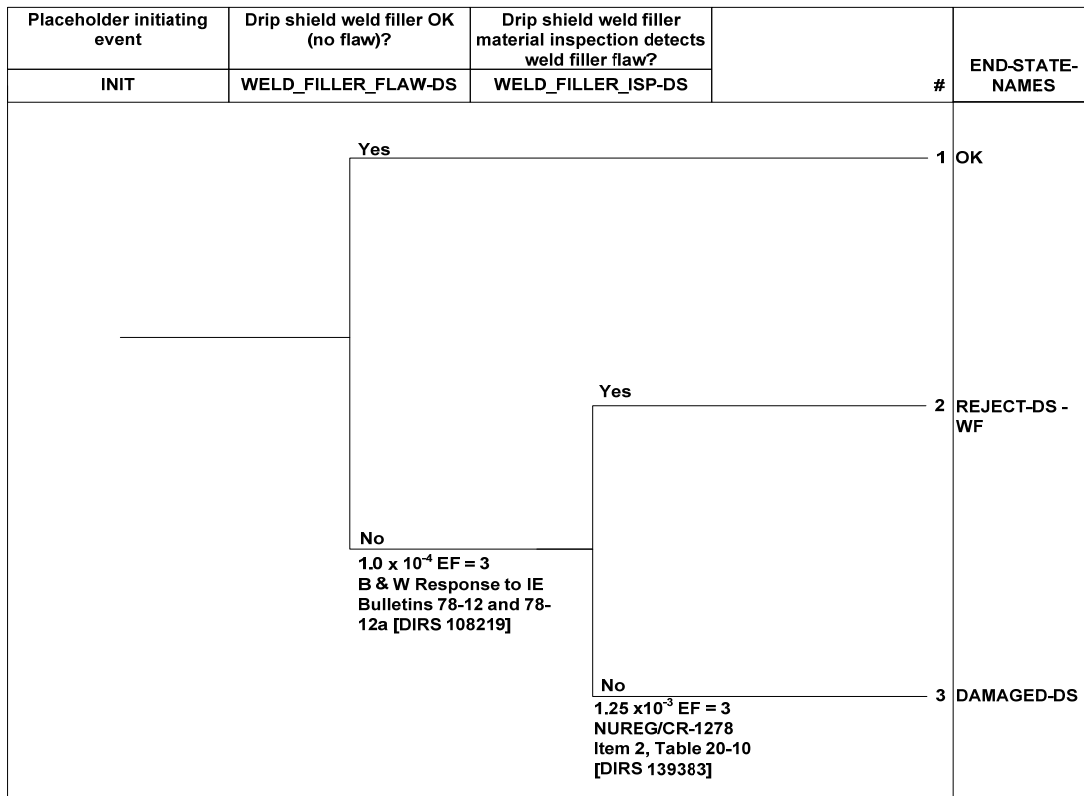


Figure 6-18. Event Tree for Evaluating Weld-Filler Material Flaws in the Drip Shield

6.4.4 Drip Shield Emplacement Failure

The probability that a drip shield is improperly emplaced in the repository, leaving a gap between adjacent drip shields, is evaluated with HEPs. It is expected that inspections will be performed on the drip shields during emplacement to detect misalignments and/or gaps (SNL 2007 [DIRS 179354], Table 4-2, Items 07-02 and 07-02B). These inspections are expected to include a visual inspection of the drip shield while in the surface facilities of the repository when the drip shield is received, remote inspections (via camera) at various times through emplacement. It is assumed that the inspections will be independently checked and documented (Assumption 5.9, Section 5). The probabilities of the events involved in drip shield emplacement error are shown in Figure 6-19 and are as follows:

- The top event (Figure 6-19, DS_INTRLCK) tests whether or not the operator properly interlocks the drip shield to be emplaced with the adjacent drip shield, where the top branch represents success and the lower branch failure. This probability is approximated by the HEP “improperly mate a connector” (Item 5 of Table 4-1), which has a median of 3×10^{-3} , a mean value of 3.75×10^{-3} , and an error factor of 3.

- The top event (Figure 6-19, CAM_DET) tests whether or not the QA check, performed remotely by camera, detects that adjacent drip shields are correctly interlocked, where the upper branch is success and the lower branch is a failure. This event is represented by the HEP derived from “error of commission in check-reading analog meter...” (Item 3 of Table 4-1), which has a median value of 2×10^{-3} , a mean value of 2.50×10^{-3} , and an error factor of 3.
- The top event (Figure 6-19, DS_EMP_ANN) tests whether or not the operator responds to an annunciator. This event is represented by the HEP derived from the low-competing-signals evaluation for “failure to respond to a compelling signal” (Benhardt et al. 1994 [DIRS 157684], Table 4, Item 2), which has a mean value of 3×10^{-3} per demand and an error factor of 10.
- The top event (Figure 6-19, DS_EMP_CKR) tests whether or not the checker detects failure of the operator to respond properly to a process malfunction annunciator, where the upper branch is success and the lower branch is a failure. This event is represented by the HEP derived from “checking routine tasks with alerting factors” (Item 8 of Table 4-1), which has a median value of 5×10^{-2} per demand, a mean value of 8.1×10^{-2} , and an error factor of 5.

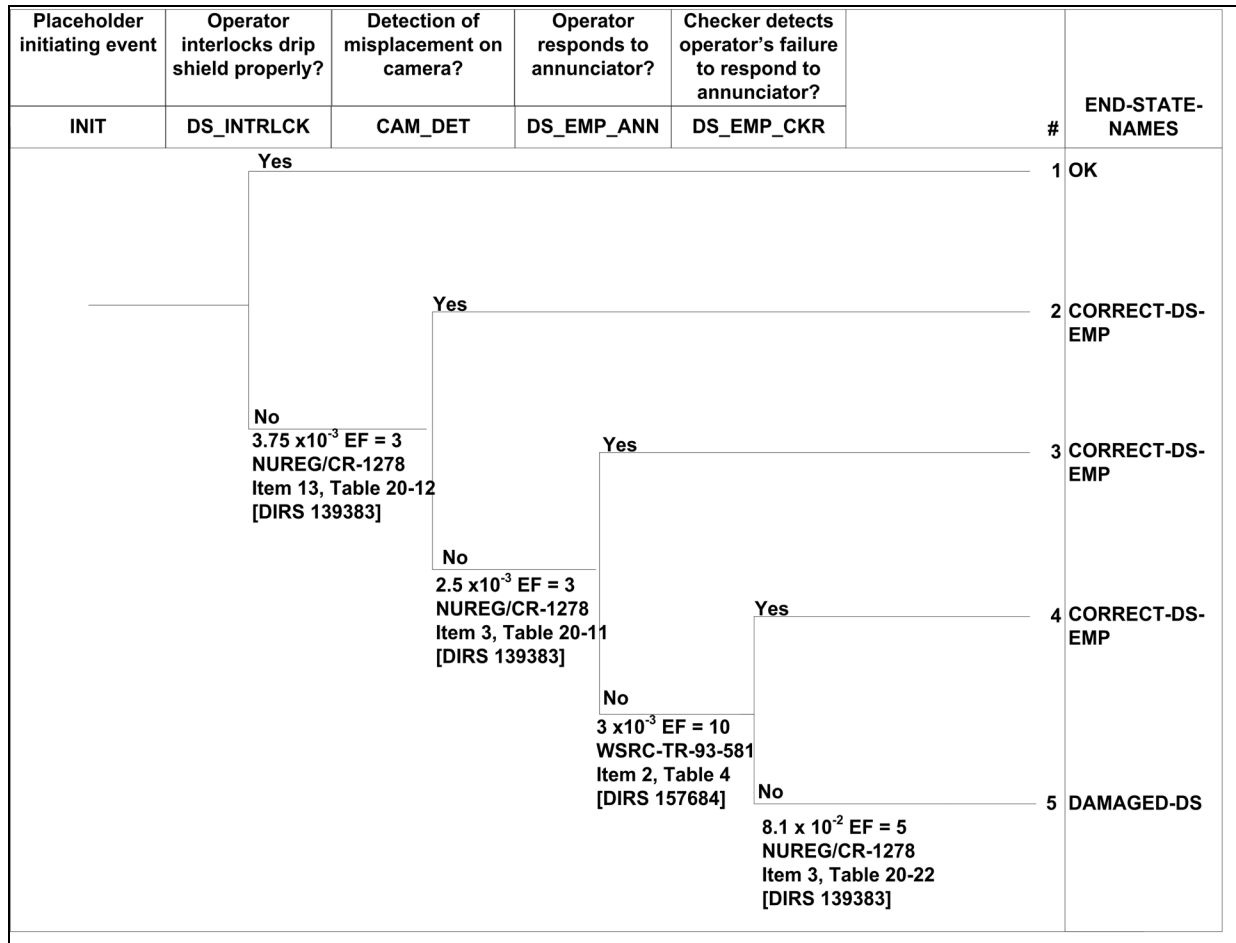


Figure 6-19. Event Tree for Evaluating Improper Emplacement of the Drip Shield

6.5 WASTE PACKAGE AND DRIP SHIELD DEFECT SUMMARY PROBABILITIES AND CONSEQUENCES

6.5.1 Combining Defect Probabilities

As stated in Section 6.3, the quantification of events using the event tree approach and in particular, uncertainty analyses, incorporates the premise that the events are independent, i.e., that events are not correlated by common causes (Apostolakis and Kaplan 1981 [DIRS 160971], pp. 136 to 139). However, note that the probabilities of nominally identical events have been correlated together by class where nominally identical events are those that are distinct (i.e., independent) but for which the state of knowledge for determining their distributions is identical. The net effect on the analysis results of correlating probability classes is to somewhat broaden the uncertainty distributions.

Results from an uncertainty analysis of the waste package and drip shield event sequences were collected into the end states DAMAGED-WP (e.g., Figure 6-9) and DAMAGED-DS (e.g., Figure 6-16), respectively. The comprehensive probability distributions for the presence of

undetected defects per waste package and per drip shield were developed by running 90,000 realizations for these end states with Monte Carlo sampling starting with a seed of 48,524.

In order to perform an uncertainty analysis for the combined set of early failure mechanisms applicable to either the waste package outer corrosion barrier or drip shield, the SAPHIRE code generates uncertainty distributions for each scenario sequence contributing to the defective end state (e.g., DAMAGED-DS). The uncertainty for each basic event in a sequence was characterized as a lognormal distribution by specifying a mean value and error factor. The individual event probability distributions in these sequences may have different error factors. Thus, the mean value of the uncertainty distribution for the end state of the scenario is not just a simple product from each basic event in the sequence but derived from the generated distribution. Furthermore, since the uncertainty distribution for a grouped end states is generated by sampling over all of the end-state distributions for that particular combination, the final distribution is a weighted average (with the weight factors implicit but not actually calculated) of all the scenarios in the group.

The parameters for the uncertainty distributions for the grouped end states are listed in Table 6-7 where all values were generated by the SAPHIRE software with the exception of the error factors, which were evaluated using Equation 2. The error factor for the drip shield distribution was subsequently adjusted to permit the distribution to more closely approximate the upper part of the SAPHIRE data. CDFs were generated in the Excel file *lognormalresults vs uncertainty.xls* in the output DTN: MO0701PASHIELD.000 with these parameters and are shown in Figures 6-20 and 6-21 for the waste package and drip shield, respectively. The mean and median values for the various uncertainty distributions for the end states of the event sequences for early failure mechanism scenarios culminating in the combined end states, DAMAGED-WP and DAMAGED-DS, are given in Table 6-8 and in the output DTN: MO0705EARLYEND.000.

Table 6-7. Parameters for End-State Uncertainty Distributions of Undetected Defects

Distribution Parameter	Waste Package	Drip Shield
Mean ^a	1.13×10^{-4}	2.21×10^{-6}
Median ^b	4.14×10^{-5}	4.30×10^{-7}
95th Percentile ^b	4.07×10^{-4}	6.97×10^{-6}
5th Percentile ^b	6.10×10^{-6}	7.86×10^{-8}
Standard Deviation ^a	3.27×10^{-4}	1.68×10^{-5}
Error Factor ^b	8.17	14

^a Output DTN: MO0701PASHIELD.000, file *SAPHIRE OUTPUT.zip*.

^b Output DTN: MO0701PASHIELD.000, file *lognormalresults vs uncertainty.xls*.

Table 6-8. Parameters from Scenario End-State Uncertainty Distributions for Undetected Defects

Event Sequence	Mean Value	Median Value
Base metal flaw (waste package outer corrosion barrier)	1.25×10^{-7}	8.76×10^{-8}
Base metal flaw (drip shield)	2.53×10^{-7}	1.77×10^{-7}
Improper heat treatment (waste package outer corrosion barrier)	7.70×10^{-5}	4.25×10^{-5}
Improper heat treatment (waste package outer corrosion barrier lid)	7.51×10^{-5}	4.09×10^{-5}
Improper heat treatment (drip shield)	3.23×10^{-6}	5.33×10^{-7}
Weld filler flaws (waste package outer corrosion barrier)	1.25×10^{-7}	8.76×10^{-8}
Weld filler Flaws (drip shield)	2.53×10^{-7}	1.77×10^{-7}
Emplacement error (drip shield)	4.36×10^{-9}	6.76×10^{-10}
Handling error (waste package outer corrosion barrier)	9.63×10^{-7}	7.71×10^{-7}
Low-plasticity burnishing (waste package outer corrosion barrier)	3.84×10^{-5}	7.28×10^{-6}

Output DTN: MO0705EARLYEND.000, SAPHIRE OUTPUT.zip.

The mechanisms of early failure implementation consist of specifying the likelihood (probability) that waste packages and drip shields can be considered as potentially subject to early failure (i.e., have undetected defects). The probability of having an undetected defect per waste package or drip shield, \bar{p}_{defect} , in the repository is given by Equation 25:

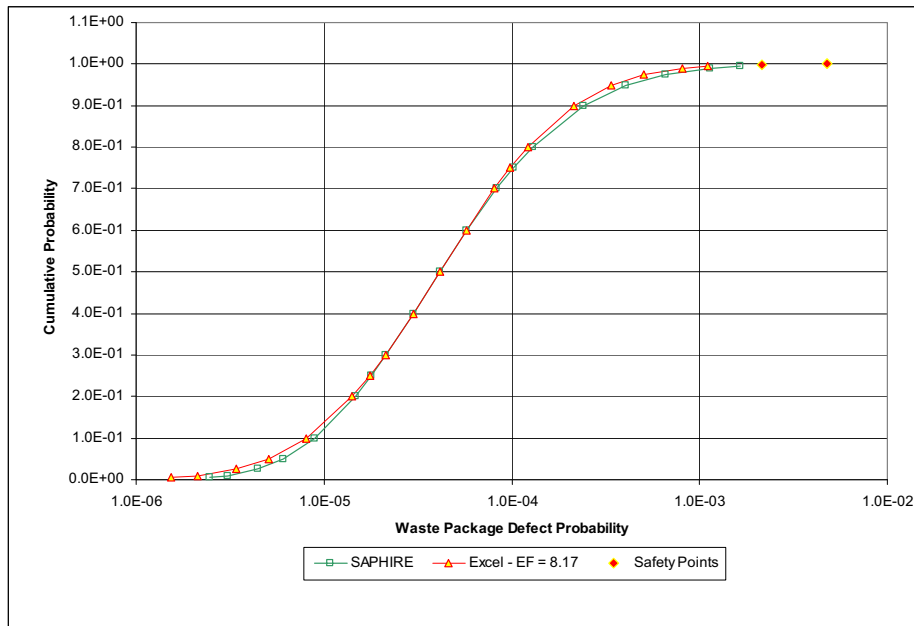
$$\bar{p}_{defect} = \text{mean of } p_{defect} \quad (\text{Eq. 25})$$

The cumulative probability distribution of having an undetected defect per waste package, (p_{defect}), is listed in Table 6-9 and shown graphically in Figure 6-20. Similar results for a drip shield are given in Table 6-10 and Figure 6-21.

Table 6-9. Cumulative Uncertainty Distribution for Undetected Waste Package Defects

End State	Distribution Quantile (%)	Probability Values	Lower Bound 95% Confidence Interval	Upper Bound 95% Confidence Interval
Damaged Waste Package	0.5	2.447×10^{-6}	2.377×10^{-6}	2.519×10^{-6}
	1.0	3.086×10^{-6}	3.008×10^{-6}	3.152×10^{-6}
	2.5	4.426×10^{-6}	4.335×10^{-6}	4.504×10^{-6}
	5.0	6.099×10^{-6}	6.015×10^{-6}	6.196×10^{-6}
	10.0	8.973×10^{-6}	8.876×10^{-6}	9.078×10^{-6}
	20.0	1.470×10^{-5}	1.452×10^{-5}	1.485×10^{-5}
	25.0	1.792×10^{-5}	1.772×10^{-5}	1.812×10^{-5}
	30.0	2.149×10^{-5}	2.124×10^{-5}	2.172×10^{-5}
	40.0	3.000×10^{-5}	2.967×10^{-5}	3.031×10^{-5}
	50.0	4.138×10^{-5}	4.096×10^{-5}	4.181×10^{-5}
	60.0	5.778×10^{-5}	5.712×10^{-5}	5.844×10^{-5}
	70.0	8.354×10^{-5}	8.256×10^{-5}	8.463×10^{-5}
	75.0	1.029×10^{-4}	1.016×10^{-4}	1.041×10^{-4}
	80.0	1.295×10^{-4}	1.279×10^{-4}	1.312×10^{-4}
	90.0	2.409×10^{-4}	2.369×10^{-4}	2.453×10^{-4}
	95.0	4.073×10^{-4}	3.995×10^{-4}	4.153×10^{-4}
	97.5	6.538×10^{-4}	6.354×10^{-4}	6.712×10^{-4}
	99.0	1.139×10^{-3}	1.091×10^{-3}	1.192×10^{-3}
99.5	1.649×10^{-3}	1.591×10^{-3}	1.786×10^{-3}	

Output DTN: MO0701PASHIELD.000, files *SAPHIRE OUTPUT.zip* and *lognormalresults vs uncertainty.xls*.



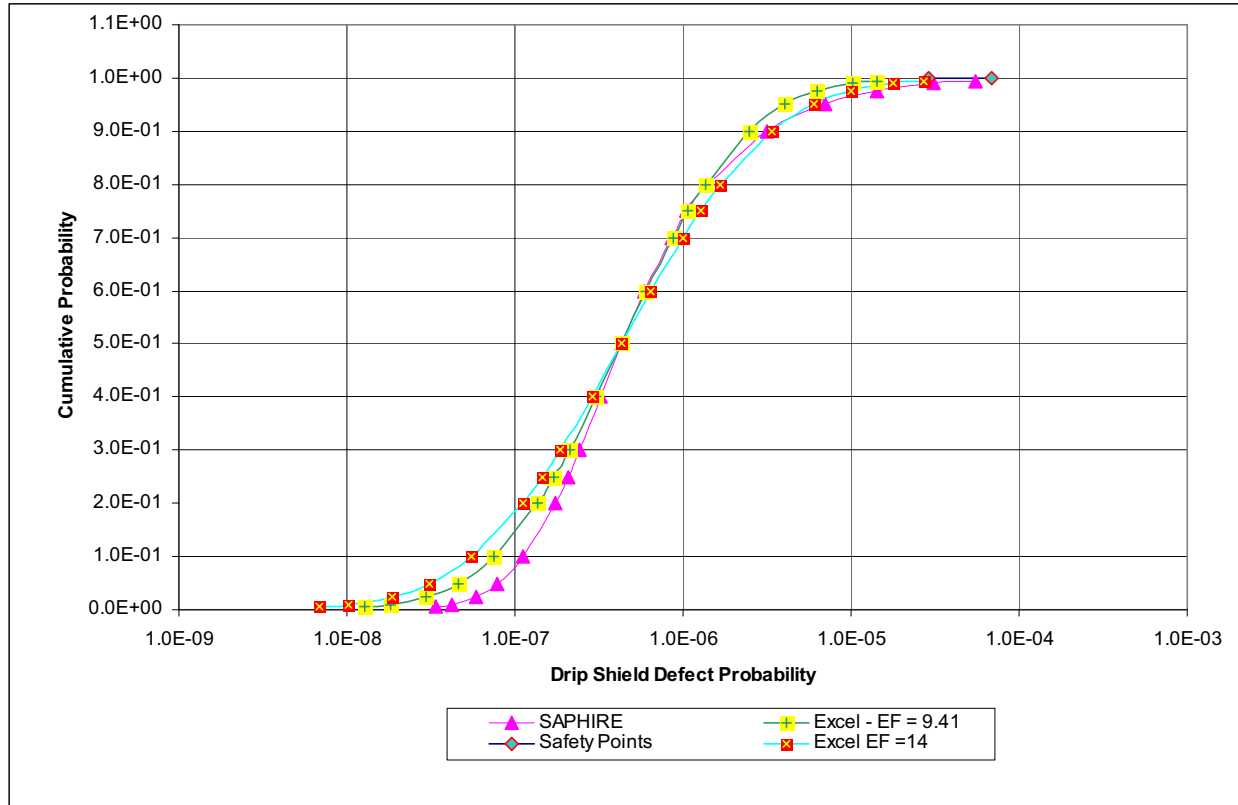
Output DTN: MO0701PASHIELD.000, *lognormalresults vs uncertainty.xls*.

Figure 6-20. Cumulative Uncertainty Distribution for Undetected Waste Package Defects (UNC_WP_EF)

Table 6-10. Cumulative Uncertainty Distribution for Undetected Drip Shield Defects

End State	Distribution Quantile (%)	Probability Values	Lower Bound 95% Confidence Interval	Upper Bound 95% Confidence Interval
Damaged Drip Shield	0.5	3.379×10^{-8}	3.297×10^{-8}	3.480×10^{-8}
	1.0	4.243×10^{-8}	4.135×10^{-8}	4.348×10^{-8}
	2.5	5.882×10^{-8}	5.773×10^{-8}	5.986×10^{-8}
	5.0	7.864×10^{-8}	7.766×10^{-8}	7.956×10^{-8}
	10.0	1.118×10^{-7}	1.107×10^{-7}	1.129×10^{-7}
	20.0	1.739×10^{-7}	1.723×10^{-7}	1.755×10^{-7}
	25.0	2.065×10^{-7}	2.046×10^{-7}	2.082×10^{-7}
	30.0	2.408×10^{-7}	2.386×10^{-7}	2.431×10^{-7}
	40.0	3.231×10^{-7}	3.202×10^{-7}	3.258×10^{-7}
	50.0	4.302×10^{-7}	4.264×10^{-7}	4.340×10^{-7}
	60.0	5.858×10^{-7}	5.798×10^{-7}	5.922×10^{-7}
	70.0	8.486×10^{-7}	8.381×10^{-7}	8.599×10^{-7}
	75.0	1.056×10^{-6}	1.043×10^{-6}	1.069×10^{-6}
	80.0	1.382×10^{-6}	1.359×10^{-6}	1.402×10^{-6}
	90.0	3.171×10^{-6}	3.095×10^{-6}	3.239×10^{-6}
	95.0	6.968×10^{-6}	6.757×10^{-6}	7.181×10^{-6}
	97.5	1.421×10^{-5}	1.356×10^{-5}	1.481×10^{-5}
99.0	3.106×10^{-5}	2.976×10^{-5}	3.275×10^{-5}	
99.5	5.510×10^{-5}	5.153×10^{-5}	5.838×10^{-5}	

Output DTN: MO0701PASHIELD.000, files *SAPHIRE OUTPUT.zip* and *lognormalresults vs uncertainty.xls*.



Output DTN: MO0701PASHIELD.000, *lognormalresults vs uncertainty.xls*.

Figure 6-21. Cumulative Uncertainty Distribution for Undetected Drip Shield Defects (UNC_DS_EF)

The CDFs in the figures were developed in the Excel file *lognormalresults vs uncertainty.xls* in the output DTN: MO0701PASHIELD.000 using the quantile median values and error factors based on the 5th and 95th quantiles. Figure 6-20 shows the CDF of the direct output from SAPHIRE along with a developed lognormal distribution using the median value and error factor based on the 5th and 95th percentiles for the waste package. The lognormal distribution is the curve TSPA should use when calculating the number of waste packages for each realization that have an undetected defect that can lead to an early failure. Figure 6-21 shows the CDF of the direct output from SAPHIRE along with a developed lognormal distribution using the median value and error factor based on the 5th and 95th percentiles for the drip shield. The lognormal CDF that was constructed for the drip shield in the Excel file *lognormalresults vs uncertainty.xls* uses the quantile median values and an error factor of 14 that more closely captures the upper part of the SAPHIRE CDF than does the CDF that used the error factor based on the 5th and 95th percentiles. This latter CDF is also shown in Figure 6-21. Tables 6-9 and 6-10, included in the output DTN: MO0701PASHIELD.000, list the uncertainty output from SAPHIRE in quantile form in Columns 2 and 3. Columns 4 and 5 represent the statistical confidence (5th and 95th percent bounds) about the quantile probability values.

As a safety calculation, the joint probability that a waste package and drip shield, both with undetected flaws, could be co-located in the repository is estimated with combinatorial methods. The joint probability is based on the likelihood of placing a drip shield with an undetected flaw

at the same location as a waste package with an undetected flaw. The probability, p_i , that a drip shield with undetected flaws is placed in a specific location (i.e., over any specific waste package) is given by the number of possible combinations (in this case, distributions), N , of k identical objects in n total objects, as shown in Equation 26:

$$N = \frac{n!}{(n-k)! \times k!} \times \frac{k}{n} = \frac{(n-1)!}{(n-k)! \times (k-1)!} \quad (\text{Eq. 26})$$

normalized by the overall number of combinations resulting in the probability, p_i , given by Equation 27:

$$p_i = \frac{N}{\frac{n!}{(n-k)! \times k!}} = \frac{k}{n} \quad (\text{Eq. 27})$$

The total probability of placing a flawed drip shield at the location of a flawed waste package is given by Equation 28:

$$P = p_i \times F_{wp} \quad (\text{Eq. 28})$$

where F_{WP} is the probability that any given waste package has undetected flaws (i.e., $N_{WP-flaw}/11,184$ where $N_{WP-flaw}$ is the number of waste packages at the selected quantile value having undetected flaws and 11,184 is the estimated repository inventory used for evaluating Equation 28). The results from Equation 28 are insensitive to an inventory range between 10,990 and 11,190. The estimated repository waste package inventory ranges from 11,162 to 11,629 (DTN: MO0702PASTREAM.001 [DIRS 179925], Spreadsheet UNIT CELL) where 11,162 is the nominal value.

To illustrate this calculation, it is assumed there are 11,184 waste packages and the same number of drip shields. Based on the 0.999 and 0.9999 quantile values from the lognormal distribution fit to the waste package and drip shield undetected-flaw distribution, the total number of waste packages with an undetected defect is 24 and 53, respectively; and the total number of drip shields with an undetected defect is 1 and 1, respectively (see Table 6-11). Therefore, the joint probability at the 0.9999 case is $[(53/11,184) \times (1/11,184) \approx 4.2 \times 10^{-7}]$. The results, from output DTN: MO0701PASHIELD.000, file *lognormalresults vs uncertainty.xls*, are listed in Table 6-11.

Table 6-11. Joint Probability for Co-Location of Flawed Drip Shield and Waste Package

Quantile	Number of Waste Packages with Flaws	Number of Drip Shields with Flaws	Joint Probability
0.999	24	1	$\approx 1.9 \times 10^{-7}$
0.9999	53	1	$\approx 4.2 \times 10^{-7}$

Output DTN: MO0701PASHIELD.000, file *lognormalresults vs uncertainty.xls*.

6.5.2 Assessing Consequences of Defects

The above analyses predict rates for defects to be introduced during drip shield and waste package fabrication, handling, and emplacement operations. It is necessary to develop a method to apply these defect estimates in order to calculate the impacts on repository performance, that is, to determine the impact on radionuclide dose to the reasonably maximally exposed individual to contribute to a calculated dose comparison to the regulatory standard. As stated in Section 1, if a waste package is affected by a type of defect that may lead to its early failure, it does not mean that this waste package is due to fail at emplacement in the repository. Failure of the waste package will only occur after degradation processes take place, which may happen hundreds or even thousands of years after emplacement. Even if a waste package were to fail soon after emplacement because of a defect, its radionuclide inventory might not necessarily be available for transport. This is because most through-wall penetrations, especially cracks from SCC, are usually tight and of limited length. Parallel arguments apply to a drip shield relative to its ability to perform its function.

A realistic estimate of when components with defects will fail would be difficult to develop and justify given the nature of the problem:

- Physical failure of highly corrosion resistant metallic structures with very small loads under nominal conditions
- The time frames involved—centuries to millennia or longer
- The lack of long-term experience with such engineered systems in standard industrial or engineering practice.

Because of such considerations, an assumption of complete failure of the components with respect to radionuclide containment (waste package) or seepage (drip shield) at the time of repository closure is recommended for implementation in the TSPA model, because this will lead to an overestimation of the potential for radionuclide release early in the life of the repository. However, a similar approach for criticality evaluations is not necessarily conservative since the geometrical configuration is only one of several parameters that determine the criticality potential of configurations. Thus, criticality evaluations must analyze a series of configurations to quantify their criticality potential.

7. CONCLUSIONS

The intended use of this scientific analysis is to provide input to:

- Repository licensing activities
- Performance assessment for implementation of the early failure mechanisms for waste packages and drip shields in TSPA
- Screening analysis of postclosure criticality features, events, and processes.

The various parameters to be used as inputs to the repository licensing activities have been developed from analyses of mechanisms for early failure, as presented in Sections 6.3 and 6.4. Information developed from this analysis is provided in the output DTNs: MO0701PASHIELD.000 and MO0705EARLYEND.000.

7.1 WASTE PACKAGE AND DRIP SHIELD EARLY FAILURE IMPLEMENTATION

A complete list of early waste package and drip shield failure parameter inputs into TSPA from this analysis is provided in Table 7-1 and is included in the output DTN: MO0701PASHIELD.000. As shown in Table 7-1, the waste package and drip shield early failure parameters include:

- The fraction of defects capable of propagation based on orientation (Section 6.3.1.5)
- Characteristic flaw size for ultrasonic testing and PND (Section 6.3.1.6)
- Shape factor for PND (Section 6.3.1.6)
- Lower limit for PND (Section 6.3.1.6)
- Total volume of weld examined during testing (Appendix A, Section A.1)
- Number of flaws found during testing
- Cumulative size of weld flaws
- Flaw-density parameter (Section 6.3.1.3)
- Flaw-size parameter (Section 6.3.1.2)
- Uncertainty distribution for the occurrence of undetected defects in waste package outer corrosion barriers (Table 6-9 and Figure 6-20)
- Uncertainty distribution for the occurrence of undetected defects in drip shields (Table 6-10 and Figure 6-21).

Table 7-1. TSPA Waste Package and Drip Shield Early Failure Parameter Specification

Parameter Name	Parameter Description	Parameter Type	Parameter Value and Uncertainty/Variability
Defect_Frac_Orientation	Fraction of defects capable of propagation based on orientation.	Constant	0.008
Location_PND (s_0)	Characteristic flaw size for ultrasonic testing PND in mm.	Constant	1.5875 mm
Shape_PND (ν)	Shape factor for PND.	Constant	1.5
Detection_Thresh_PND (ϵ_t)	Lower limit for ultrasonic testing PND.	Constant	0.005
Cumulative_Sample_Weld_Volume (V_f)	Total volume of weld examined during testing.	Constant	$1.656 \times 10^{-2} \text{ m}^3$
Num_Weld_Flaws (n_f)	Number of flaws found during testing.	Constant	7
Cum_Size_Flaws (s_t)	Cumulative size of weld flaws.	Constant	31.75 mm
CS ^a	Cross-sectional area of weld examined during testing.	Constant	$2.135 \times 10^{-4} \text{ m}^2$
Defect_Count_a	Flaw density parameter (flaws per m^3 of weld, λ_d).	Stochastic	Gamma distribution with a mean of $(n_f + 1/2) / V_f$ and a standard deviation of $\text{sqrt}(n_f + 1/2) / V_f$
Defect_Size_a	Flaw-size parameter (λ_s , per mm).	Stochastic	Gamma distribution with a mean of n_f / s_t and a standard deviation of $\text{sqrt}(n_f) / s_t$
UNC_WP_EF	Parameters for probability distribution for undetected defects in waste packages. For TSPA purposes, this distribution is the probability that a waste package will fail soon after emplacement.	Stochastic	Log normal distribution with a median of 4.14×10^{-5} and an error factor of 8.17. The quantile data points are also included.
UNC_DS_EF	Parameters for probability distribution for undetected defects in drip shields. For TSPA purposes, this distribution is the probability that a drip shield will fail soon after emplacement.	Stochastic	Log normal distribution with a median of 4.30×10^{-7} and an error factor of 14. The CDF data points are also included.

^a The weld cross-sectional (CS) area is provided as a parameter, and the total weld volume for a waste package depends on the diameter of the particular waste package.

Output DTN: MO0701PASHIELD.000, file *Tables for DTN Readme.doc*.

There is only one input parameter feeding the TSPA from the analysis of early failure mechanisms in the drip shield; the other eleven parameters are from the analysis of early failure mechanisms in the waste package.

The weld flaw analysis applies only to the waste package outer corrosion barrier closure welds. Other welds in the waste package outer corrosion barrier are heat-treated for stress relief during the solution annealing of the outer corrosion barrier for phase control. In addition, these latter welds are examined with ultrasonic testing, radiographic examination, and visual penetrant testing methods that result in a lower (nonquantified) PND.

It is important to note that, even if a waste package outer corrosion barrier or drip shield has a type of defect that may lead to its early failure, that does not mean that the particular unit is due to fail immediately upon emplacement in the repository. Failure will only occur after degradation processes take place, which may happen hundreds of years after emplacement.

However, if a simplifying assumption is made (in the TSPA model) that units with defects fail immediately, then the distributions for occurrence of defects become distributions for failed units.

The output DTN: MO0701PASHIELD.000 includes the combined uncertainty distributions for undetected defects in the waste package outer corrosion barrier and drip shield with the individual end-state uncertainty distributions provided in output DTN: MO0705EARLYEND.000.

7.2 TSPA WELD-FLAW IMPLEMENTATION

Flaws in the closure-lid welds are potential sites for stress corrosion crack initiation. The characteristics of weld flaws in the closure welds are important to consider in regards to the waste package SCC mechanism. Residual stress analyses showed that the hoop stress is the dominant stress driving crack growth; thus, only radially oriented weld flaws are potential sites for SCC initiation. In addition, while size plays a role in the potential severity of a flaw, no minimum size is defined, and all remaining weld flaws are considered for potential propagation; however, the flaw-density distribution is based only upon the (non-spherical) detected flaws and may therefore underestimate the number of small (sub-millimeter) flaws.

To quantitatively estimate the number of remaining flaws in the waste package outer barrier closure weld, several steps are needed. This analysis is presented in Section 6.3.1. The size distribution (Section 6.3.1.2, Equation 7 and gamma distribution parameter λ_s), based upon ultrasonic testing-detected flaws in Alloy 22 specimen rings, is screened by the detection capability of ultrasonic testing (Section 6.3.1.6, Equation 17). This results in a determination of the fraction of weld flaws that are not detected (Section 6.3.1.7). That fraction is multiplied by the initial weld-flaw density (Section 6.3.1.3, Equation 12 and gamma distribution parameter λ_d , from Equation 11) to provide a distribution for the remaining weld flaws of potential concern (Section 6.3.1.8). Only a small fraction (0.8%, Section 6.3.1.5) of those flaws may be oriented along the hoop stress direction such that they might propagate by SCC action. The depth of these flaws is considered to be uniformly distributed through the weld thickness (Section 6.3.1.4).

7.3 EVALUATION OF YUCCA MOUNTAIN REVIEW PLAN CRITERIA

Because this report serves, in part, as the basis for the repository license application, the information contained herein conforms to applicable acceptance criteria. The YMRP (NRC 2003 [DIRS 163274]) contains acceptance criteria intended to establish the basis for the review of the material contained in the license application and, in particular, material applicable to the barrier system. This analysis addresses the degradation of two features of the engineered barrier system—the waste package outer corrosion barrier and the drip shield. Thus, based on the processes involved with the degradation of the waste package outer corrosion barrier and drip shield and the potential impact of such degradation, the acceptance criteria that are applicable to this analysis are evaluated below.

YMRP Acceptance Criteria 2.2.1.1.3—System Description and Demonstration of Multiple Barriers

Acceptance Criterion 1—Identification of Barriers Is Adequate.

Barriers relied upon to achieve compliance with 10 CFR 63.113(b), as demonstrated in the total system performance assessment, are adequately identified and clearly linked to their capability.

Evaluation of Criterion: The discussion contained in Sections 6.2, 6.3, and 6.4 of this report establishes the configurations of the drip shields and waste packages. The capability of these items to function as barriers is evaluated in the context of how that capability could be compromised. The rates at which the capabilities could be compromised are estimated, and functional representations are developed in Section 6.5 for inclusion in the TSPA.

Acceptance Criterion 2—Description of Barrier Capability Is Acceptable.

The capability of the identified barriers to prevent or substantially reduce the movement of water or radionuclides from the Yucca Mountain repository to the accessible environment or prevent the release or substantially reduce the release rate of radionuclides from the waste is adequately identified and described:

(1) The information on the time period over which each barrier performs its intended function, including any changes during the compliance period, is provided;

(2) The uncertainty associated with barrier capabilities is adequately described;

(3) The described capabilities are consistent with the results from the total system performance assessment;

(4) The described capabilities are consistent with the definition of a barrier at 10 CFR 63.2

Evaluation of Criterion: The capability of the drip shields and waste packages to prevent or substantially reduce the release rate of radionuclides from the waste is evaluated in the context of undetected manufacturing defects or handling accidents that could compromise the capability prematurely (before it would degrade through expected mechanisms such as corrosion or seismic events). Time periods for these early failure scenarios are not explicitly estimated; instead, the failures are assumed to occur concurrently with closure of the repository, because this is expected to overestimate the consequences of the undetected defects. Uncertainty is included in these estimates through application of error factors, typical of those discussed in Section 4.1.

Acceptance Criterion 3—Technical Basis for Barrier Capability Is Adequately Presented.

The technical bases are consistent with the technical basis for the performance assessment. The technical basis for assertions of barrier capability is commensurate with the importance of each barrier's capability and the associated uncertainties.

Evaluation of Criterion: The technical bases for the predictions of early failure rates of drip shields and waste packages are provided to enable inclusion of these estimates in the TSPA. These bases are commensurate with the importance of the barriers provided by these components. Uncertainties are incorporated in the input data as discussed in Section 4.1, and summary data are discussed in Section 6.5.

YMRP Acceptance Criterion 2.2.1.3.1.3—Degradation of Engineered Barriers

Acceptance Criterion 3—Data Uncertainty Is Characterized and Propagated Through the Model Abstraction.

(4) The US Department of Energy uses appropriate methods for nondestructive examination of fabricated engineered barriers to assess the type, size, and location of fabrication defects that might lead to premature failure as a result of rapidly initiated engineered barriers degradation. The US Department of Energy specifies and justifies the allowable distribution of fabrication defects in the engineered barriers and assesses the effects that cannot be detected on the performance of the engineered barriers.

Evaluation of Criterion: The analyses contained in this report consider the potential existence of fabrication defects, the probability of their occurrence, and their potential impact. Possible defects and their probability of occurrence, including appropriate uncertainty, are developed in Sections 6.2, 6.3, and 6.4. The summation of these defect probabilities is calculated in Section 6.5.

INTENTIONALLY LEFT BLANK

8. INPUTS AND REFERENCES

8.1 DOCUMENTS CITED

- 100441 Doubt, G. 1984. *Assessing Reliability and Useful Life of Containers for Disposal of Irradiated Fuel Waste*. AECL-8328. Chalk River, Ontario, Canada: Atomic Energy of Canada Limited. TIC: 227332.
- 100444 EPRI (Electric Power Research Institute) 1997. *The Technical Basis for the Classification of Failed Fuel in the Back-End of the Fuel Cycle*. EPRI TR-108237. Palo Alto, California: Electric Power Research Institute. TIC: 236839.
- 101978 Holman, J.P. 1997. *Heat Transfer*. 8th Edition. New York, New York: McGraw-Hill. TIC: 239954.
- 102049 Yang, R.L. 1997. "Meeting the Challenge of Managing Nuclear Fuel in a Competitive Environment." *Proceedings of the 1997 International Topical Meeting on LWR Fuel Performance, Portland, Oregon, March 2-6, 1997*. Pages 3-10. La Grange Park, Illinois: American Nuclear Society. TIC: 232556.
- 104667 Modarres, M. 1993. *What Every Engineer Should Know About Reliability and Risk Analysis*. New York, New York: Marcel Dekker. TIC: 238168.
- 106591 NRC (U.S. Nuclear Regulatory Commission) 1983. *PRA Procedures Guide, A Guide to the Performance of Probabilistic Risk Assessments for Nuclear Power Plants*. NUREG/CR-2300. Two volumes. Washington, D.C.: U.S. Nuclear Regulatory Commission. TIC: 205084.
- 106780 ASM International 1990. *Properties and Selection: Irons, Steels, and High-Performance Alloys*. Volume 1 of *Metals Handbook*. 10th Edition. Materials Park, Ohio: ASM International. TIC: 245666.
- 107504 Babcock & Wilcox 1970. Analysis and Resolution of Dye-Penetrant Indications in Submerged Arc Weld Cladding of Reactor Coolant System Straight Piping. BAW-1363. Barberton, Ohio: Babcock & Wilcox. TIC: 245525.
- 107509 Babcock & Wilcox 1970. Analysis and Resolution of Dye-Penetrant Indications in AISI-304 Alloy Cladding of Reactor Coolant System Elbows. BAW-1364. Barberton, Ohio: Babcock & Wilcox. TIC: 245526.
- 107696 Bush, S.H. 1983. *Reliability of Nondestructive Examination*. NUREG/CR-3110. Volume 3. Washington, D.C.: U.S. Nuclear Regulatory Commission. TIC: 218323.

- 107749 EPA (U.S. Environmental Protection Agency) 1987. *Causes of Release from UST Systems*. EPA 510-R-92-702. Washington, D.C.: Environmental Protection Agency. TIC: 244679.
- 107751 EPA 1987. *Causes of Release from UST Systems: Attachments*. EPA 510-R-92-703. Washington, D.C.: Environmental Protection Agency. TIC: 244678.
- 107754 Framatome Cogema Fuels 1996. *Fuel Integrity*. Proprietary 12-1244558-00. Lynchburg, Virginia: Framatome Cogema Fuels. ACC: MOL.19990930.0110.
- 107755 Grainawi, L. 1999. "Manufacturing Defects." Memo from L. Grainawi (Steel Tank Institute) to J. Massari (Framatome Technologies), April 20, 1999. TIC: 244544.
- 107758 Heasler, P.G. and Doctor, S.R. 1996. *Piping Inspection Round Robin*. NUREG/CR-5068. Washington, D.C.: U.S. Nuclear Regulatory Commission. TIC: 244618.
- 107764 Khaleel, M.A.; Chapman, O.J.V.; Harris, D.O.; and Simonen, F.A. 1999. "Flaw Size Distribution and Flaw Existence Frequencies in Nuclear Piping." *Probabilistic and Environmental Aspects of Fracture and Fatigue: The 1999 ASME Pressure Vessels and Piping Conference*. PVP-386. Pages 127-144. New York, New York: American Society of Mechanical Engineers. TIC: 245621.
- 107765 National Board of Boiler and Pressure Vessel Inspectors 1999. "Incident Reports." Columbus, Ohio: National Board of Boiler and Pressure Vessel Inspectors. Accessed September 29, 1999. TIC: 245629. URL: <http://www.nationalboard.com/incidents.html>
- 107766 S.M. Stoller and Company 1976. *Nuclear Power Experience*. Pages 5 and 44. Boulder, Colorado: S.M. Stoller and Company. TIC: 245630.
- 107767 Hodges, M.W. 1998. "Confirmatory Action Letter 97-7-001, Technical Evaluation, Docket No: 72-1007." Washington, D.C.: U.S. Nuclear Regulatory Commission. Accessed November 2, 1999. TIC: 244630. URL: <http://www.nrc.gov/OPA/reports/sn072298.htm>
- 107774 Potts, G.A. and Proebstle, R.A. 1994. "Recent GE BWR Fuel Experience." *Proceedings of the 1994 International Topical Meeting on Light Water Reactor Fuel Performance, West Palm Beach, Florida, April 17-21, 1994*. Pages 87-95. La Grange Park, Illinois: American Nuclear Society. TIC: 243043.
- 107783 Smith, T.A. and Warwick, W.A. 1978. "Survey of Defects in Pressure Vessels Built to High Standards of Construction." *The Annual Winter Meeting of the American Society of Mechanical Engineers, San Francisco, California, December 10-15, 1978*. PVP-PB-032. Pages 21-53. New York, New York: American Society of Mechanical Engineers. TIC: 244550.

- 107789 Tschoepe, E., III; Lyle, F.F., Jr.; Dancer, D.M.; Interrante, C.G.; and Nair, P.K. 1994. *Field Engineering Experience with Structural Materials*. San Antonio, Texas: Center for Nuclear Waste Regulatory Analyses. TIC: 244536.
- 107799 NRC 1975. *Reactor Safety Study: An Assessment of Accident Risks in U.S. Commercial Nuclear Power Plants*. WASH-1400. Washington, D.C.: U.S. Nuclear Regulatory Commission. TIC: 236923.
- 108219 Babcock & Wilcox 1979. *Records Investigation Report Related to Off-Chemistry Welds in Material Surveillance Specimens and Response to IE Bulletins 78-12 and 78-12A - Supplement*. Mt. Vernon, Indiana: Babcock & Wilcox. TIC: 244621.
- 119579 SAE (Society of Automotive Engineers) 1993. *Metals & Alloys in the Unified Numbering System*. 6th Edition. Warrendale, Pennsylvania: Society of Automotive Engineers. TIC: 243414.
- 139383 Swain, A.D. and Guttman, H.E. 1983. *Handbook of Human Reliability Analysis with Emphasis on Nuclear Power Plant Applications Final Report*. NUREG/CR-1278. Washington, D.C.: U.S. Nuclear Regulatory Commission. TIC: 246563.
- 141700 Blanton, C.H. and Eide, S.A. 1993. *Savannah River Site, Generic Data Base Development (U)*. WSRC-TR-93-262. Aiken, South Carolina: Westinghouse Savannah River Company. TIC: 246444.
- 149953 Shcherbinskii, V.G. and Myakishev, V.M. 1970. "Statistical Distribution of Welding Defects with Respect to Azimuth." *Translated from Defektoskopiya, No. 4*, 143-144. New York, New York: Plenum Publishing. TIC: 247890.
- 157560 BSC (Bechtel SAIC Company) 2001. *Waste Package Misload Probability*. CAL-WHS-MD-000001 REV 00. Las Vegas, Nevada: Bechtel SAIC Company. ACC: MOL.20011212.0186.
- 157684 Benhardt, H.C.; Eide, S.A.; Held, J.E.; Olsen, L.M.; and Vail, R.E. 1994. *Savannah River Site Human Error Data Base Development for Nonreactor Nuclear Facilities (U)*. WSRC-TR-93-581. Aiken, South Carolina: Westinghouse Savannah River Company, Savannah River Site. ACC: MOL.20061201.0160.
- 157687 Gertman, D.I.; Gilbert, B.G.; Gilmore, W.E.; and Galyean, W.J. 1989. *Nuclear Computerized Library for Assessing Reactor Reliability (NUCLARR): Data Manual, Part 4: Summary Aggregations*. NUREG/CR-4639, Vol. 5, Part 4, Rev. 2. Washington, D.C.: U.S. Nuclear Regulatory Commission. TIC: 252112.
- 160078 Schuster, G.J.; Doctor, S.R.; and Heasler, P.G. 1998. *Density and Distribution of Flaw Indications in PVRUF*. Volume 1 of *Characterization of Flaws in U.S. Reactor Pressure Vessels*. NUREG/CR-6471. Washington, D.C.: U.S. Nuclear Regulatory Commission. TIC: 253278.

- 160924 Martz, H.F. and Waller, R.A. 1991. *Bayesian Reliability Analysis*. Malabar, Florida: Krieger Publishing Company. TIC: 252996.
- 160971 Apostolakis, G. and Kaplan, S. 1981. "Pitfalls in Risk Calculations." *Reliability Engineering*, 2, 135-145. Barking, England: Applied Science Publishers. TIC: 253648.
- 163114 Smith, D. 2003. Weld Flaw Evaluation and Nondestructive Examination Process Comparison Results for High-Level Radioactive Waste Package Manufacturing Program. TDR-EBS-ND-000007 REV 01. Las Vegas, Nevada: Bechtel SAIC Company. ACC: ENG.20030515.0003.
- 163274 NRC 2003. *Yucca Mountain Review Plan, Final Report*. NUREG-1804, Rev. 2. Washington, D.C.: U.S. Nuclear Regulatory Commission, Office of Nuclear Material Safety and Safeguards. TIC: 254568.
- 165403 NRC 1978. *Atypical Weld Material in Reactor Pressure Vessel Welds*. IE Bulletin No. 78-12. Washington, D.C.: U.S. Nuclear Regulatory Commission, Office of Inspection and Enforcement. ACC: MOL.20030922.0136.
- 167564 DOE (U.S. Department of Energy) 2003. *Software Management Report: CWD Version Number 2.0*. Document ID: 10363-SMR-2.0-00. Las Vegas, Nevada: U.S. Department of Energy, Office of Repository Development. ACC: MOL.20030501.0182.
- 170024 BSC 2004. *Analysis of Mechanisms for Early Waste Package/Drip Shield Failure*. CAL-EBS-MD-000030 REV 00C. Las Vegas, Nevada: Bechtel SAIC Company. ACC: DOC.20040913.0006; DOC.20050606.0005; DOC.20050830.0002.
- 173869 SNL (Sandia National Laboratories) 2007. *Screening Analysis of Criticality Features, Events, and Processes for License Application*. ANL-DS0-NU-000001 REV 00. Las Vegas, Nevada: Sandia National Laboratories.
- 174757 Lloyd, R.L. 2003. *A Survey of Crane Operating Experience at U.S. Nuclear Power Plants from 1968 through 2002*. NUREG-1774. Washington, D.C.: U.S. Nuclear Regulatory Commission. ACC: MOL.20050802.0185.
- 175539 BSC 2005. *Q-List*. 000-30R-MGR0-00500-000-003. Las Vegas, Nevada: Bechtel SAIC Company. ACC: ENG.20050929.0008.
- 176937 DOE 2006. *Yucca Mountain Project Conceptual Design Report*. TDR-MGR-MD-000014, Rev. 05. Las Vegas, Nevada: U.S. Department of Energy, Office of Repository Development. ACC: ENG.20060505.0003.

- 177092 DOE 2006. *Quality Assurance Requirements and Description*. DOE/RW-0333P, Rev. 18. Washington, D.C.: U.S. Department of Energy, Office of Civilian Radioactive Waste Management. ACC: DOC.20060602.0001.
- 177417 SNL 2007. *Stress Corrosion Cracking of Waste Package Outer Barrier and Drip Shield Materials*. ANL-EBS-MD-000005 REV 03. Las Vegas, Nevada: Sandia National Laboratories. ACC: DOC.20070530.0012.
- 178849 SNL 2007. *Technical Work Plan for Postclosure Engineered Barrier Degradation Modeling*. TWP-EBS-MD-000020 REV 00. Las Vegas, Nevada: Sandia National Laboratories. ACC: DOC.20070216.0001.
- 178871 SNL 2007. *Total System Performance Assessment Model /Analysis for the License Application*. MDL-WIS-PA-000005 REV 00. Las Vegas, Nevada: Sandia National Laboratories.
- 179354 SNL 2007. *Total System Performance Assessment Data Input Package for Requirements Analysis for EBS In-Drift Configuration*. TDR-TDIP-ES-000010 REV 00. Las Vegas, Nevada: Sandia National Laboratories.
- 179394 SNL 2007. *Total System Performance Assessment Data Input Package for Requirements Analysis for TAD Canister and Related Waste Package Overpack Physical Attributes Basis for Performance Assessment*. TDR-TDIP-ES-000006 REV 00. Las Vegas, Nevada: Sandia National Laboratories.
- 179567 SNL 2007. *Total System Performance Assessment Data Input Package for Requirements Analysis for DOE SNF/HLW and Navy SNF Waste Package Overpack Physical Attributes Basis for Performance Assessment*. TDR-TDIP-ES-000009 REV 00. Las Vegas, Nevada: Sandia National Laboratories.
- 180190 BSC 2007. *Waste Package Fabrication*. 000-3SS-DSC0-00100-000-001. Las Vegas, Nevada: Bechtel SAIC Company. ACC: ENG.20070315.0001.

8.2 CODES, STANDARDS, REGULATIONS, AND PROCEDURES

- 180319 10 CFR 63. 2007. Energy: Disposal of High-Level Radioactive Wastes in a Geologic Repository at Yucca Mountain, Nevada. Internet Accessible.
- LS-PRO-0203. *Q-List and Classification of Structures, Systems, Components and Barriers*.
- SCI-PRO-001. *Qualification of Unqualified Data*.
- SCI-PRO-005. *Scientific Analyses and Calculations*.
- SCI-PRO-004. *Managing Technical Product Inputs*.

IM-PRO-001. *Managing Electronic Mail Records.*

IM-PRO-002. *Control of the Electronic Management of Information.*

IM-PRO-003. *Software Management.*

8.3 SOURCE DATA, LISTED BY DATA TRACKING NUMBER

179925 MO0702PASTREAM.001. Waste Stream Composition and Thermal Decay Histories for LA. Submittal date: 02/15/2007.

8.4 OUTPUT DATA, LISTED BY DATA TRACKING NUMBER

MO0701PASHIELD.000. Waste Package/Drip Shield Early Failure Probabilities. Submittal date: 04/24/2007.

MO0705EARLYEND.000. Waste Package/Drip Shield Early Failure End State Probabilities. Submittal date: 05/18/2007.

8.5 SOFTWARE CODES

162809 CWD V. 2.0. 2003. WINDOWS 2000. STN: 10363-2.0-00.

177010 SAPHIRE V. 7.26. 2006. Windows 2000, XP. STN: 10325-7.26-00.

APPENDIX A
EVALUATION OF WELD-FLAW TEST DATA

APPENDIX A – EVALUATION OF WELD-FLAW TEST DATA

The weld-flaw data from *Analysis of Mechanisms for Early Waste Package/Drip Shield Failure* (BSC 2004 [DIRS 170024]) have been re-analyzed with the Mathcad® computational file *Early Fail-Weld Flaw-rlj.xmcd* in the output DTN: MO0701PASHIELD.000 as depicted in this appendix. The weld-flaw data are derived from the drawing cited in *Total System Performance Assessment Data Input Package for Requirements Analysis for TAD Canister and Related Waste Package Overpack Physical Attributes Basis for Performance Assessment* (SNL 2007 [DIRS 179394], Section 4.1.2.3). The waste package outer corrosion barrier data are derived from *Total System Performance Assessment Data Input Package for Requirements Analysis for TAD Canister and Related Waste Package Overpack Physical Attributes Basis for Performance Assessment* (SNL 2007 [DIRS 179394], Table 4.3).

Set Mathcad sheet preferences

ORIGIN:= 1 sd1 := Seed(1381285117)

A.1 Inputs from Specimen Rings

The source references and justifications for the values presented here are from Section 4.1 of the associated report (*Analysis of Mechanisms for Early Waste Package/Drip Shield Failure*). Note that Section numbers refer to the associated report. Briefly, there were 16 specimen rings that were extensively examined for flaws. The breakdown of the number of confirmed flaws by specimen ring is as follows: specimen K two flaws, specimen R three flaws, specimen W one flaw, specimen X one flaw.

Total of seven flaws. Flaw size components, units entered in 1/16th of an inch.

Actual flaw distribution used in A.3 for comparison only.

$$X := \begin{pmatrix} 2 \\ 10 \\ 12 \\ 22 \\ 6 \\ 8 \\ 6 \end{pmatrix} \quad Y := \begin{pmatrix} 1 \\ 1 \\ 2 \\ 2 \\ 2 \\ 3 \\ 9 \end{pmatrix} \quad Z := \begin{pmatrix} 1 \\ 1 \\ 1 \\ 1 \\ 1 \\ 2 \\ 0 \end{pmatrix}$$

$$\text{FlawDistribution} := \begin{pmatrix} 12 \\ 2 \\ 1 \\ 1 \\ 0 \\ 0 \end{pmatrix} \quad \begin{array}{l} \text{Zero flaws in specimen} \\ \text{one flaw} \\ \text{two flaws} \\ \text{three flaws} \end{array}$$

$$\text{Normal_FlawDistribution} := \frac{\text{FlawDistribution}}{16}$$

Sum of flaw sizes in Y-direction in units of mm

$$s_t := \left(\frac{25.4}{16} \right) \cdot \sum Y \quad s_t = 31.750 \quad s_t = \text{Length of weld flaws}$$

Number of flaws detected

$$n_f := \text{length}(Y) \quad n_f = 7.000$$

Weld Cross Section (CS) Calculation (results in units of meter squared)

Calculation of the cross-area of weld in a specimen ring: Refer to Section 4.1 of *Analysis of Mechanisms for Early Waste Package/Drip Shield Failure* for direct input schematic representation with dimensions.

$$d_{OC} := 0.97(0.0254) \quad d_{AO} := 0.125(0.0254) \quad d_{BC} := 0.30(0.0254) \quad d_{AB} := d_{OC} - d_{AO} - d_{BC}$$

$$\theta_1 := 25 \cdot \left(\frac{\pi}{180} \right) \quad \theta_2 := 3 \cdot \left(\frac{\pi}{180} \right) \quad \theta_3 := 6 \cdot \left(\frac{\pi}{180} \right) \quad \theta_4 := 29 \cdot \left(\frac{\pi}{180} \right)$$

$$CS := \frac{\pi \cdot d_{AO}^2}{2} + 2 \cdot d_{AO} \cdot (d_{BC} + d_{AB}) + (\tan(\theta_3) + \tan(\theta_2)) \cdot \left(\frac{d_{AB}^2}{2} + d_{BC} \cdot d_{AB} \right) + \frac{d_{BC}^2}{2} \cdot (\tan(\theta_4) + \tan(\theta_1))$$

$$CS = 2.135 \times 10^{-4}$$

Total weld volume in the sixteen weld specimens in units of meters cubed (diameter is 60.765 in)

$$V_f := 16 \cdot \pi \cdot (60.765) \cdot (0.0254) \cdot CS \quad V_f = 1.656 \times 10^{-2} \text{ m}^3$$

Individual Specimen Weld Volume

$$V_{sw} := \pi \cdot (60.765) \cdot (0.0254) \cdot CS \quad V_{sw} = 1.035 \times 10^{-3} \text{ m}^3$$

Specimen and current Waste Package weld thickness, rounded-off to nearest mm.

$$TH := 25 \text{ mm}$$

Waste package (TAD) closure weld diameter and resulting weld volume estimate (SNL 2007 [DIRS 179394], Table 4.3):

$$D_{wp} := 72.08 \text{ inches} \quad V_{wp} := \pi \cdot (D_{wp}) \cdot (0.0254) \cdot CS \quad V_{wp} = 1.228 \times 10^{-3} \text{ m}^3$$

Flaw angles (in units of degrees)

$$\theta := \left(\frac{180}{\pi} \right) \cdot \text{atan} \left(\frac{Z}{X} \right) \quad \theta = \begin{pmatrix} 26.565 \\ 5.711 \\ 4.764 \\ 2.603 \\ 9.462 \\ 14.036 \\ 0.000 \end{pmatrix}$$

A.2 Development of Distribution for Flaws in the Y direction

Flaw Size Parameter Distribution

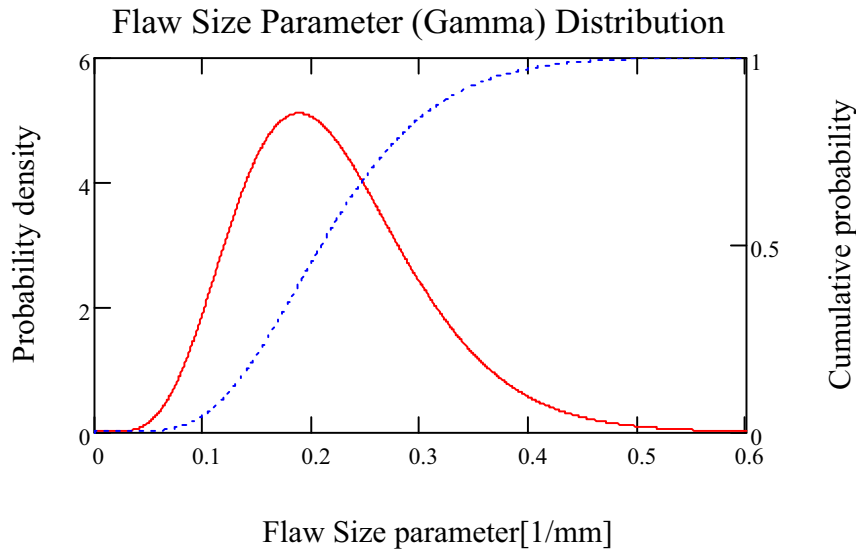
An exponential distribution is used to characterize the size in the Y direction of the flaws in the specimen rings. First, using the Bayesian approach with a noninformative prior, the parameter f_s of the exponential distribution is determined by a posterior PDF given by Equation 6, Section 6.3.1.2 as follows:

$$f_s(x) := \frac{s_t (s_t \cdot x)^{n_f - 1}}{\Gamma(n_f)} \cdot \exp(-s_t \cdot x) \quad \text{Equation 6, Section 6.3.1.2}$$

Flaw size parameter pdf, x is Flaw Size parameter (mm⁻¹), described as λ_s in the report.

$$F_s(x) := 1 - \frac{\Gamma(n_f, s_t \cdot x)}{\Gamma(n_f)}$$

Flaw size parameter CDF



Mean	Standard deviation	Mode
$\frac{n_f}{s_t} = 0.220$	$\frac{\sqrt{n_f}}{s_t} = 0.083$	$\frac{n_f - 1}{s_t} = 0.189$

$$Q := \begin{pmatrix} 0.01 \\ 0.05 \\ 0.25 \\ 0.50 \\ 0.75 \\ 0.95 \\ 0.99 \end{pmatrix} \quad \text{augment} \left(Q, \frac{\text{qgamma}(Q, n_f)}{s_t} \right) = \begin{pmatrix} 0.010 & 0.073 \\ 0.050 & 0.103 \\ 0.250 & 0.160 \\ 0.500 & 0.210 \\ 0.750 & 0.270 \\ 0.950 & 0.373 \\ 0.990 & 0.459 \end{pmatrix} \quad \text{Quantile Values}$$

Marginal Flaw Size Distribution for a Weld of Thickness (TH:=25 mm)

$$p_{sg}(x, \lambda) := \frac{\lambda \cdot \exp(-\lambda \cdot x)}{1 - \exp(-\lambda \cdot TH)}$$

joint PDF of flaw size as an upper-bounded exponential; used later in A.6. Equation 8, Section 6.3.1.2

Alternate fixed thickness exponential distribution function (g2), plotted as p2(25-x):

$$p1(x) := \int_0^\infty p_{sg}(x, \lambda) \cdot f_s(\lambda) d\lambda$$

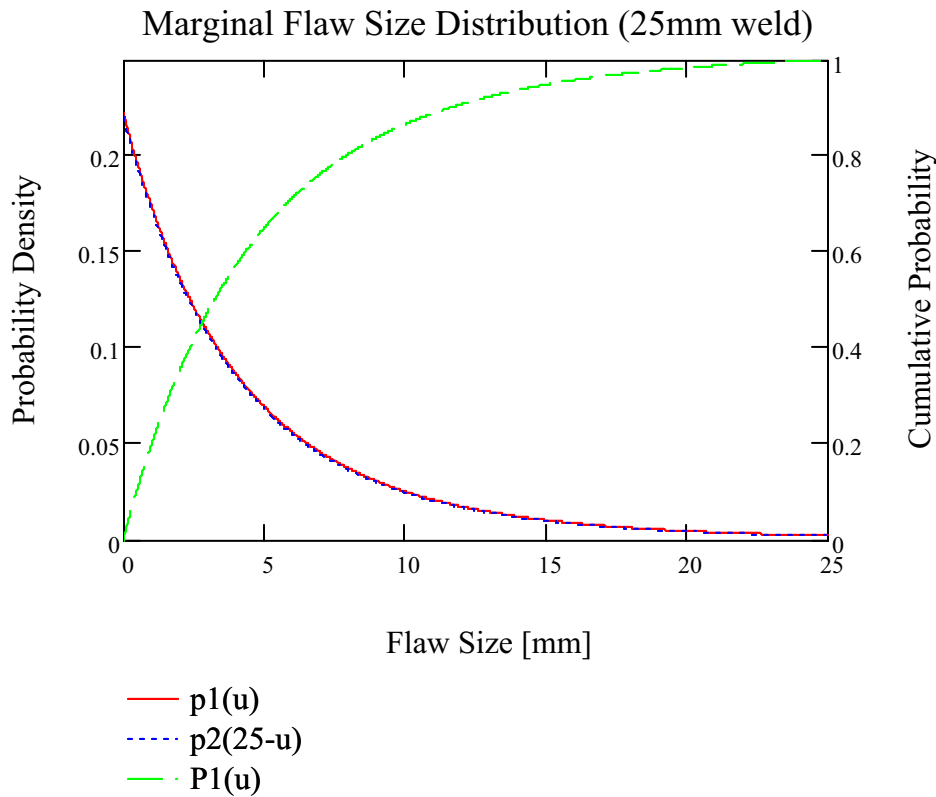
Marginal PDF for flaw size Equation 9, Section 6.3.1.2

$$g2(x, \lambda) := \lambda \cdot \exp[-\lambda \cdot (TH - x)]$$

$$P1(x) := \int_0^x p1(s) ds$$

Marginal CDF for flaw size Equation 10, Section 6.3.1.2

$$p2(x) := \int_0^\infty g2(x, \lambda) \cdot f_s(\lambda) d\lambda$$



$$\int_0^{TH} s \cdot p1(s) ds = 4.823 \text{ mm} \quad \text{Mean value of } p1 \text{ (flaw size PDF)}$$

jj := 1..7

$$xQ_{jj} := \text{root}[(P1(x) - Q_{jj}), x, 0, TH]$$

$$\text{augment}(Q, xQ) = \begin{pmatrix} 0.010 & 0.045 \\ 0.050 & 0.231 \\ 0.250 & 1.315 \\ 0.500 & 3.246 \\ 0.750 & 6.738 \\ 0.950 & 15.169 \\ 0.990 & 21.548 \end{pmatrix}$$

Quantile Values for P1(x), Determine the values of x where P1(x) = Q_{jj} for each jj

A.3 Development of Distribution for Flaw Density Weld

Flaw Density Parameter Distribution (flaws per volume of weld)

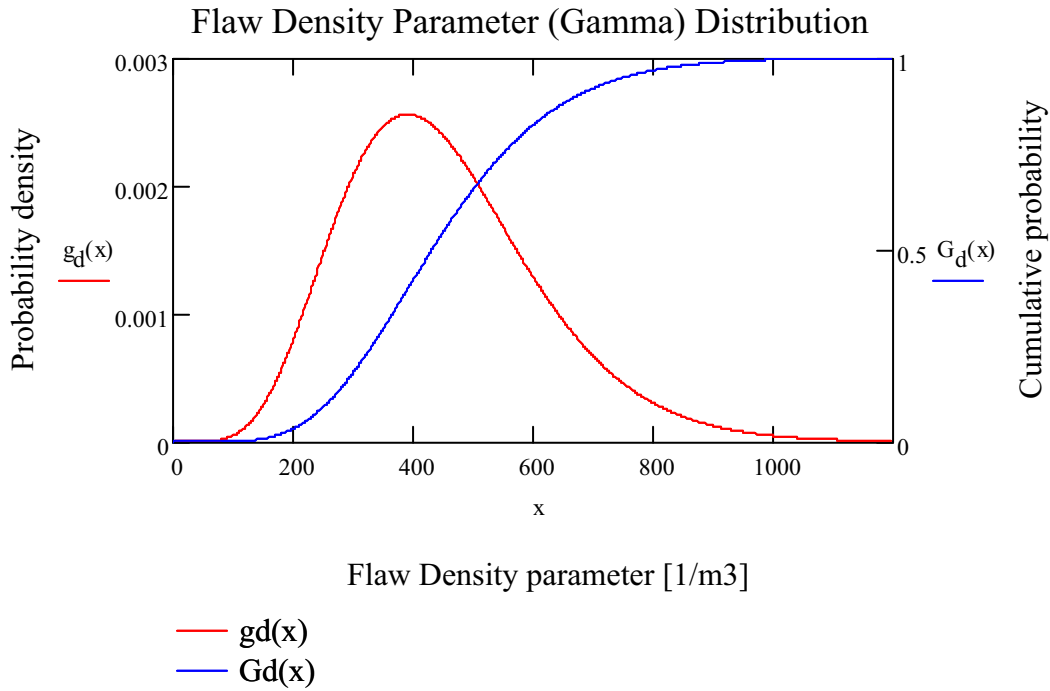
The number of flaws observed in a given specimen rings is characterized by a Poisson distribution. The parameter of the Poisson distribution, i.e., the flaw density parameter, is called λ_d (termed x in this first calculation here). Using the Bayesian approach with a noninformative prior, the posterior PDF for g_d is given by Equation 11 in Section 6.3.1.3.

Flaw density parameter pdf,
Equation 11, Section 6.3.1.3

$$g_d(x) := \frac{V_f (V_f x)^{n_f - \frac{1}{2}}}{\Gamma\left(n_f + \frac{1}{2}\right)} \cdot \exp(-V_f x)$$

Flaw density parameter CDF

$$G_d(x) := 1 - \frac{\Gamma\left(n_f + \frac{1}{2}, V_f x\right)}{\Gamma\left(n_f + \frac{1}{2}\right)}$$



Mean no.
of flaws per
cubic meter

$$\frac{n_f + \frac{1}{2}}{V_f} = 452.880$$

Standard Deviation

$$\frac{\sqrt{n_f + \frac{1}{2}}}{V_f} = 165.368$$

Mode

$$\frac{n_f - \frac{1}{2}}{V_f} = 392.496 \quad \text{Flaws per cubic meter of weld}$$

$$\text{augment} \left(Q, \frac{\text{qgamma} \left(Q, n_f + \frac{1}{2} \right)}{V_f} \right) = \begin{pmatrix} 0.010 & 157.884 \\ 0.050 & 219.222 \\ 0.250 & 333.215 \\ 0.500 & 432.919 \\ 0.750 & 550.856 \\ 0.950 & 754.672 \\ 0.990 & 923.208 \end{pmatrix}$$

Quantile Values

Marginal Number of Flaws (per Specimen Weld Volume)

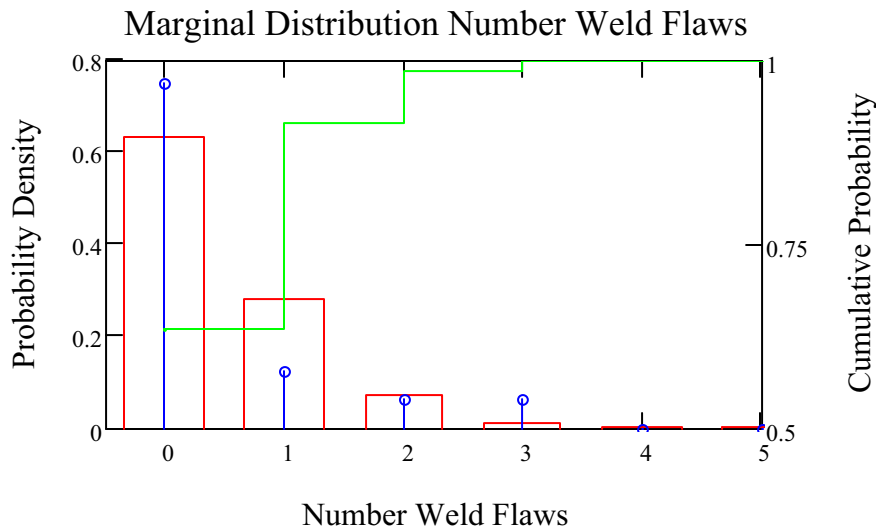
$$\frac{n_f + \frac{1}{2}}{V_f} \cdot V_{sw} = 0.46875 \quad \text{Mean Number of flaws per Sample Weld volume } V_{sw}$$

$$pf(n) := \int_0^{3000} (\lambda \cdot V_{sw})^n \cdot \frac{\exp(-\lambda \cdot V_{sw})}{n!} \cdot g_d(\lambda) d\lambda$$

Integral of Equation 12, Section 6.3.1.3 weighted by the probability density of λ given by Equation 11

$$Pf(n) := \sum_{i=0}^n pf(i)$$

kk := 0..5



Expected Probability of the number of specimen ring flaws as: zero, one, two or more.

$$pf(0) = 0.635$$

$$pf(1) = 0.280$$

$$1 - Pf(1) = 0.085$$

An example using these formula for the Waste Package expected weld flaw probability:

$$pfWP(n) := \int_0^{3000} (\lambda \cdot V_{WP})^n \cdot \frac{\exp(-\lambda \cdot V_{WP})}{n!} \cdot g_d(\lambda) d\lambda$$

pfWP(0) = 0.585	pfWP(2) = 0.089	pfWP(4) = 3.517 × 10 ⁻³	$\left(\sum_{x=2}^{30} pfWP(x) \right) = 0.112$
pfWP(1) = 0.303	pfWP(3) = 0.019	pfWP(5) = 5.583 × 10 ⁻⁴	

A.4 Flaw Orientation Distribution

Determination of the fraction of flaws that deviate by more than 45 degrees from the direction of the weld. Assumes normal distribution about zero degrees.

The PDF of θ is based on Equation 13 of Section 6.3.1.5 as:

$$p_{\theta}(\theta, \sigma) := 2 \cdot \text{dnorm}(\theta, 0, \sigma) \quad \text{where } \sigma \text{ is the standard deviation of the normal distribution associated with the orientation of the flaw.}$$

The CDF is therefore:

$$P_{\theta}(\theta, \sigma) := 2 \cdot \text{pnorm}(\theta, 0, \sigma) - 1$$

The likelihood function related to the observed angles is:

$$L_{\theta}(\sigma) := \prod_{i=1}^7 p_{\theta}(\theta_i, \sigma)$$

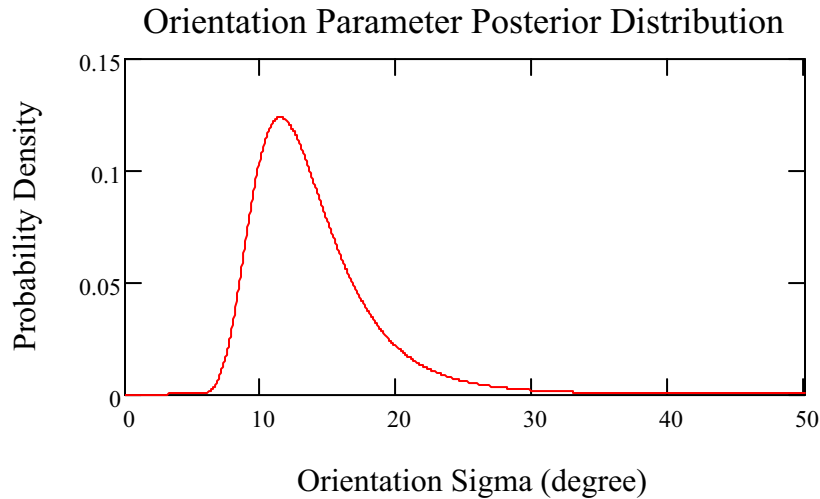
Application of Bayes' theorem (Equation 15 of Section 6.3.1.5) yields the posterior PDF for σ :

$$p_{\sigma}(\sigma) := \frac{\frac{L_{\theta}(\sigma)}{\sigma}}{\int_0^{\infty} \frac{L_{\theta}(u)}{u} du}$$

The mean value for σ is:

$$\sigma_m := \int_0^{\infty} x p_{\sigma}(x) dx$$

$$\sigma_m = 13.905 \quad \text{degrees}$$



The 5th percentile is: $\sigma_{0.05} := \text{root} \left(\int_0^a p_{\sigma}(x) dx - 0.05, a, 2, 20 \right)$ $\sigma_{0.05} = 8.652$ degrees

The 95th percentile is: $\sigma_{0.95} := \text{root} \left(\int_0^a p_{\sigma}(x) dx - 0.95, a, 10, 60 \right)$ $\sigma_{0.95} = 21.594$ degrees

Expected fraction of flaws with an angle θ greater than 45 degrees

The foregoing results yielded by the specimen rings are used to determine the fraction of flaws in waste packages that are expected to deviate by more than 45 degrees from the direction of the weld. Accounting for all the possible values that can be taken by σ , this fraction is calculated as:

$$F_{\theta} := \int_0^{\infty} (1 - P_{\theta}(45, u)) \cdot p_{\sigma}(u) du$$

$F_{\theta} = 8.050 \times 10^{-3}$ This corresponds to around 0.8% of the flaws.

A.5 Characterization of Capability of UT Inspection to Detect Weld Flaws

- $\epsilon_1 := 0.005$ detection limit - probability of failing to detect a flaw of any size
- $s_0 := \frac{25.4}{16}$ is a characteristic flaw size, in mm, for which around 50 percent of flaws are detected.
- $v := 1.5$ shape parameter

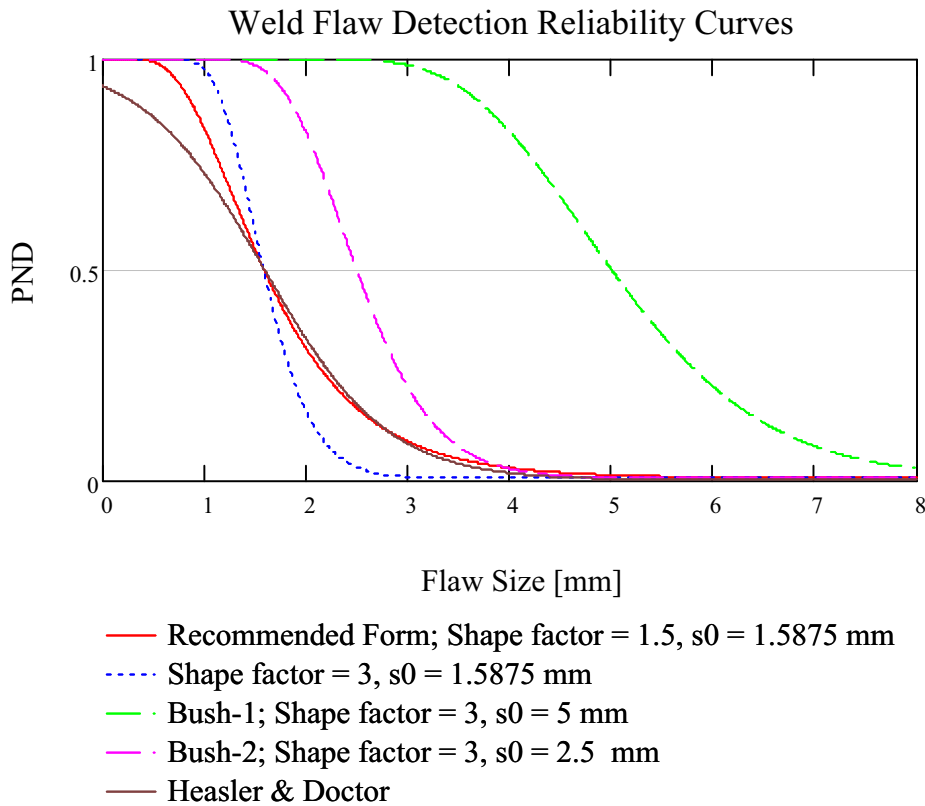
$$P_{nd}(x, s_0, v) := \epsilon_1 + \frac{1 - \epsilon_1}{2} \cdot \operatorname{erfc}\left(v \cdot \ln\left(\frac{x}{s_0}\right)\right)$$

Equational form of Bush 1983 [DIRS 107696],
Equation 17, Section 6.3.1.6

Alternate detection function from Heasler and Doctor 1996 [DIRS 107758]:
Equation 18, Section 6.3.1.6

$$P_{nd2}(s, \beta_1, \beta_2) := 1 - \frac{1}{1 + \exp(-\beta_1 - \beta_2 \cdot s)}$$

s is size (in mm)
 $\beta_1 := -2.67$ $\beta_2 := 1.6709$ per mm



Fraction of flaws that remain in the weld after UT inspection and repair is determined by the convolution of the size distribution (A.2, g_1) with the UT inspection PND (A.5, P_{nd}).

$$F_{nd}(x) := \int_0^{TH} p_{sg}(s, x) \cdot P_{nd}(s, s_0, v) ds \quad \text{Equation 19, Section 6.3.1.7}$$

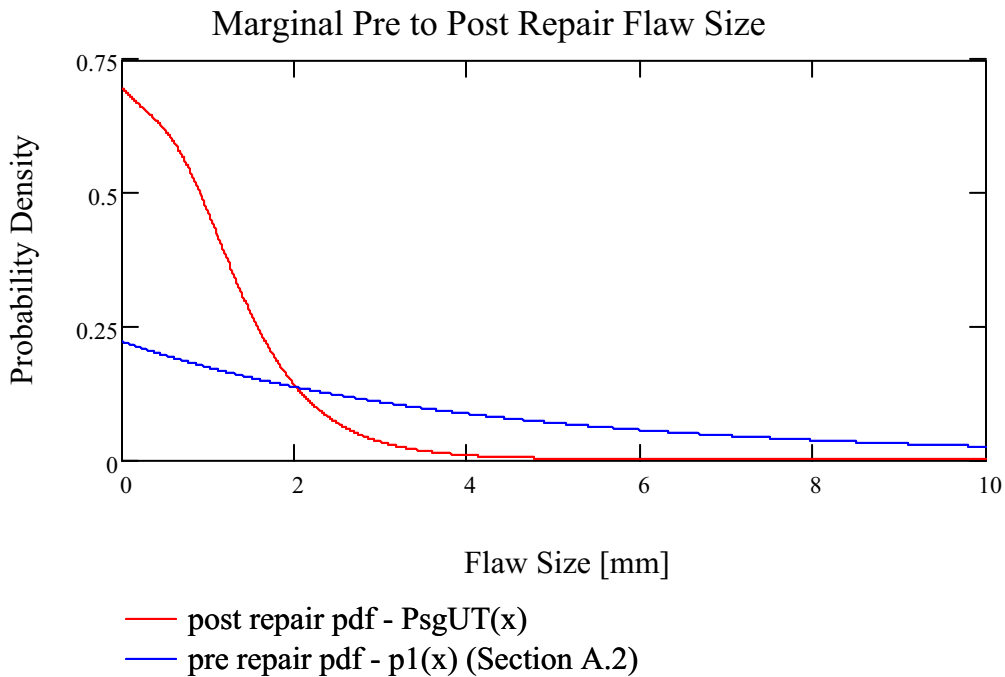
The following PDF/CDF determinations are as a informational only and are not TSPA-relevant equations. These calculate the distribution of the remaining flaw sizes.

$$p_{sgUT}(s) := \int_0^{\infty} \frac{p_{sg}(s, u) \cdot P_{nd}(s, s_0, v)}{F_{nd}(u)} \cdot f_s(u) du \quad \text{Equation 20, Section 6.3.1.7}$$

$$\int_0^{TH} s \cdot p_{sgUT}(s) ds = 1.030 \quad \text{mean value (mm), Equation 22, Section 6.3.1.7}$$

$$P_{sgUT}(x) := \int_0^x p_{sgUT}(s) ds \quad \text{Equation 21, Section 6.3.1.7}$$

CDF P_{sgUT} is not plotted as it would take an inordinate amount of time and is only for demonstration. See the quantile calculations below instead.



$$x1Q_{jj} := \text{root}\left[\left(P_{\text{sgUT}}(x) - Q_{jj}\right), x, 0, TH\right]$$

$$\text{augment}(Q, x1Q) = \begin{pmatrix} 0.010 & 0.014 \\ 0.050 & 0.072 \\ 0.250 & 0.373 \\ 0.500 & 0.790 \\ 0.750 & 1.362 \\ 0.950 & 2.602 \\ 0.990 & 4.513 \end{pmatrix}$$

Percentage of remaining weld flaws greater than 1/16th of an inch.

$$1.0 - P_{\text{sgUT}}\left(\frac{25.4}{16}\right) = 0.186$$

A.7 Undetected Flaw Density

The distribution on the number of flaws remaining in the weld after inspection and repair. Using Monte Carlo simple random sampling with B realizations.

$$B := 50000$$

$$ii := 1..B$$

$$pp_{ii} := \frac{ii}{B + 1}$$

$$\lambda_s := \frac{\text{rgamma}(B, n_f)}{s_t}$$

$$\lambda_d := \frac{\text{rgamma}\left(B, n_f + \frac{1}{2}\right)}{V_f}$$

Function *rgamma* returns the random vector of numbers with a gamma distribution.

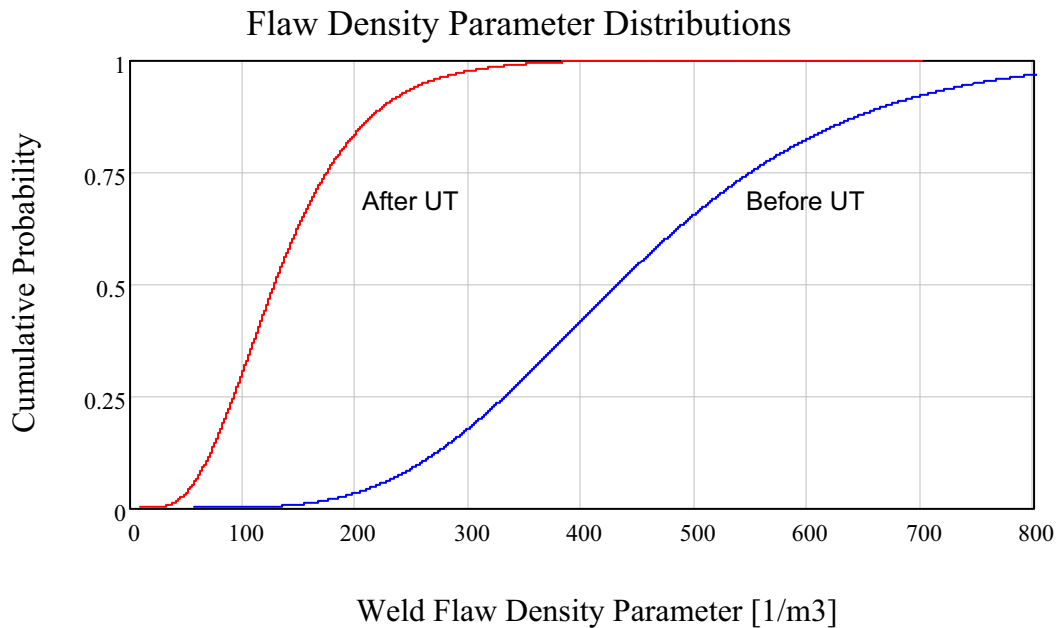
$$\lambda_{\text{dPR}_{ii}} := \lambda_{d_{ii}} \cdot F_{\text{nd}}(\lambda_{s_{ii}})$$

Equation 23, Section 6.3.1.8

$$\lambda_{\text{dPR}} := \text{sort}(\lambda_{\text{dPR}})$$

$$\text{mean}(\lambda_{\text{dPR}}) = 140.422$$

$$\text{augment}(Q, \text{linterp}(pp, \lambda_{\text{dPR}}, Q)) = \begin{pmatrix} 0.0100 & 38.5117 \\ 0.0500 & 55.9053 \\ 0.2500 & 92.9264 \\ 0.5000 & 128.6926 \\ 0.7500 & 175.4984 \\ 0.9500 & 263.6242 \\ 0.9900 & 345.1955 \end{pmatrix}$$



Expected probability of the number of post-inspection flaws in a specimen weld volume (25 mm thickness), zero, one, two or more.

$$\text{mean}(\text{dpois}(0, \lambda_{\text{dPR}} \cdot V_{\text{sw}})) = 0.867$$

Equation 24, Section 6.3.1.8

$$\text{mean}(\text{dpois}(1, \lambda_{\text{dPR}} \cdot V_{\text{sw}})) = 0.122$$

$$\text{mean}(1 - \text{ppois}(1, \lambda_{\text{dPR}} \cdot V_{\text{sw}})) = 0.011$$

Expected probability of the number of post-inspection flaws in a TAD waste package weld volume (thickness as 25 mm), zero, one, two or more.

$$\text{mean}(\text{dpois}(0, \lambda_{\text{dPR}} \cdot V_{\text{wp}})) = 0.844$$

$$\text{mean}(\text{dpois}(1, \lambda_{\text{dPR}} \cdot V_{\text{wp}})) = 0.140$$

$$\text{mean}(1 - \text{ppois}(1, \lambda_{\text{dPR}} \cdot V_{\text{wp}})) = 0.015$$

INTENTIONALLY LEFT BLANK

APPENDIX B
EVENT TREES AND FAULT TREES

APPENDIX B – EVENT TREES AND FAULT TREES

The full set of event trees and fault trees from the SAPHIRE model used in the analysis of early failure mechanisms in waste package outer corrosion barriers and drip shields are shown graphically in this appendix. These event trees and fault trees have been abstracted from the compressed dataset labeled “SAPHIRE OUTPUT” that is included in both of the output DTNs: MO0701PASHIELD.000 and MO0705EARLYEND.000.

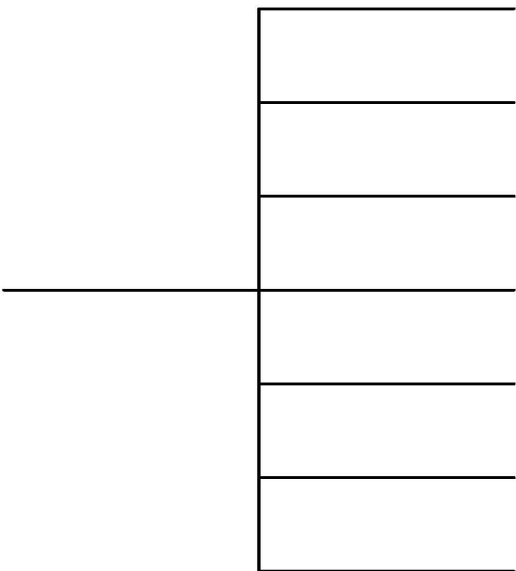
Placeholder initiating event	Dummy Top Event			
INIT	PASS		#	END-STATE-NAMES
			1	OK
			2	T HEAT_TREATMENT_SHELL
			3	T HEAT_TREATMENT_LID
			4	T LOW-PLASTICITY-BURNISH
			5	T MISHANDLING-WP
			6	T BASE-METAL-WP
			7	T WELD-FILLER-WP

Figure B-1. Basic Waste Package Defect Event Tree

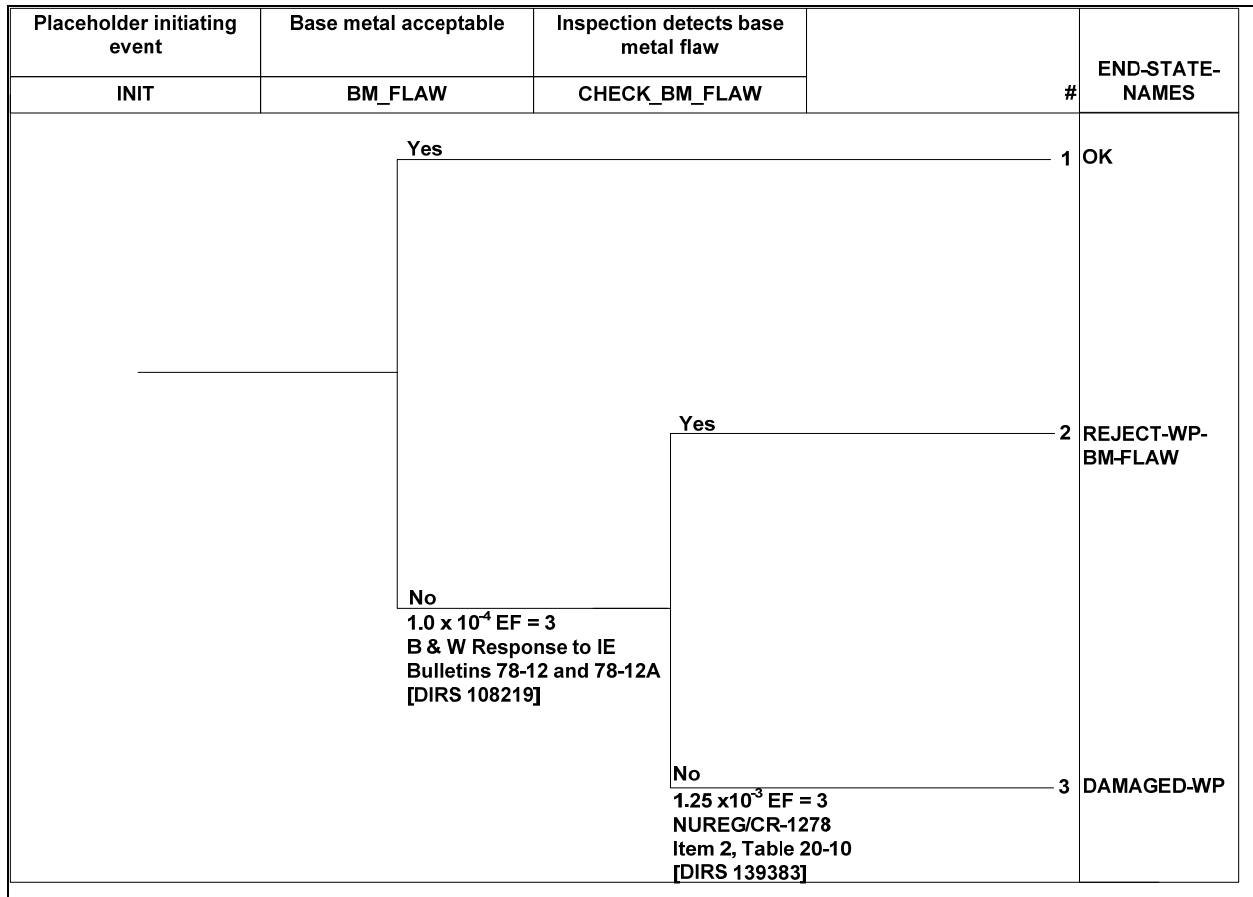


Figure B-2. Event Tree for Evaluating Improper Base Metal Selection for Waste Package Outer Corrosion Barrier

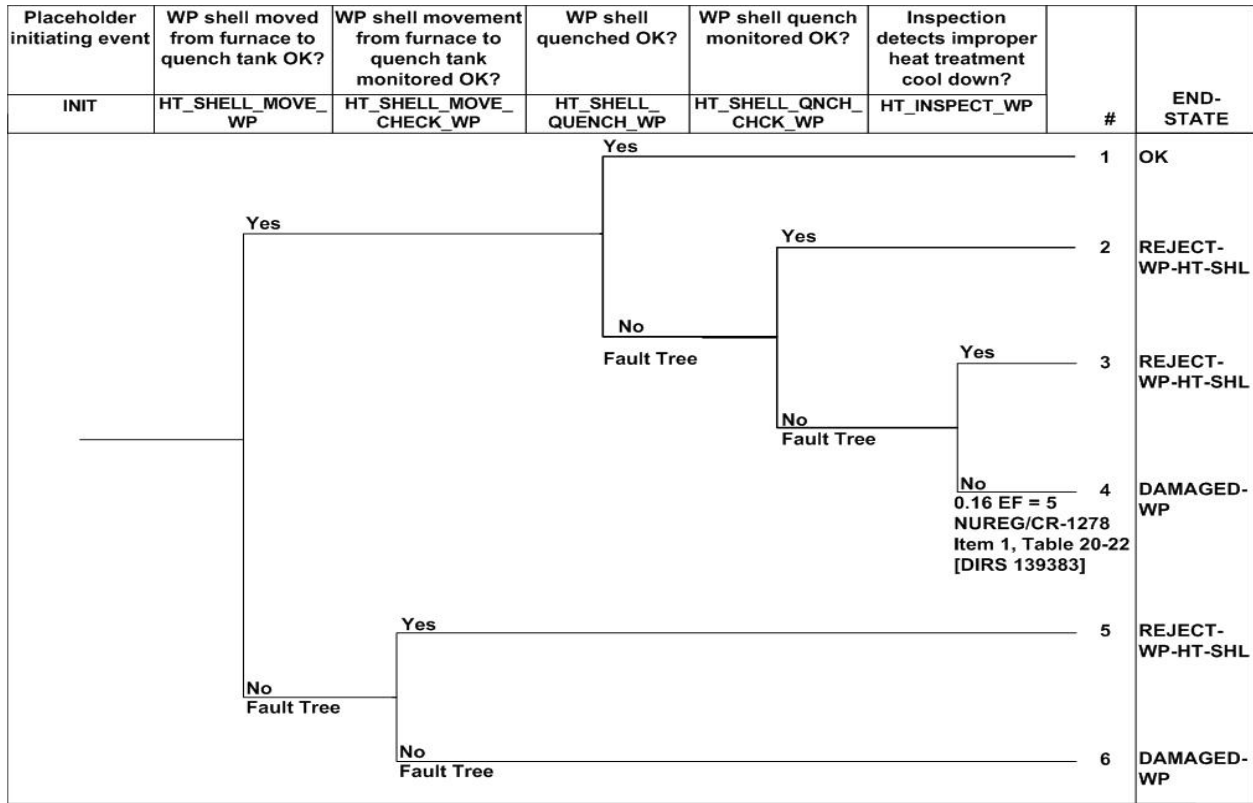


Figure B-3. Event Tree for Evaluating Improper Heat Treatment of the Waste Package Outer Corrosion Barrier

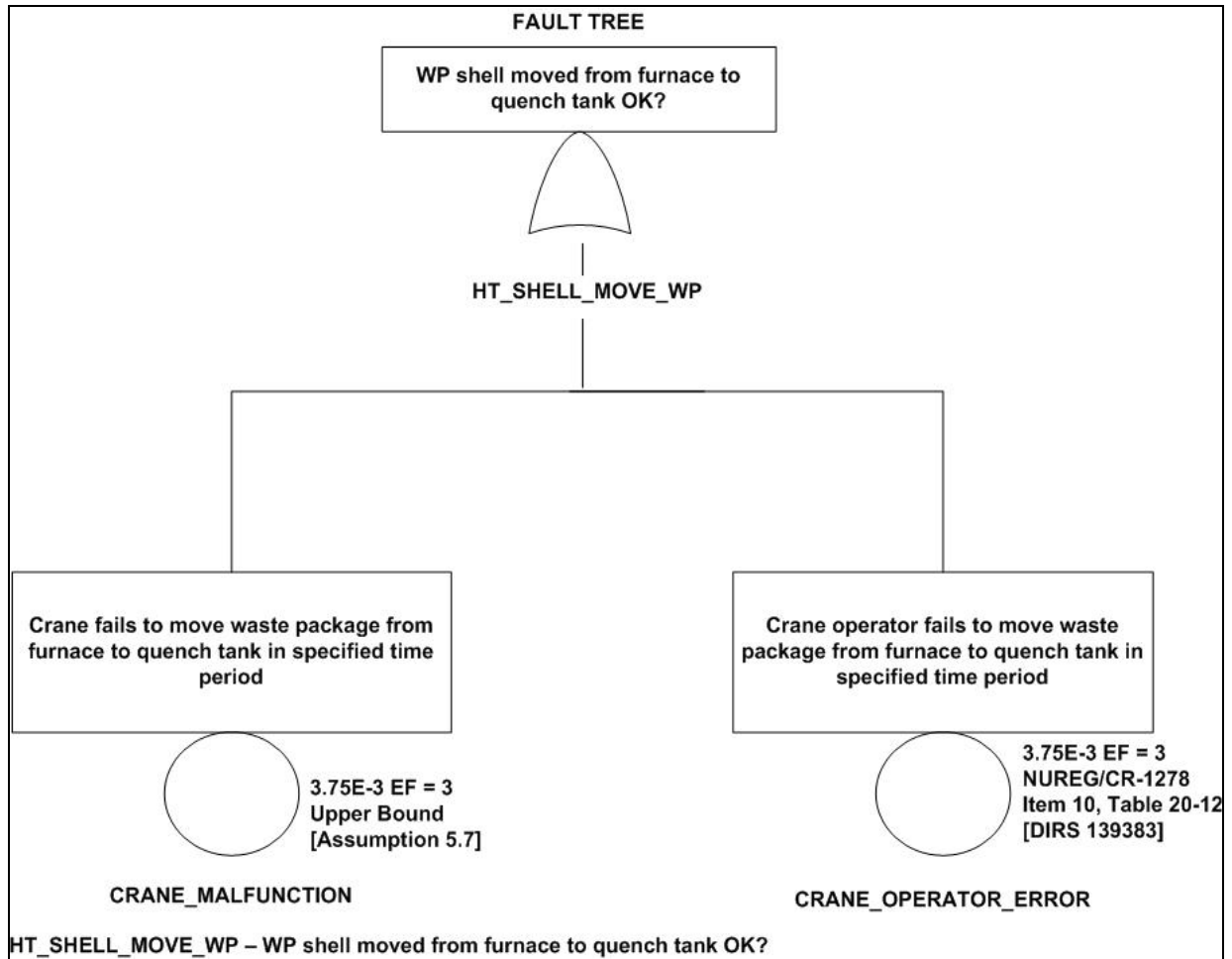


Figure B-4. Fault Tree for Waste Package Outer Corrosion Barrier Heat Treatment Move

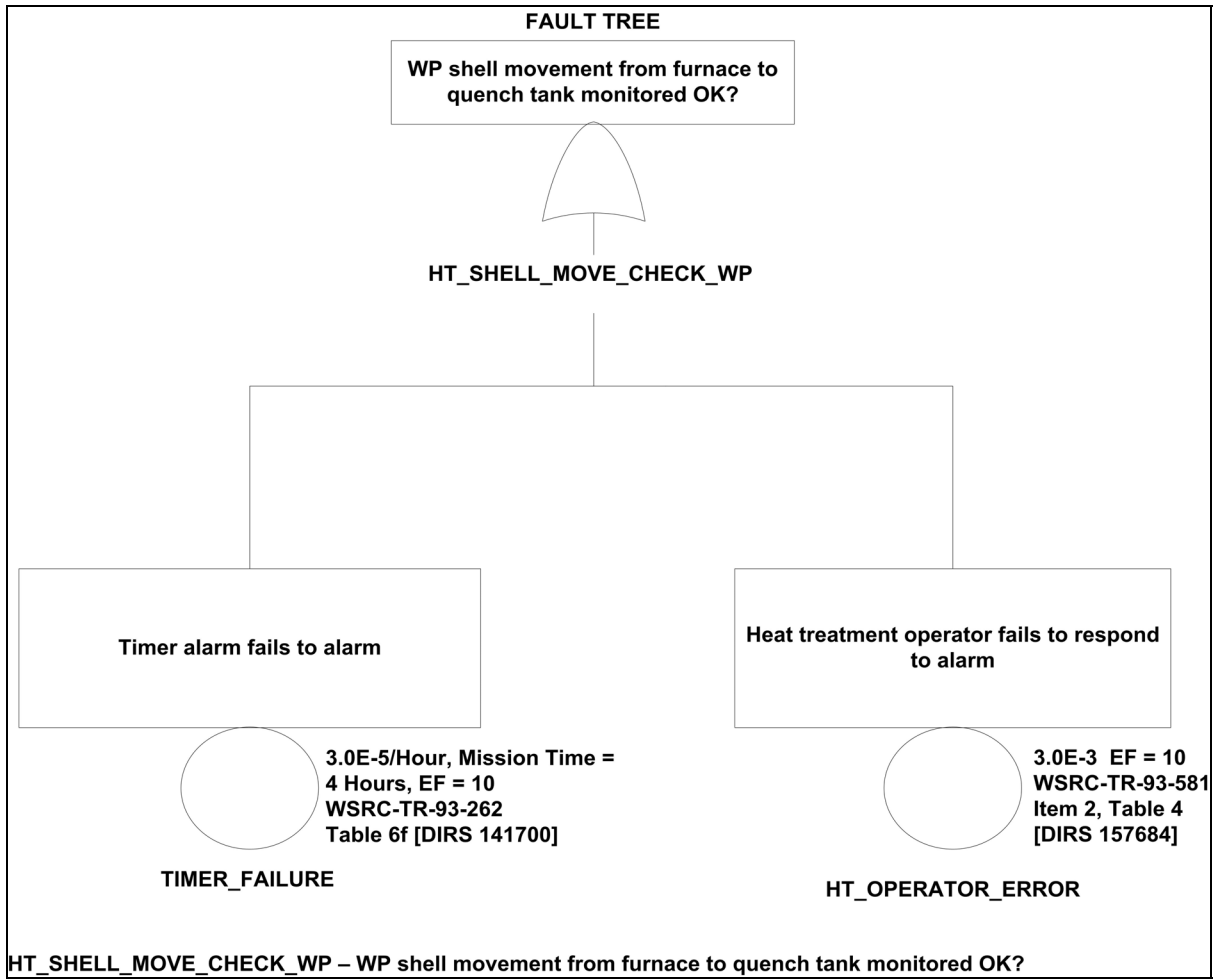


Figure B-5. Fault Tree for Waste Package Outer Corrosion Barrier Heat Treatment Move Check

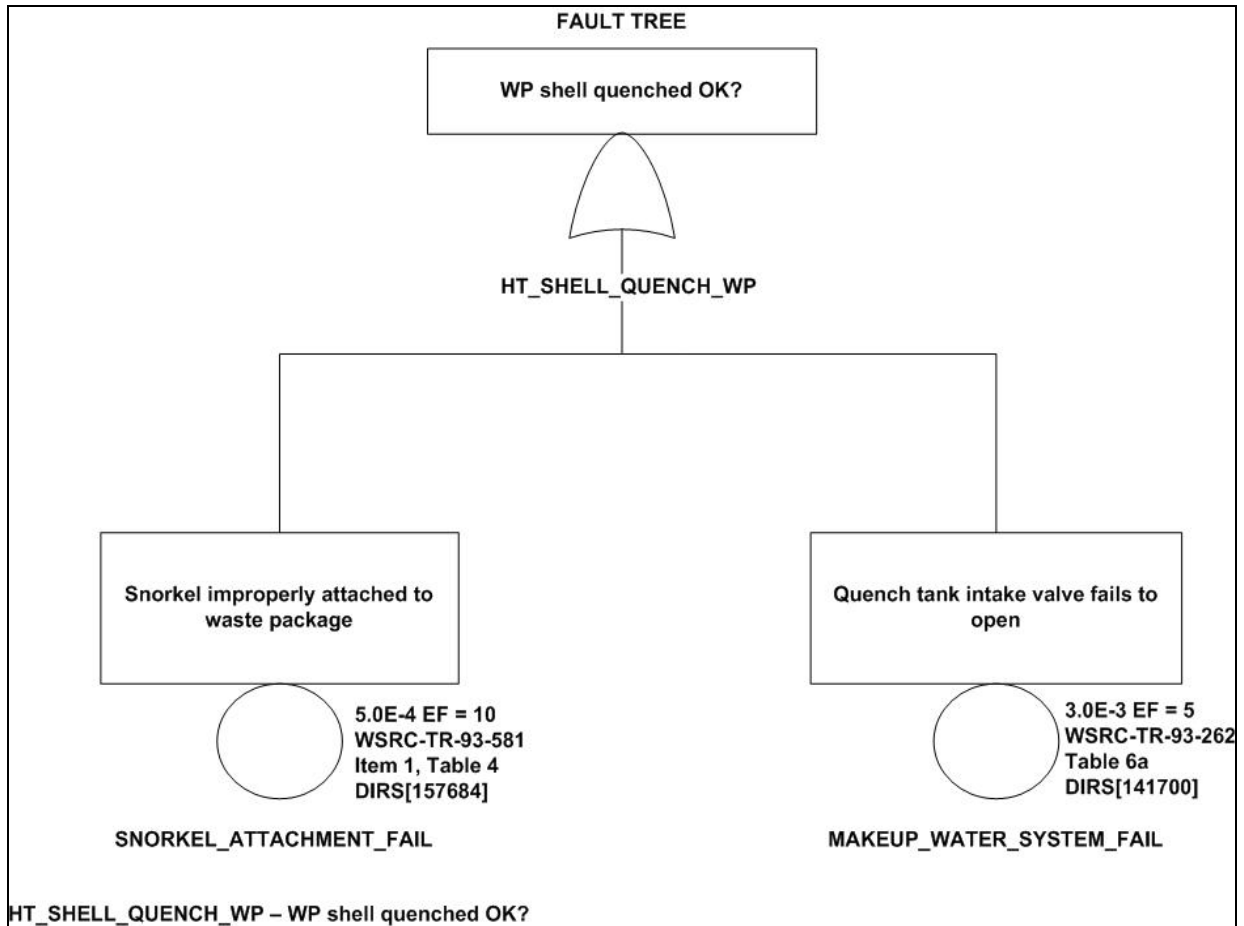


Figure B-6. Fault Tree for Waste Package Outer Corrosion Barrier Heat Treatment Quench

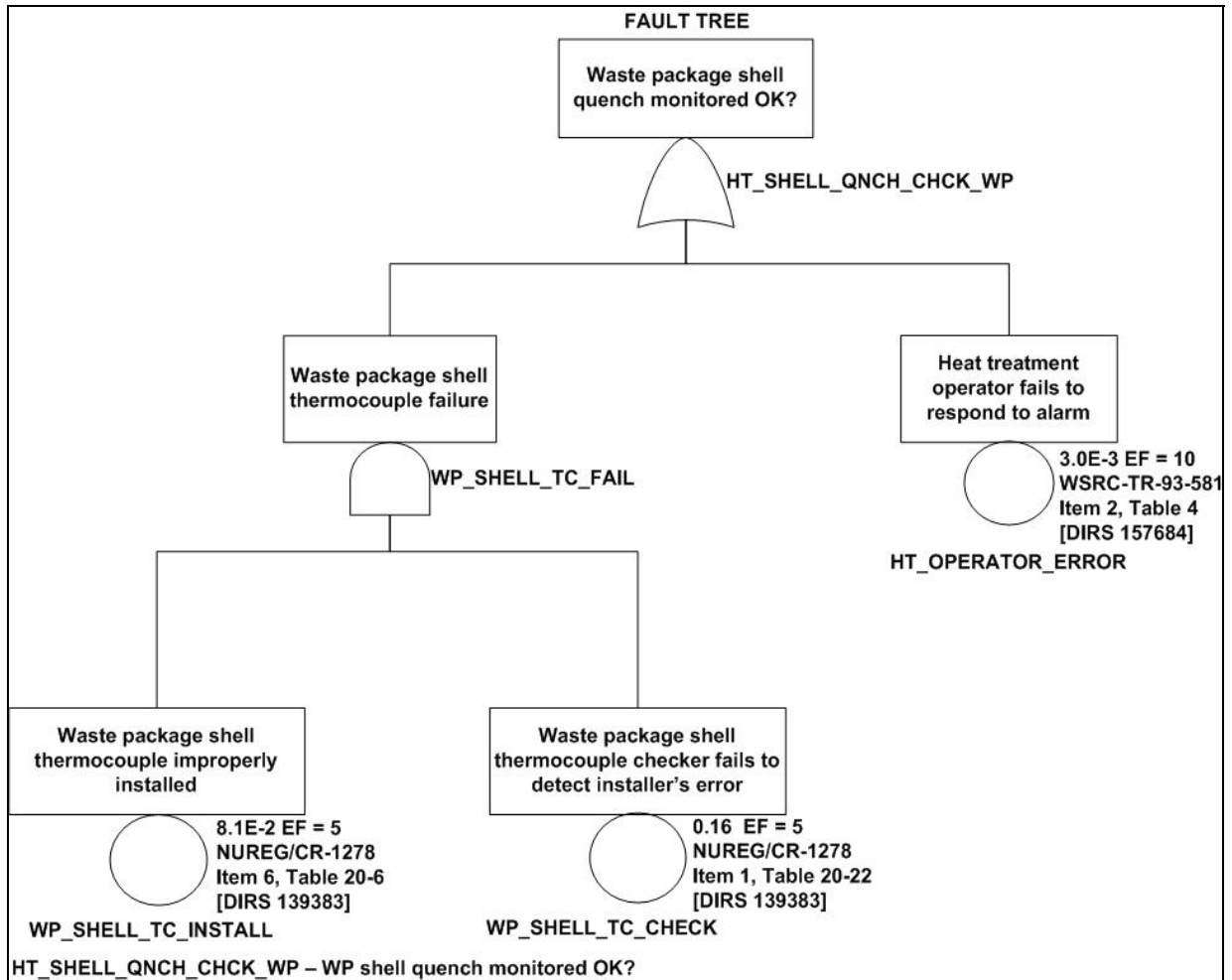


Figure B-7. Fault Tree for Waste Package Outer Corrosion Barrier Heat Treatment Quench Check

Placeholder initiating event	WP lid moved from furnace to quench tank OK?	WP lid movement from furnace to quench tank monitored OK?	WP lid quenched OK?	WP lid quench monitored OK?	Inspection detects improper heat treatment cool down?	#	END-STATE
INIT	HT_LID_MOVE_WP	HT_LID_MOVE_CHECK_WP	HT_LID_QUENCH_WP	HT_SHELL_QNCH_CHK_WP	HT_INSPECT_WP		
						1	OK
						2	REJECT-WP-HT-LID
						3	REJECT-WP-HT-LID
						4	DAMAGED-WP 0.16 EF = 5 NUREG/CR-1278 Item 1, Table 20-22 [DIRS 139383]
						5	REJECT-WP-HT-LID
						6	DAMAGED-WP

Figure B-8. Event Tree for Evaluating Improper Heat Treatment of the Waste Package Outer Corrosion Barrier Lid

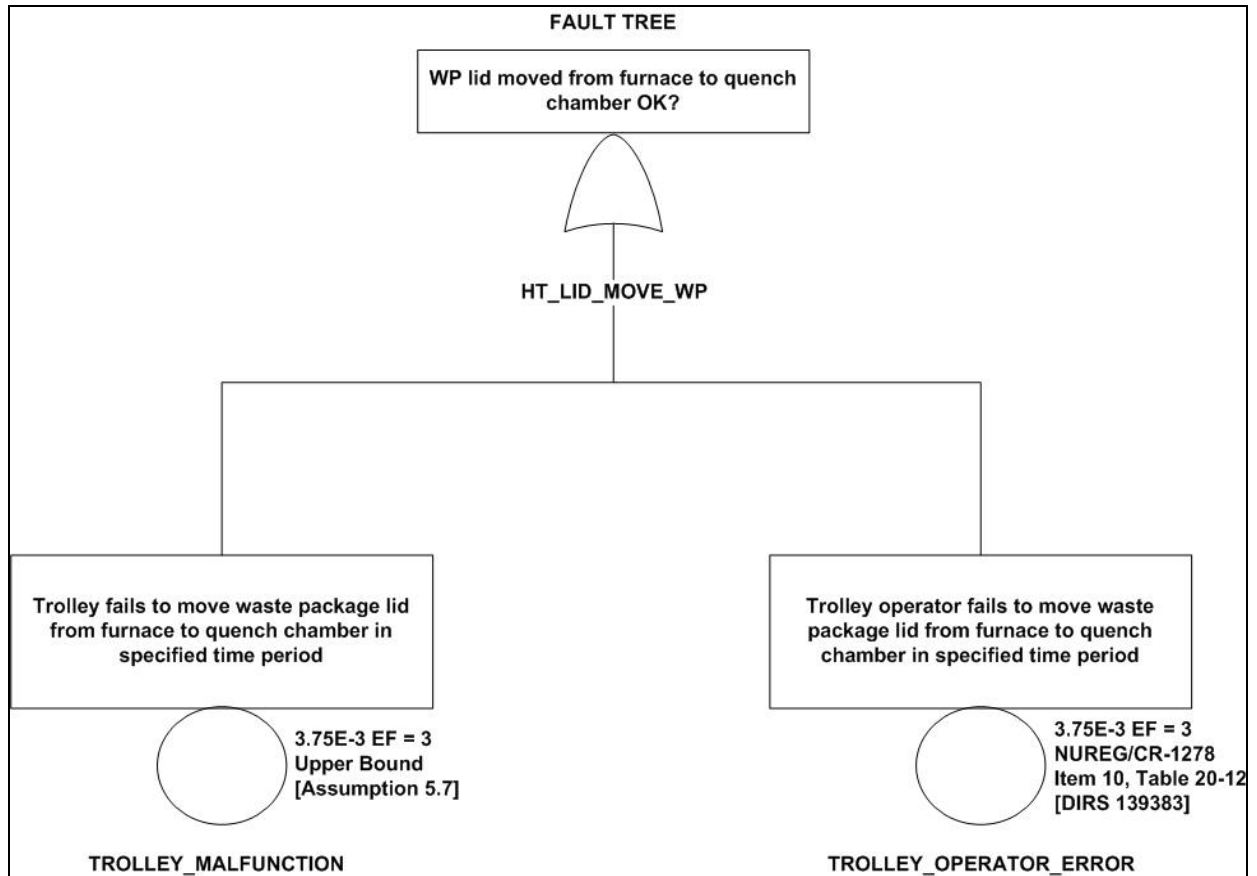


Figure B-9. Fault Tree for Waste Package Outer Corrosion Barrier Lid Heat Treatment Move

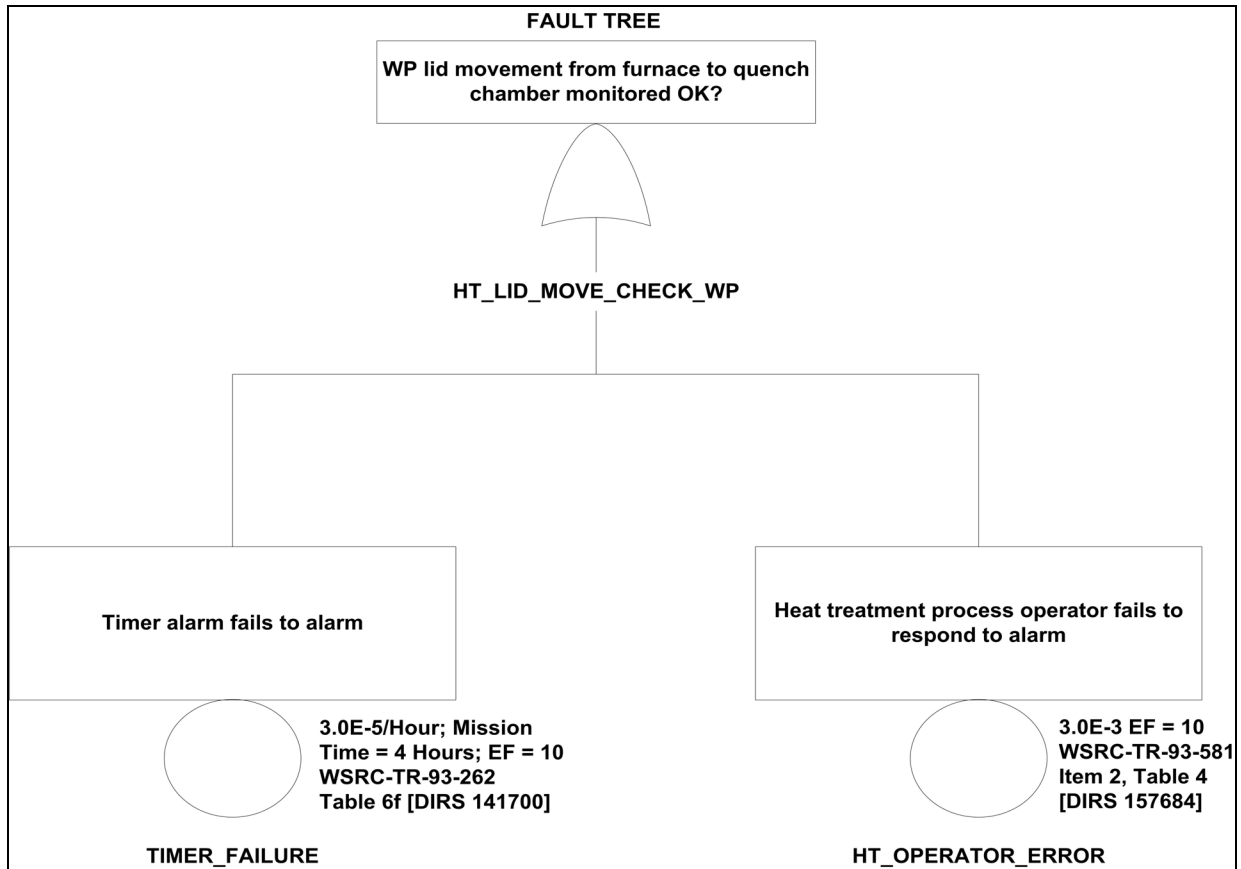


Figure B-10. Fault Tree for Waste Package Outer Corrosion Barrier Lid Heat Treatment Move Check

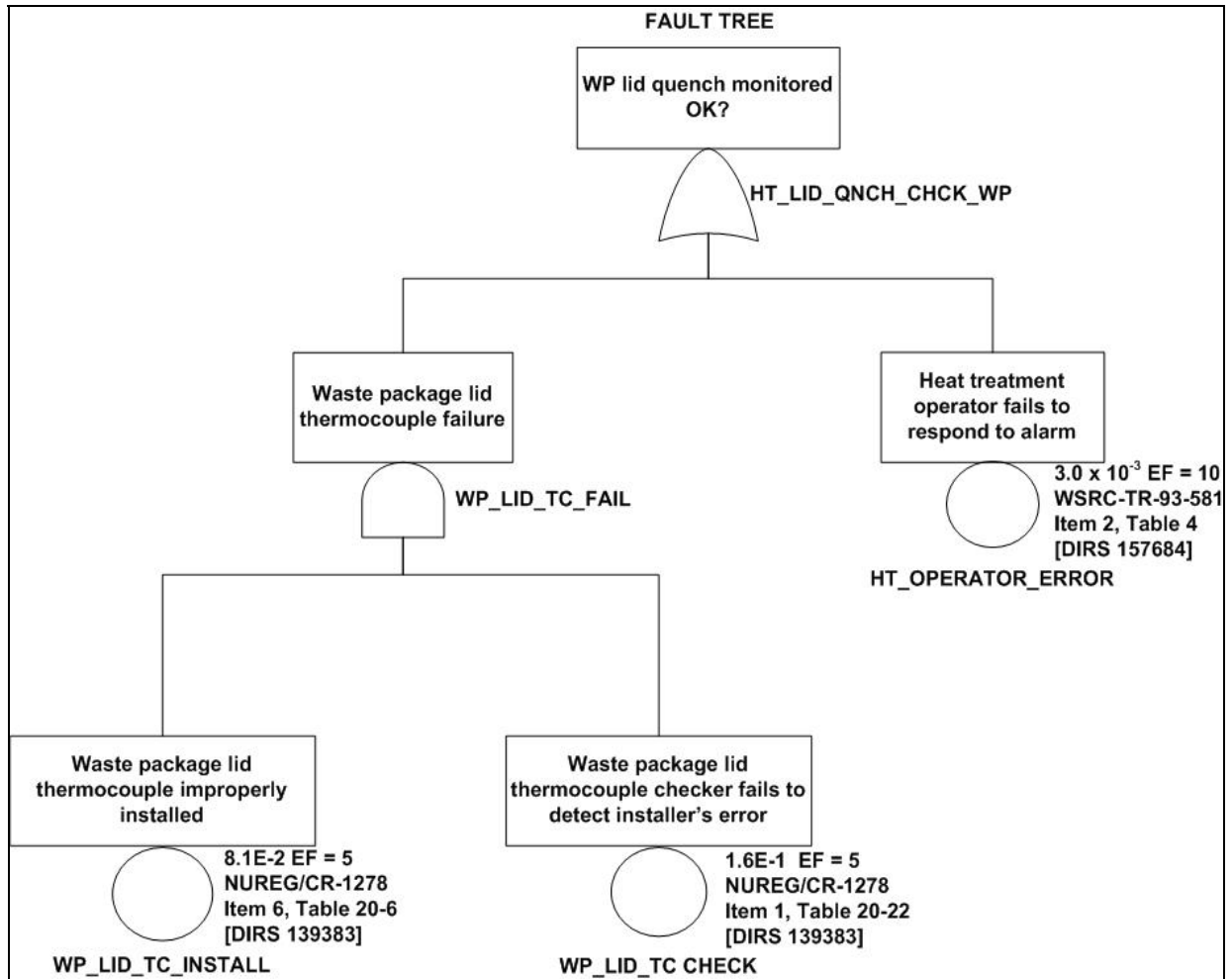


Figure B-11. Fault Tree for Waste Package Outer Corrosion Barrier Lid Heat Treatment Quench Check

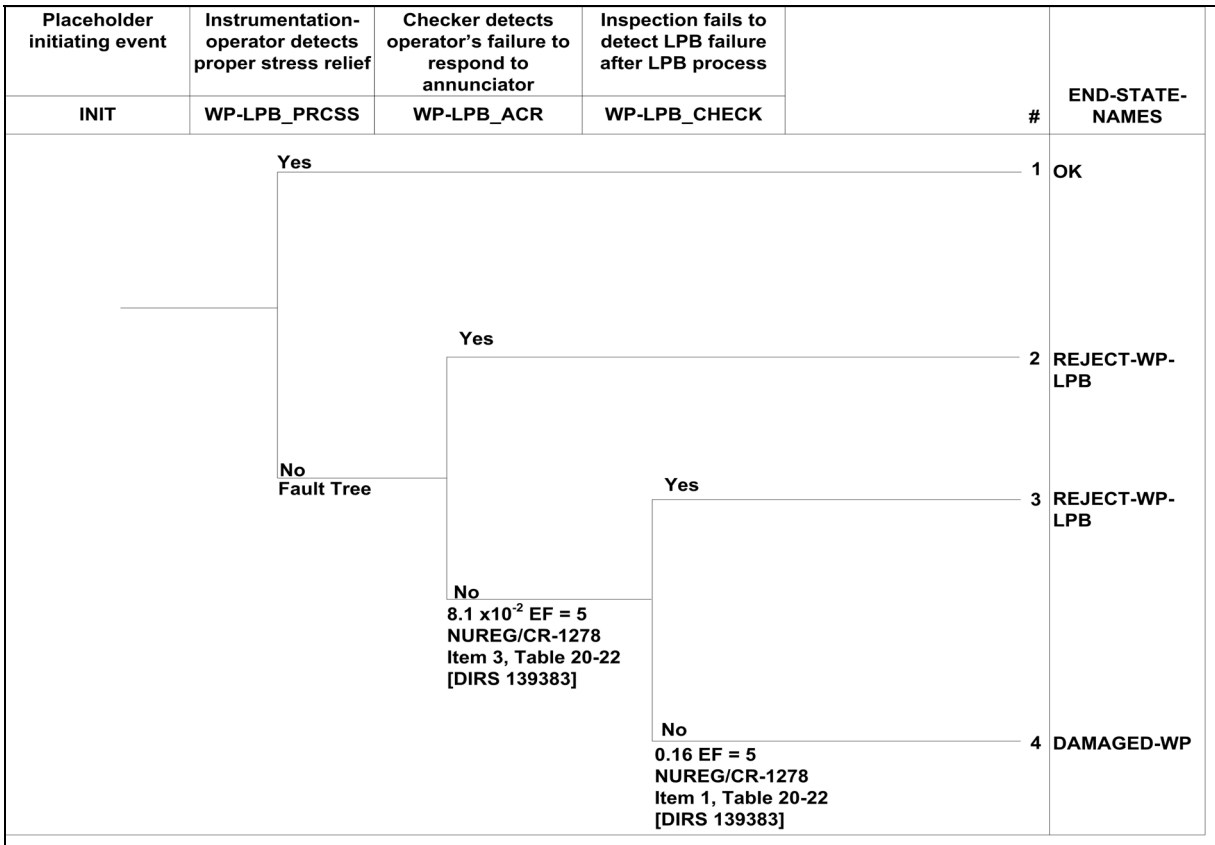


Figure B-12. Event Tree for Evaluating Low-Plasticity Burnishing Treatment of the Waste Package Outer Corrosion Barrier Lid

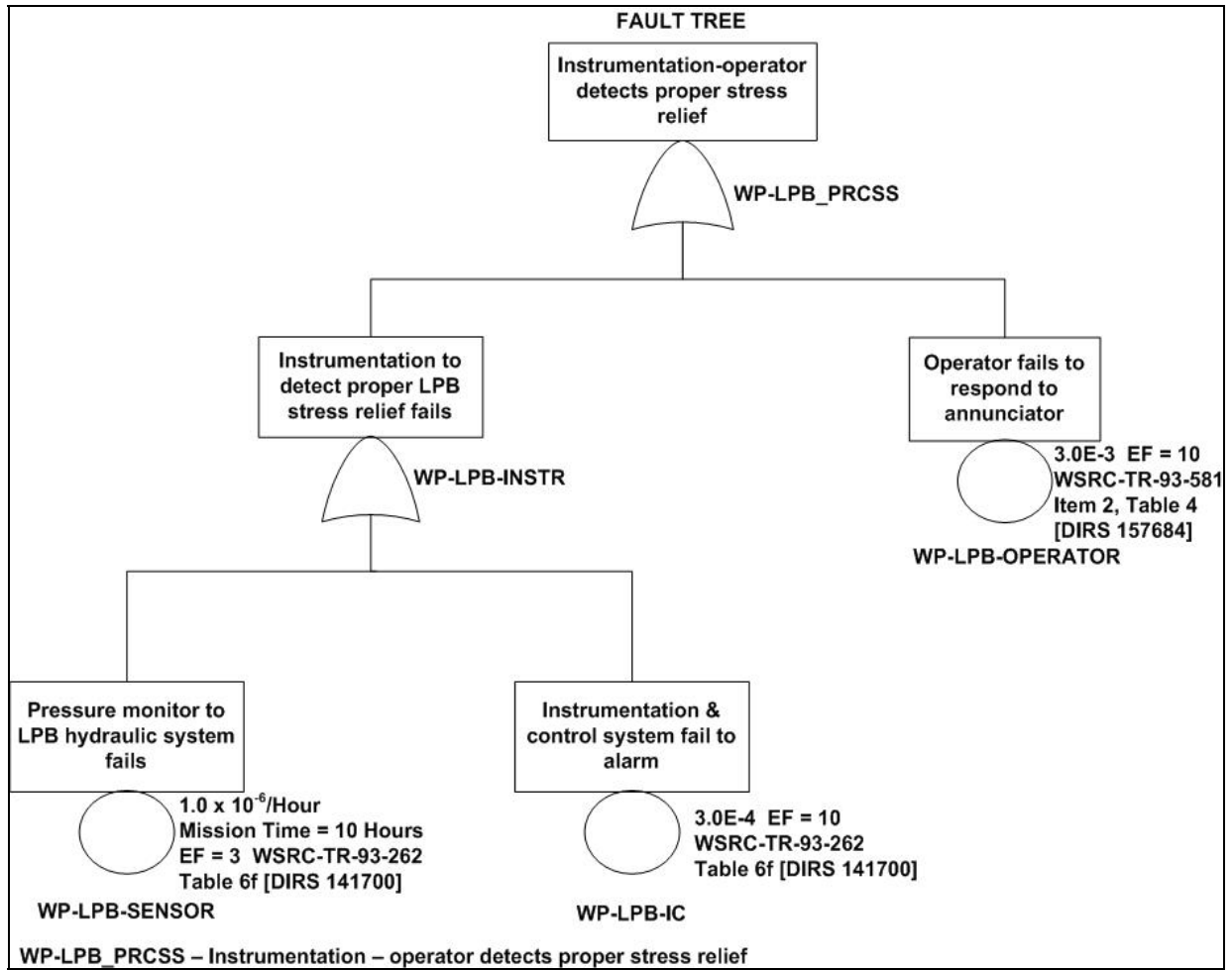


Figure B-13. Fault Tree for Evaluating Low-Plasticity Burnishing Process for the Waste Package Outer Corrosion Barrier Lid

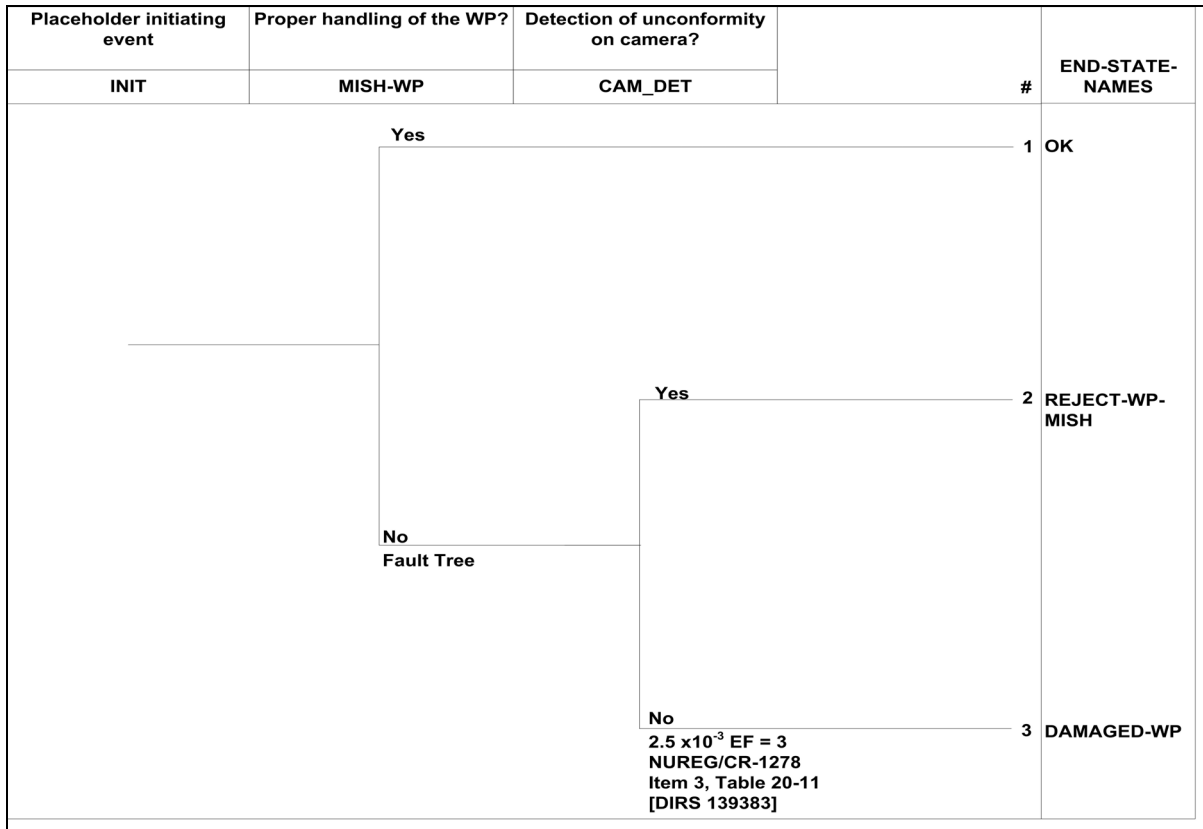
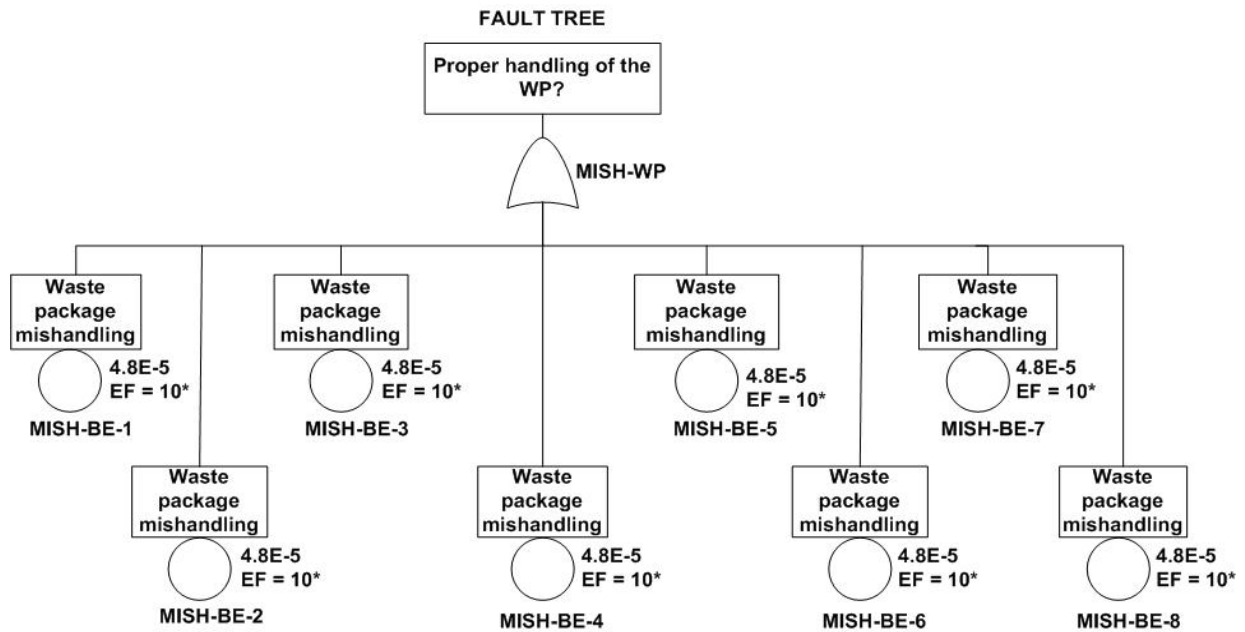


Figure B-14. Event Tree for Evaluating Mishandling of the Waste Package Outer Corrosion Barrier



*CAL-WHS-MD-000001, Table 5 [DIRS 157560]

MISH-WP – Proper handling of the WP?

Figure B-15. Fault Tree for Evaluating Mishandling of the Waste Package Outer Corrosion Barrier

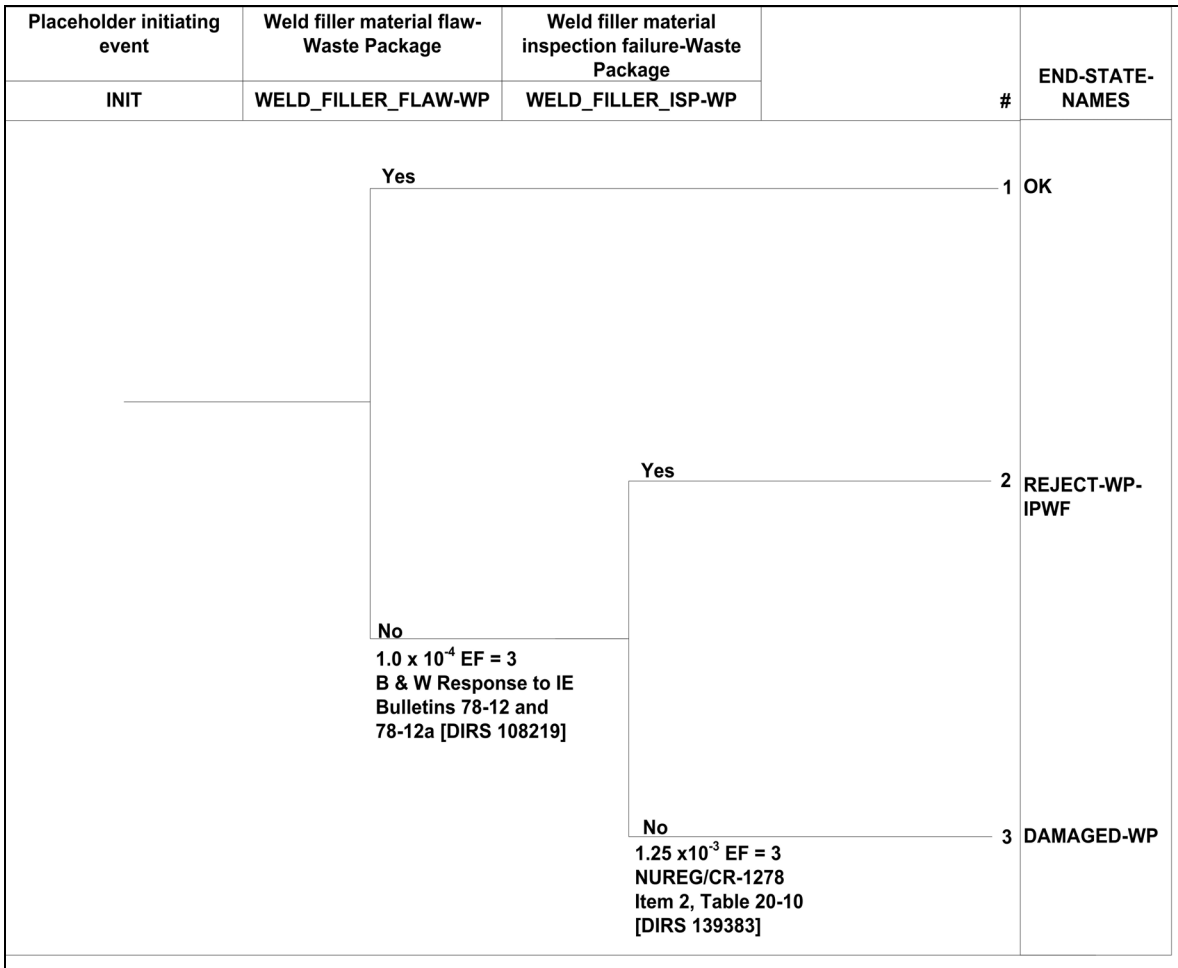


Figure B-16. Event Tree for Evaluating Weld Filler Material Defects for the Waste Package Outer Corrosion Barrier

Placeholder Initiating Event	Dummy Top Event			
INIT	PASS		#	END-STATE-NAMES
		1		OK
		2	T	HEAT_TREATMENT_DS
		3	T	BASE-METAL-DS
		4	T	WELD-FILLER-DS
		5	T	EMPLACEMENT-DS

Figure B-17. Basic Drip Shield Defect Event Tree

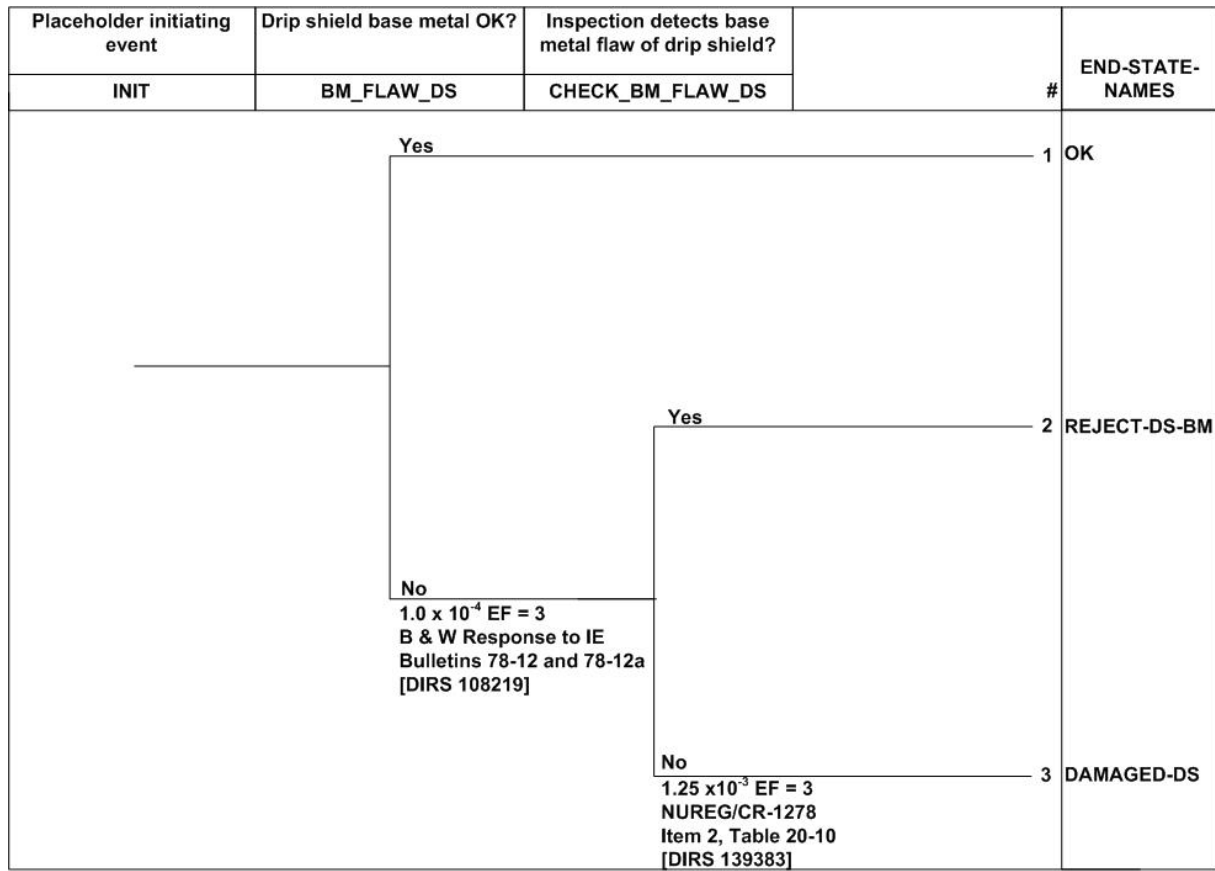


Figure B-18. Event Tree for Evaluating Improper Base Metal Selection for the Drip Shield

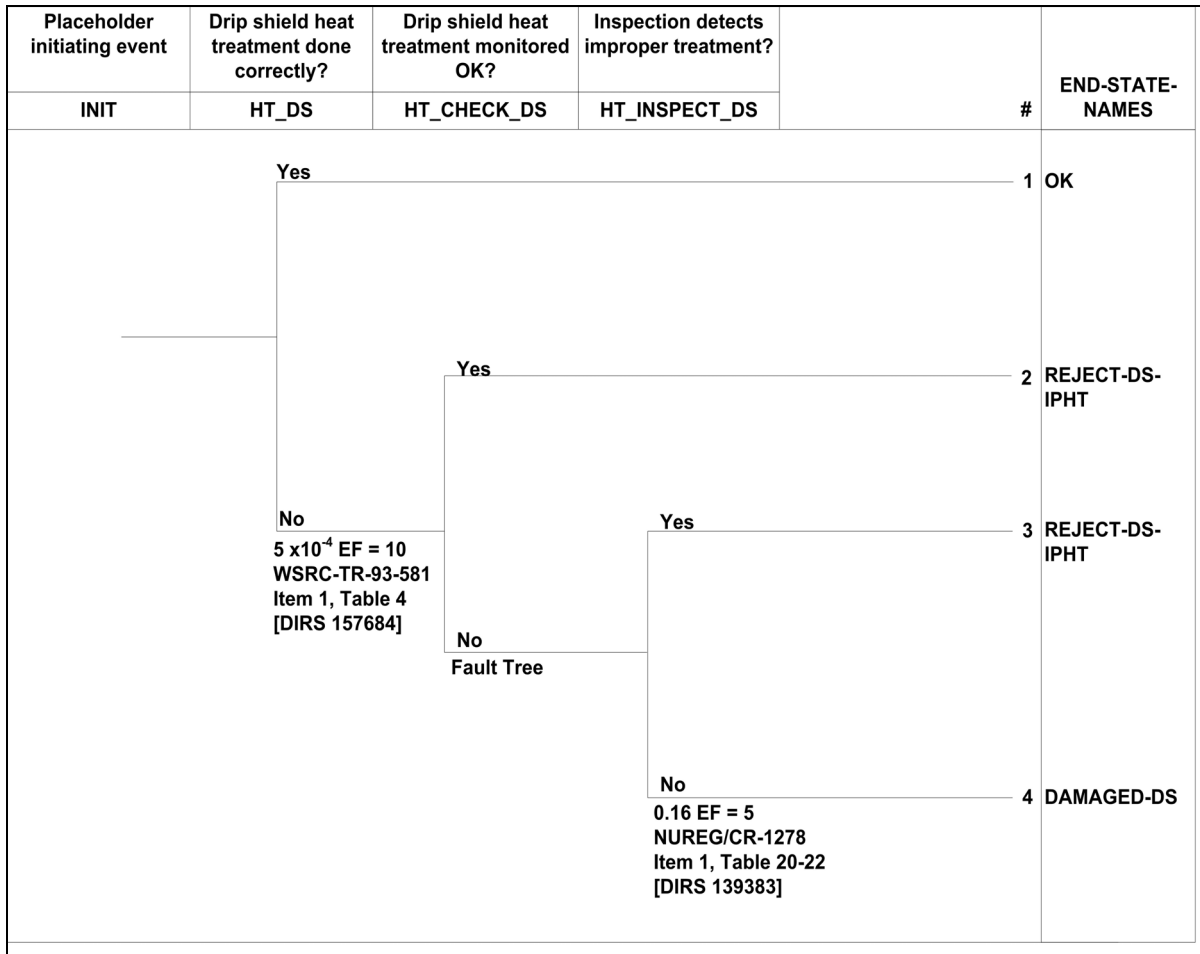


Figure B-19. Event Tree for Evaluating Improper Heat Treatment of the Drip Shield

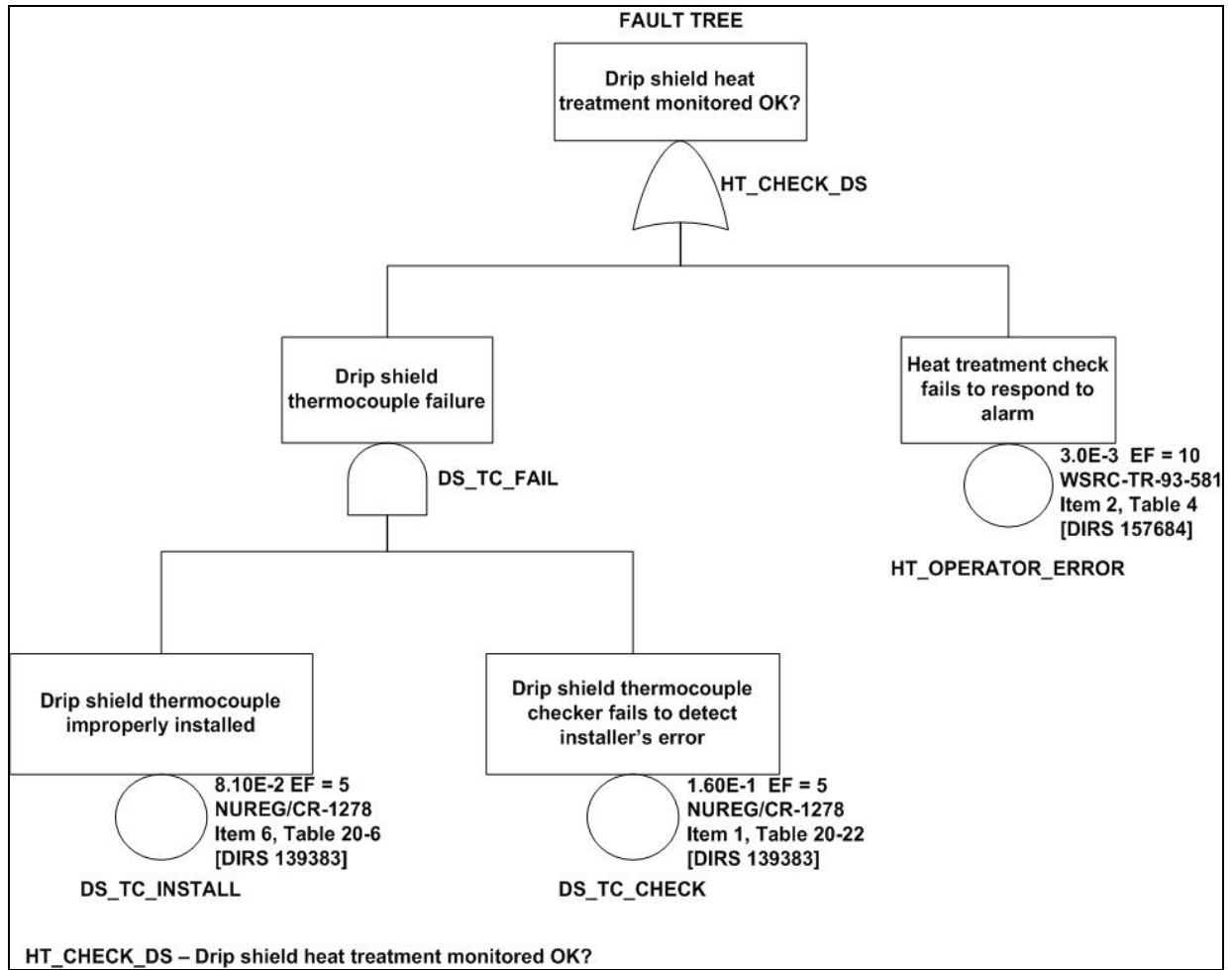


Figure B-20. Fault Tree for Check on Improper Heat Treatment of the Drip Shield

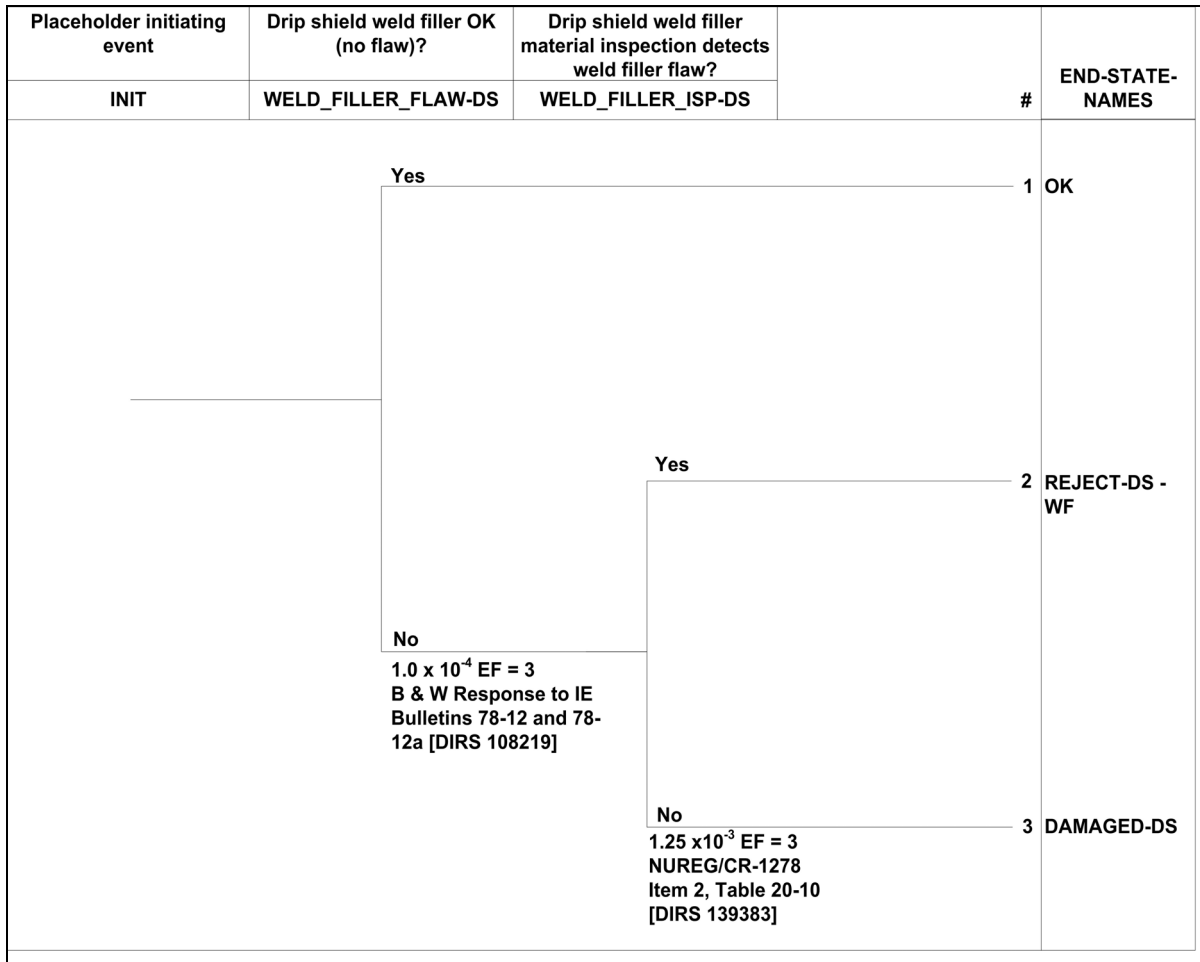


Figure B-21. Event Tree for Evaluating Weld Filler Material Flaws in the Drip Shield

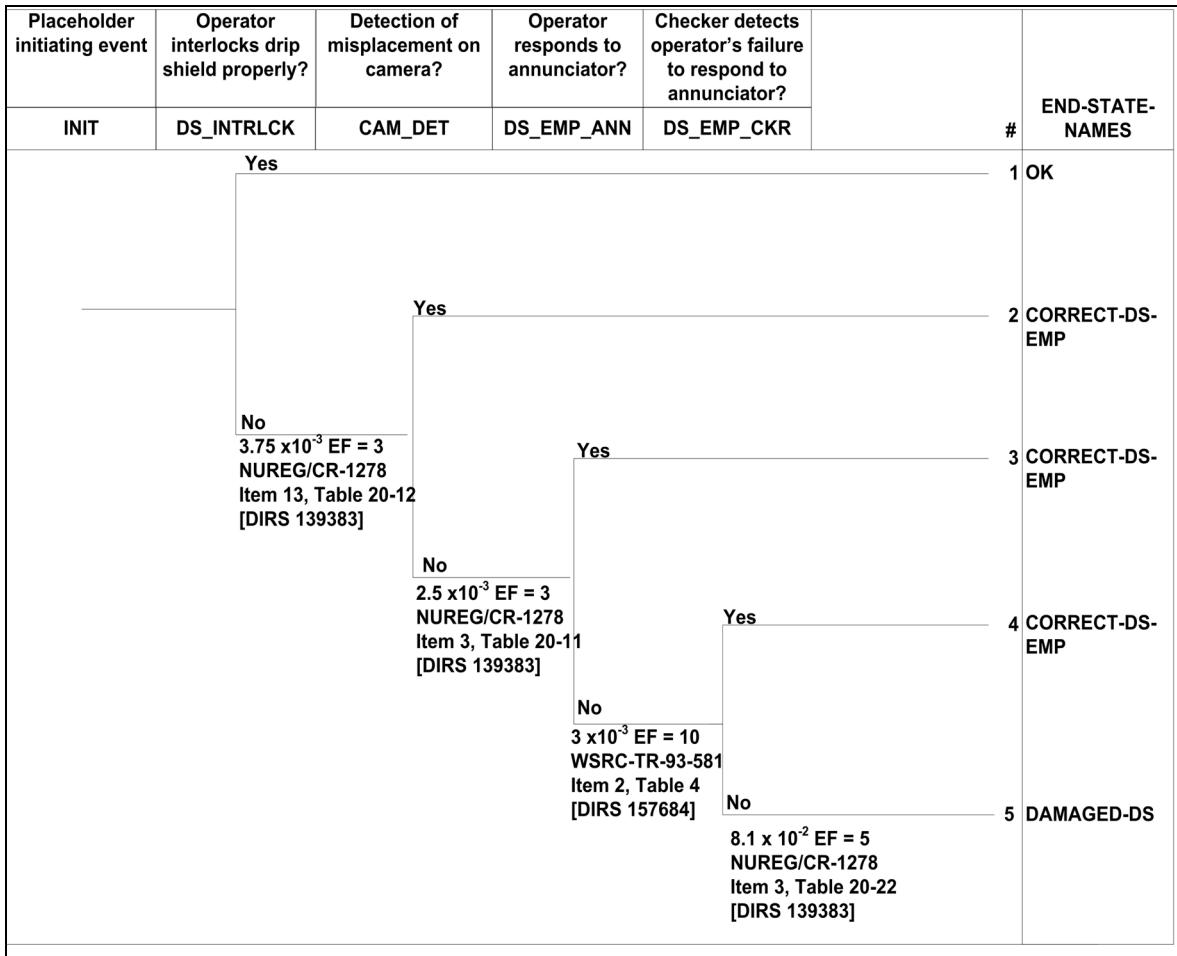


Figure B-22. Event Tree for Evaluating Improper Emplacement of the Drip Shield

APPENDIX C

TESTS ON PROTOTYPE WASTE PACKAGE OUTER CORROSION BARRIER

APPENDIX C – TESTS ON PROTOTYPE WASTE PACKAGE OUTER CORROSION BARRIER

Fabrication processes for the waste package outer corrosion barrier have been tested using a prototype waste package shell. Photographs from these tests are included in this appendix as collaborative information for possible fabrication processes as assumed in this analysis. Figure C-1 shows a full size Alloy 22 prototype shell being lowered by a crane into the quench tank after being furnace-heated per specification. Quenching is carried out on both sides of the shell by using gas purge pipes in the shell interior, one of which can be seen along the length of the shell.



Figure C-1. Prototype Waste Package Outer Corrosion Barrier Entering Quench Tank

A view of the post-annealed Alloy 22 prototype waste package outer corrosion barrier is shown in Figure C-2. The gas sparger purge pipes are clearly evident in this view.

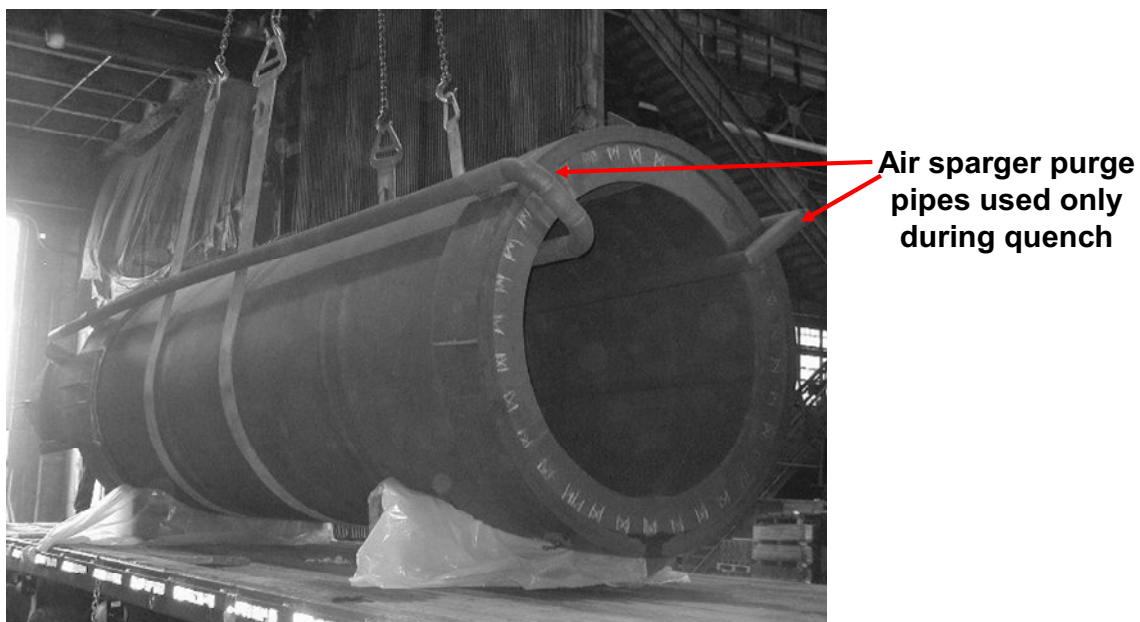


Figure C-2. Postannealed View of the Prototype Waste Package Outer Corrosion Barrier